ISTITUTO NAZIONALE DI FISICA NUCLEARE

Sezione di Trieste

INFN/AE-95/12

31 marzo 1995

A. Fridman

INTRODUCTION TO BEAUTY-HADRON PHYSICS

S.I.S. Pubblicazioni
Laboratori Nazionali di Frascati

INFN/AE-95/12
31/03/1995

INTRODUCTION TO BEAUTY-HADRON PHYSICS

A. Fridman*

Based on the lectures given in May 1994
at the University of Trieste
Via A. Valerio 2, Trieste

Centre National de la Recherche Scientifique, France

All the rivers run into the sea;
yet the sea is not full...
Ecclesiastes 1,7

Foreword

These lectures discuss methods for analyzing the decay of beauty hadrons (B mesons and beauty baryons) produced in pp interactions. At the c.m. energies around 14 TeV planned for the Large Hadron Collider (LHC) at CERN, the B meson production rate is expected to be $\sim 10^5$ larger than in an e^+e^- B factory. The pp collider could then offer, in principle, important advantages. However, the detection of beauty hadrons produced in a pp collider will be a task of great complexity. In particular, the triggering difficulties of events in a large background will be one of the major problems. Therefore, it would be useful to discuss the various aspects that can be investigated in beauty physics arising from pp interactions.

We first describe the general features of the formalisms of B mixing and search for CP violation in the meson decays. Then the specific problems appearing for beauty hadrons produced in pN interactions are considered. Some comparison between investigations which could be carried out with B factories and pp colliders are also mentioned, although this is not the main concern of these lectures. Finally, we also present some elements of beauty baryon decays which can only be studied efficiently by means of pN interactions.

Introduction in beauty-hadron physics

Content

1 - Generalities

1.1 - Quarks and hadrons

Before discussing the physics related to the decay and production of beauty particles, let us recall some general comments about hadrons. All the hadrons are assumed to be formed by quarks and/or antiquarks. All these quarks have spin S = 1/2 ($S_z = \pm 1/2$). The fundamental SU(3) triplet is formed by an isospin doublet u, d ($I = 1/2$, $I_z = \pm 1/2$) and an isospin singlet s ($I = 0$), the last having a strangeness quantum number $S = -1$. The quantum numbers can be summarized as follows where e_q represents the charge of the q quark[1,2]:

Quark	I	I_z	e_q	S
u	1/2	+1/2	2/3	0
d	1/2	-1/2	-1/3	0
s	0	0	-1/3	-1

The charge and the quantum numbers I_z, S_z, S are reversed for the charge conjugate (c.c.) triplet ($\bar{u}, \bar{d}, \bar{s}$). Later, two additional quarks have been introduced in order to describe new hadrons discovered in several experiments. They are:

- the charmed quark c having charge $e_c = 2/3$ and a mass $m_c \sim 1.5$ GeV
- the beauty quark b having charge $e_b = -1/3$ and a mass $m_b \sim 5.2$ GeV.

In the standard model, the weak decays of hadrons are described by the decay of the heavy quarks contained in these hadrons. For these processes, the quarks are classified into left-handed weak isodoublet fields (Chapter 2). In this approach each doublet has an up quark of charge $e_{up} = 2/3$ and another, the down quark, with $e_{down} = -1/3$. Within this approach an expected top quark was missing. Recent experimental results[3] found to be in favor of a sixth (t) quark ($e_t = 2/3$ and a mass of $m_t \sim 150$ GeV) yield the following six quark model:

$$\begin{pmatrix} u \\ d \end{pmatrix}_{left}, \quad \begin{pmatrix} c \\ s \end{pmatrix}_{left}, \quad \begin{pmatrix} t \\ b \end{pmatrix}_{left}. \qquad (1.1)$$

The charged current reactions in the weak decay processes relate the up to the down quarks through V - A interactions. This will be discussed in Chapter 2.

The main aim of these lectures will be the study of particles containing a b or $\bar{b}$ quark. In general, the light quark will be denoted by q (u, d, s) while Q will be used for the heavy quark (b, c, t). The mesons and baryons that will be considered have the following quark contents:

$\overline{B} \Rightarrow$	$B^- \equiv b\bar{u}$ $\overline{B}^0_d \equiv b\bar{d}$ $\overline{B}^0_s \equiv b\bar{s}$ $\overline{B}^0_c \equiv b\bar{c}$	$B \Rightarrow$	$B^+ \equiv \bar{b}u$ $B^0_d \equiv \bar{b}d$ $B^0_s \equiv \bar{b}s$ $B^0_c \equiv \bar{b}c$
$N_b \Rightarrow$	bqq	$\overline{N}_b \Rightarrow$	$\overline{bqq}$

Within the actual notation the meson having a b $(\bar{b})$ quark is considered to be a $\overline{B}$ (B) meson in opposition to the definitions of the beauty baryon $N_b \equiv bqq$ (antibaryon $\overline{N}_b \equiv \overline{bqq}$). One has to note that these definitions are different from those used for the charmed hadrons,

$$D \equiv c\bar{q} \qquad \overline{D} \equiv \bar{c}q$$
$$N_c \equiv cqq \qquad \overline{N}_c \equiv \overline{cqq}$$

where D $(\overline{D})$ mesons and charmed baryons (antibaryons) contain a c $(\bar{c})$ quark. In the following we will use the above notation for describing the charm and beauty hadrons. Let us now give some indications about the c and b quarks.

1.2 - Comments about the $c\bar{c}$ and $b\bar{b}$ mesons

The presence of the c and b quarks were indicated by experiments over the past ~ 20 years showing the existence of two families of heavy neutral resonances: the ψ (or charmonium) and the Υ (bottomium or beauty) families. The striking feature observed in both families[4] is that the energy level spacing between successive members in each family is small compared to the overall mass scale (the J/ψ or the Υ masses is used to represent the lowest ones in each family). This suggests interpreting the states as bound systems of heavy quarks that are moving non relativistically in the $Q\overline{Q}$ rest frame[5–8] (Q denotes here the c or the b quark). The families considered are then defined by

$$\psi \equiv c\bar{c}, \quad c \equiv \text{charmed quark}\ , \ e_c = 2/3$$
$$\Upsilon \equiv b\bar{b}, \quad b \equiv \text{beauty quark}\ , \ e_b = -1/3$$

but where the charge of these quarks has been deduced from experimental results[9].

The above remarks led to the idea of identifying the masses of the $Q\overline{Q}$ states within a quarkonium family with the energy eigenstate given by a Schrödinger type of equation[5-8,10,11]. At that time it was also necessary to know if these families are formed by quarks where some of their quantum numbers are different from those belongling to the quarks forming the hadrons known at that time. Today, we know that the c and b quarks are isosinglets and have each an additionnal quantum number called charm and beauty, respectively (and having an opposite sign for the $\overline{Q}$). This means that in strong interactions, for instance, the total charm and beauty quantum numbers have to be conserved.

The so-called Υ family in which we are here interested was discovered in 1977 by studying the effective mass of μ^+ and μ^- produced in pN interactions[12]. The observed resonances were linked to a virtual photon (see Fig. 1.1) and have then spin (J), parity (P) and charge conjugation (C) values of the photon, $J^{PC} = 1^{--}$. The convenient ways for studying these resonances were to observe them as s-channel resonances in e^+e^- collisions where the production process is dominated by a virtual photon exchange. In these cases, the precision of the mass and width measurements of the (narrow) resonances will depend essentially on the energy resolution of the e^+e^- collider (and not on the spectrometer properties). Figure 1.2 shows the diagrams contributing to the production of leptons or hadrons at c.m. energies corresponding to the s-channel resonances. The diagram representing the non-resonating background (continuum) is also shown in Fig. 1.2a and Fig. 1.2b. The third case in these figures is the so-called vacuum polarization contribution. Figure 1.2c indicates the $b\overline{q}$ and $\overline{b}q$ production above their threshold. Some $b\overline{b}$ states discovered as s-channel resonances in e^+e^- interactions are presented in Fig. 1.3. For the observed resonances the relative orbital momentum between the two (fermion) quarks is $l = 0$ in order to reach the $J^{PC} = 1^{--}$ values. These s-channel resonances will therefore be represented in the following by $\Upsilon(nS)$ where n represents the radial quantum number of the S wave describing the $b\overline{b}$ system. From the quantum number conservation a D wave between the two quarks is allowed. The existence of such an s-channel resonance is, however, negligible[13].

Other $b\overline{b}$ systems cannot be reached by the direct e^+e^- collisions when these states have not the photon quantum numbers. They can be reached by hadronic or radiative transitions. This is shown in Fig. 1.4 presenting the observed energy-level diagram of the Υ family[4]. Some of the detected transitions are indicated.

1.3 - Some properties of the $\Upsilon(nS)$

Before discussing the beauty hadrons, let us describe some properties of the $b\overline{b}$ states. The states, presented in Fig. 1.4, have been studied essentially through

Table 1.1 - Parameters of the $\Upsilon(nS)$ resonances with $n \leq 4$. The data are taken from the Particle Data Group (Phys Rev. 45D, 1992). The Γ_{ll} and Γ_t represent the $\Upsilon(nS) \to l^+l^-$ and total widths, respectively. Note that $\Gamma_{ee} = \Gamma_{\mu\mu} \simeq \Gamma_{\tau\tau}$ where the subindices indicate the type of produced leptons. The mass of the $\Upsilon(1S)$ is taken as ~ 9460 MeV.

	$\Upsilon(nS) - \Upsilon(1S)$ mass difference (MeV)	Γ_{ee} (KeV)	Γ_t (KeV)
$\Upsilon(1S)$	–	1.34 ± 0.04	52.1 ± 2.1
$\Upsilon(2S)$	563	0.586 ± 0.029	43 ± 8
$\Upsilon(3S)$	895	0.44 ± 0.03	24.3 ± 3.9
$\Upsilon(4S)$	1120	0.24 ± 0.05	$(23.8 \pm 2.2)\ 10^3$

the e^+e^- interactions. However, their production rates in pN interactions might be important at large c.m. energy, $\sqrt{s} \geq 1$ TeV. Table 1.1 indicates some proprties of the $\Upsilon(nS)$ resonances. One sees that the semileptonic decay widths have the same order of magnitude (although Γ_{ee} decreases with an increasing of n, the radial quantum number). However, the total widths of the first three resonances are narrower than the fourth by a factor of $\sim 10^3$. In fact the widths of the bound states ($n \leq 3$) observed in Fig. 1.3 correspond to the energy resolution of the e^+e^- collider. Therefore, better energy resolution of the e^+e^- collider will give a smaller background in the study of the decay of the bound $Q\overline{Q}$ state.

It should be remenbered that the partial width of the semileptonic decay of the $^3S_1$ resonances can be expressed by the Van Royen-Weisskopf formula[14], corrected here by QCD effects,

$$\Gamma(n^3S_1 \to l^+l^-) = 16\pi\ e_Q^2\alpha^2 \frac{|\psi_n(0)|^2}{M_V^2} \left[1 - \frac{16\alpha_s}{3\pi}\right] . \tag{1.1}$$

This expression gives the leptonic width of the $^3S_1$ states as a function of $|\psi_n(0)|^2$, the square of the wave function at the origin. Here M_V is the mass of the neutral vector meson, while α is the fine structure function. The QCD running coupling constant is given by

$$\alpha_s = \frac{12\pi}{(33 - 2N_t)\ ln(s/\Lambda^2)} , \tag{1.2}$$

where N_t is the number of open flavor channels at the corresponding c.m. energy $\sqrt{s}$, and Λ the QCD scale parameter ($\Lambda \sim 500$ MeV). As the increase of M_V with

n is not enough to describe the variation of the observed leptonic width (see Table 1.1), $|\psi_n(0)|^2$ has to decrease when n is increasing according to formula (1.1). The comparison of the experimental and calculated widths could allow a verification of the validity of the chosen potentials to describe the $Q\overline{Q}$ system.

In the QCD framework, the hadron production of the bound states is essentially mediated by gluons. This should occur through the minimum number of gluons allowed by the conservation rules. One gluon is not possible as the produced hadrons are color singlets. The two-gluon case is also excluded as a spin 1 object cannot decay into two massless gluons of spin 1. Therefore, three is the minimum number of gluons allowed by conservation rules. Based on this assumption the calculated three-gluon width of the $\Upsilon(nS)$ resonance is given by[15]

$$\Gamma_{3g}(nS) = \frac{160}{81}\ (\pi^2 - 9)\ \alpha_s^3\ \frac{|\psi_n(0)|^2}{M_V^2}\ . \tag{1.3}$$

The width will decrease as n increases, a consequence of the behaviour of $|\psi_n(0)|^2$ (see formula (1.1) and Table 1.1) and M_V. Note that for $n \geq 2$ one has also the decays

$$\Upsilon(2S) \to \Upsilon(1S)\pi^+\pi^-$$
$$\Upsilon(3S) \to \Upsilon(2S)\pi^+\pi^-,\ \Upsilon(1S)\pi^+\pi^-$$

which may lead to only hadrons in the final state with the additional $\Upsilon(2S), \Upsilon(1S) \to$ 3 gluons channels.

The width of the three-gluon decay together with the Van Royen-Weisskopf expression (neglecting here the QCD correction) allows an estimate of α_s through the ratio

$$\frac{\Gamma_{3g}}{\Gamma_{ee}} \simeq 1410\ \frac{(2/3)^2}{e_b^2}\ \alpha_s^3\ . \tag{1.4}$$

By using the data from the $\Upsilon(1S)$ decay one obtains the value of $\alpha_s \simeq 0.16$ at the considered e^+e^- c.m. energy[9].

Above the $b\bar{b}$ threshold, the B meson decay can be studied from the $e^+e^- \to \Upsilon(4S) \to B\overline{B}$ process. The various B decay channels could then be observed with the detector used for the experiments. This field is the dominant part of the study which was analyzed with great effort using e^+e^- colliders (Cornell and DESY laboratories).

The $\Upsilon(4S)$ mass is not large enough to produce an additionnal π in the final state. Then the relative orbital momentum between the B_d^0 and $\overline{B}_d^0$ mesons is $l = 1$ for reaching the $J^{PC} = 1^{--}$ condition. The Bose-Einstein statistics will then influence the $B_d^0 \leftrightarrow \overline{B}_d^0$ mixing (Chapter 3) as $B_d^0 B_d^0$ and $\overline{B}_d^0 \overline{B}_d^0$ final states are not allowed when l is odd. In that case the wave function describing the final state cannot be even under the permutation of the two outgoing mesons. Therefore, one meson has to decay before the second one can mix. As discussed in Chapter 4 this will also influence the search for CP violation effects in the $B_d^0, \overline{B}_d^0$ decays.

1.4 - Beauty hadrons, past and future

As already mentioned above, the experimental necessities of having c and b quarks are based on the discovery of the ψ and Υ families. Although the Υ family was discovered using pN interactions, the detailed study of the $b\bar{b}$ spectroscopy (Fig. 1.4) was essentially carried out with the e^+e^- interactions. Moreover, the $e^+e^- \rightarrow \Upsilon(4S) \rightarrow B\overline{B}$ process also allowed the study of many aspects of the B meson decays as well as the $B_d^0 \leftrightarrow \overline{B}_d^0$ mixing (see Chapter 3).

The important question now is to define what kind of new experiments should be prepared in order to improve our knowledge of (rare) B decay and to search for CP violation effects in the B decay. Two different ways can certainly be envisaged:

- the increase of the statistics of the $\Upsilon(4S) \rightarrow B\overline{B}$ using an asymmetric e^+e^- collider for the search of CP violation effects
- the study of beauty hadron produced in pp interactions where the production rate at large c.m. energy ($\sqrt{s} \geq 1$ TeV) is expected to be large.

Table 1.2 compares the production rates between an e^+e^- collider at a c.m. energy $\sqrt{s} \simeq 10$ GeV and pp interaction at $\sqrt{s} = 14$ TeV. The latter value corresponds to the c.m. energy of the Large Hadron Collider (LHC) project at CERN. For the above $\sqrt{s}$ values, we use the luminosities of $\mathcal{L} = 3 \times 10^{33}, 10^{33}$ cm^{-2}s^{-1}, respectively. The e^+e^- luminosity corresponds to the value proposed for the B-factory[16] whereas the second one is a value expected for the the study of B-physics at the LHC (Ref. 16 to 18)

The total pp cross-section at $\sqrt{s} = 14$ TeV is estimated to be $\sigma_T \simeq 110$ mb (Ref. 19, 20). However, in an experiment with a pp collider, the elastic and diffractive part of the interactions can often be neglected as the outgoing particles emitted in the forward/backward direction (defined with respect to the beam direction) will not usually be detected by the detector considered. By neglecting the diffractive and elastic cross-sections, one estimates the so-called non-diffractive cross-section

Table 1.2 - The comparison of luminosity ($\mathcal{L}$), average charged multiplicity ($\langle n \rangle$), total (σ_T) and $b\bar{b}$ [$\sigma(b\bar{b})$] cross-sections. For the LHC example we used the non-diffractive cross-section instead of σ_T (i.e. $\sigma_{in} \sim 60\ mb$). The number of $b\bar{b}$ events per year (10^7 s) of running as well as the number of interactions per second are also indicated. For pp interactions $\langle n \rangle$ does not take into account the contribution of elastic and diffractive processes.

	LHC 14 TeV	$e^+e^- \to \Upsilon(4S)$ 0.011 TeV
$\mathcal{L}$ $cm^{-2}s^{-1}$	10^{33}	$3\ 10^{33}$
$< n_c >$	~ 80	~ 12
σ_T	$\sim 60\ mb$	$4\ nb$
$\sigma(b\bar{b})$	$\sim 300\ \mu b$	$1.2\ nb$
$\sigma(b\bar{b})/\sigma_T$	$\sim 1/200$	$\sim 1/4$
$N(b\bar{b})/10^7 s$	$3\ 10^{12}$	$3.6\ 10^7$
N_{int}/s	$6\ 10^7$	$1.4\ 10^2$

$\sigma_{in} \simeq 60$ mb (Ref. 20) yielding the number of interactions per second (N_{int}/s) given in Table 1.2. At $\sqrt{s} \simeq 14$ TeV, we use a $pp \to b\bar{b}X$ of $\sigma(b\bar{b}) \simeq 300\ \mu$b ($X$ meaning anything) which is the order of magnitude utilized at this energy[21,22]. One also sees from this table that the B ($\overline{B}$) production rate is expected to be much larger in pp collisions than in the example of the $e^+e^- \to \Upsilon(4S) \to B\overline{B}$ process. However, the utilization of a pp collider is not simple, as the number of interactions per second, the average charged multiplicity $\langle n \rangle$ and the expected background (related to the $\sigma(b\bar{b})/\sigma_T$ ratio) are important[21] (Table 1.2). Moreover, one of the important difficulties of studying B-physics with a pp collider is defining efficient triggering processes[17,18].

One should also remember that difficulties can arise with a pp collider where several interactions per bunch crossing occur. The LHC project, $\mathcal{L} = 10^{33}$ cm^{-2}s^{-1} (10^{32} cm^{-2}s^{-1}) would lead to an average of 1.1 (0.11) interaction per bunch crossing using the cross-section of $\sigma_{in} \simeq 60$ mb and the example of Appendix 1.A. Assuming that the probability of n' interactions per bunch crossing follows a Poisson distribution, one obtains the average number of interactions for minimum bias events ($\overline{m}_{min}$) and for events with a specific trigger signature ($\overline{m}_{str}$) corresponding to $n' \geq 1$,

$$\mathcal{L} = 10^{32}\ \mathrm{cm^{-2}s^{-1}}: \qquad \overline{m}_{min} \simeq 1.06\ , \quad \overline{m}_{str} \simeq 1.11$$
$$\mathcal{L} = 10^{33}\ \mathrm{cm^{-2}s^{-1}}: \qquad \overline{m}_{min} \simeq 1.65\ , \quad \overline{m}_{str} \simeq 2.11$$

(Appendix 1.A). Therefore, an experimental pp run with $\overline{m}_{str} > 2$ could complicate the detection of the beauty hadron because of the large charged multiplicity given then by $\sim \overline{m}_{str} \times \langle n \rangle$.

At the end of these lectures one will have a better understanding of the usefulness of investigating B-physics in the pp collider ($\sqrt{s} \simeq 14$ TeV) and in the $e^+e^- \to \Upsilon(4S) \to B\overline{B}$ ($\sqrt{s} \simeq 10$ GeV) which are, in fact, complementary. Both methods will give access to different fields and lead to a better knowledge of the decay properties of beauty hadrons. The advantages and inconveniences of both methods can be crudely summarized in the following manner:

<u>pp collider</u>

- Advantages: large $\sigma(b\bar{b})$ cross-section, search for CP violation in the B_d^0 and B_s^0 decays, study of rare B decay, study of B_c and beauty-baryon (production and decay);
- Inconveniences: triggering difficulties, no real particle identification, large number of produced tracks and background.

<u>$e^+e^- \to \Upsilon(4S) \to B\overline{B}$</u>

- Advantages: trigger facility, particle identification, small background.
- Inconveniences: small $B\overline{B}$ production rates ($\sim 4\ 10^7$ events in one year of running), the utilization of an asymmetric e^+e^- collider to search for CP violation in the B_d^0 decays, no possibilities to search for CP violation in the B_s^0 decays, no analyzis of beauty-baryon decays.

Let us now study in some detail the properties of the beauty hadron decays. After some general discussions about B^0 mixing and CP violation effects we will investigate the difficulties of using pp interactions for studying beauty hadron decays. Some comparison between the study of beauty-meson decays produced in pN and in $e^+e^- \to \Upsilon(4S) \to B\overline{B}$ will also be mentioned.

Appendix 1.A

Minimum bias and specific events

We assume that the number of n' interactions per bunch crossing follows a Poisson distribution given by the probability

$$P(n') = e^{-m} \frac{m^{n'}}{n'!} \ , \quad \text{with} \quad \sum_{n'=0}^{\infty} P(n') = 1$$

and where $\overline{n}' = m$ is the average number of interactions per bunch crossing while the standard deviation is given by $\sigma = \sqrt{m}$.

The minimum bias event corresponds to interaction where $n' \geq 1$. In this case the probability distribution will be given by

$$P_{min}(n') = e^{-m} \frac{m^{n'}}{n'!} \frac{1}{\sum_{n=1}^{\infty} e^{-m} \, m^n/n!}$$

Since one has

$$\sum_{n=1}^{\infty} e^{-m} \frac{m^n}{n!} = -e^{-m} + 1$$

one obtains the average number of interactions for minimum bias events ($\overline{m}_{min}$), and $\overline{m}_{str}$ denoting the average number of events with a specific trigger signature. They are given by:

$$\boxed{\begin{aligned} \overline{m}_{min} &= \frac{m}{1-e^{-m}} \\ \overline{m}_{str} &= 1+m \end{aligned}} \qquad (1.A1)$$

In order to estimate $\overline{n}' = m$ let us take a pp collider with a luminosity of $\mathcal{L} = 10^{32}$ cm^{-2}s^{-1} and where $\sigma_T' \simeq 60$ mb. The number of interactions per second is then

$$N_{int}/s = \mathcal{L}\sigma_T' \simeq 6 \times 10^6 \ .$$

Taking an example of a p beam with 4810 bunches and a turning frequency of 11.2 KHz, the average number of interactions per bunch crossing will be given by

$$m = \frac{6 \times 10^6}{11200 \times 4810} = 0.11 \qquad (1.A2)$$

yielding $\overline{m}_{min}$ and $\overline{m}_{str}$. For a ten times larger luminosity, one simply has $m = 1.1$.

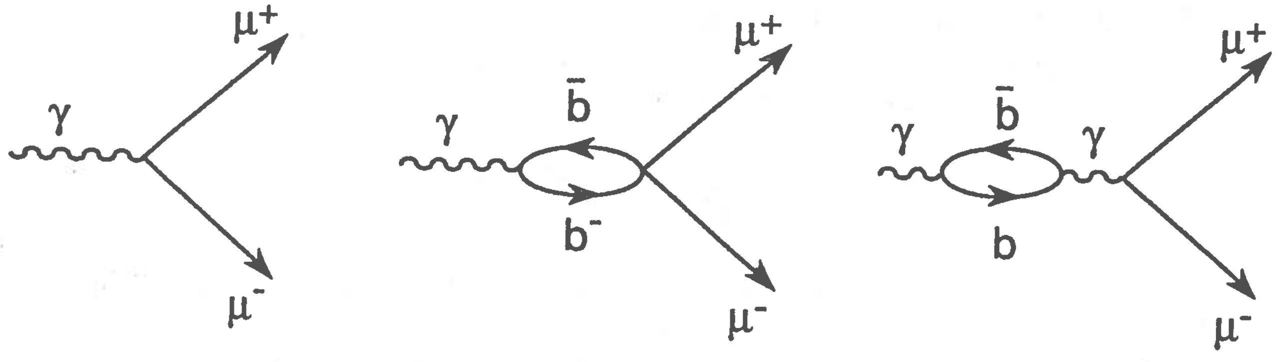

Fig. 1.1 - Diagrams leading to the $\mu^+\mu^-$ production due to background and to the $\Upsilon(nS)$ decays. Here the virtual photon is assumed to be produced in pN collisions.

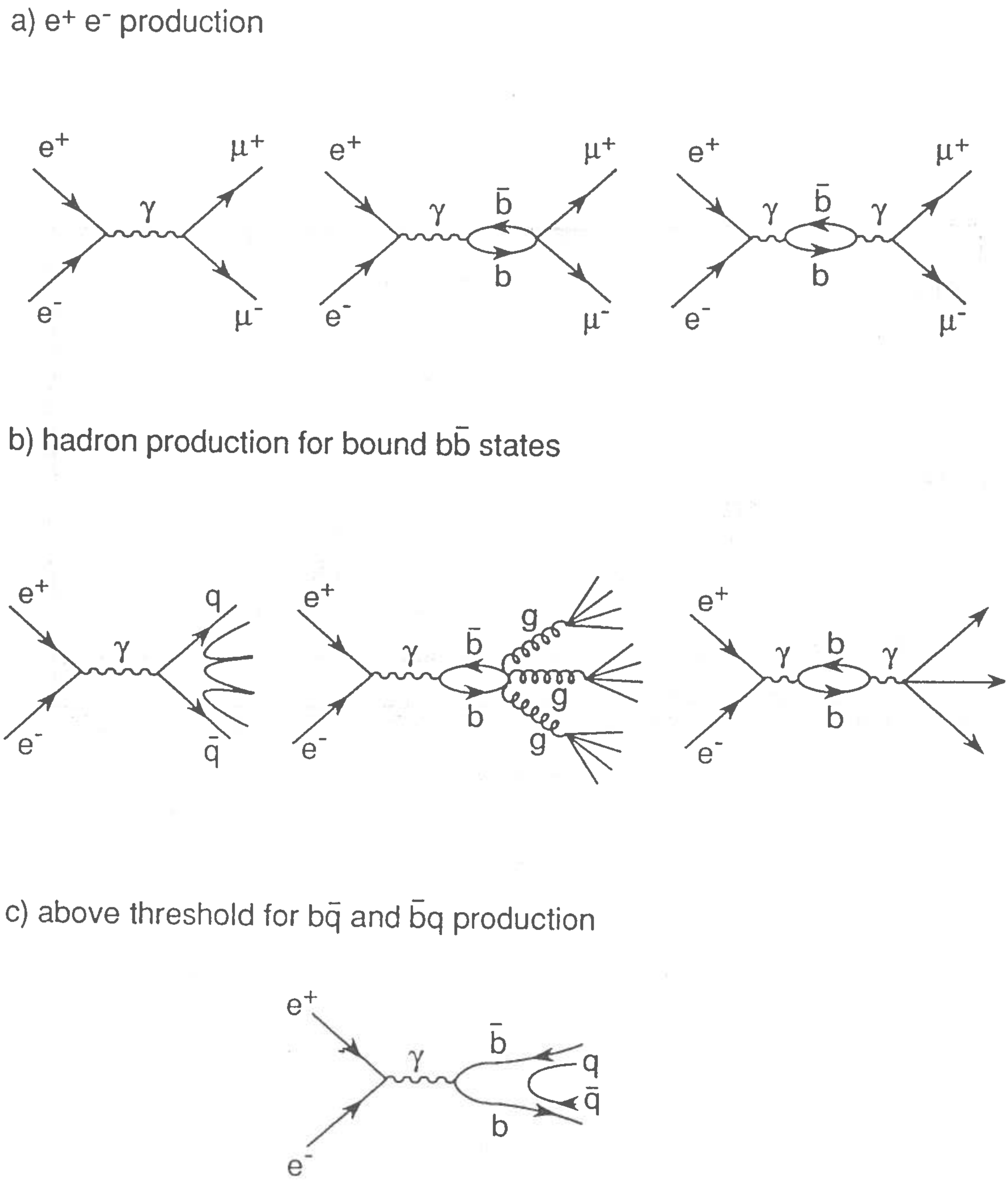

Fig. 1.2 - The $\mu^+\mu^-$ [a)] and hadron [b)] production for the decay of bound $b\bar{b}$ states produced in e^+e^- collisions. The first diagram in a) and b) indicate the background contribution. In c) the hadron production is shown for $b\bar{q}$ and $\bar{b}q$ production above their threshold.

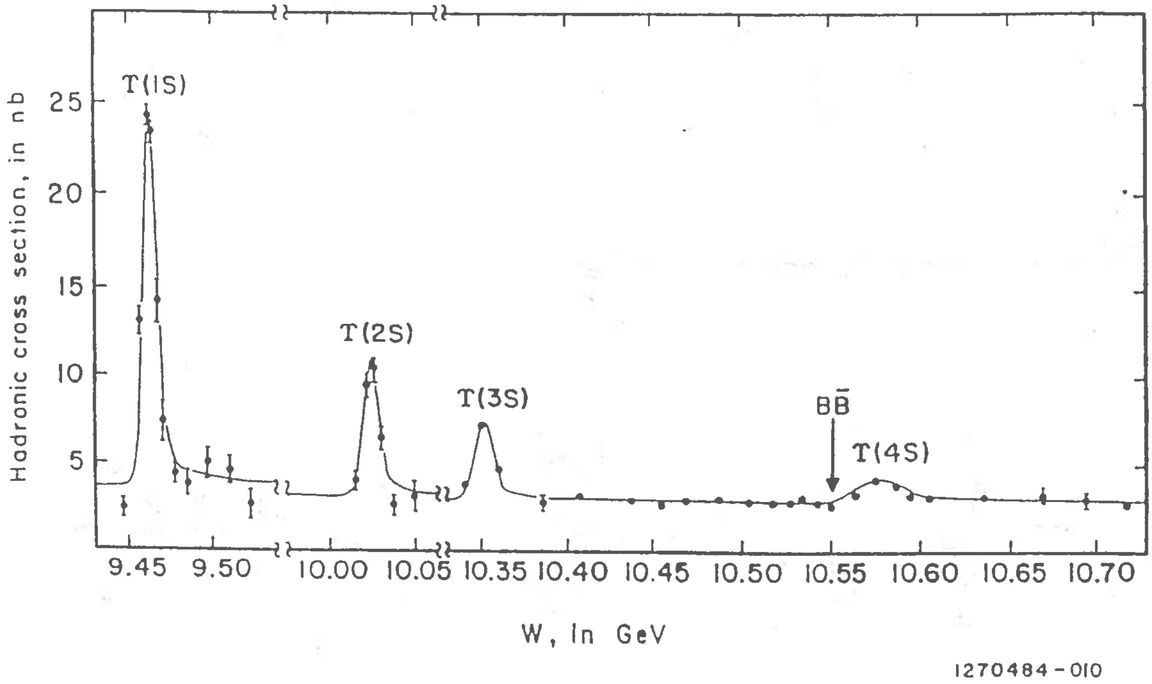

Fig. 1.3 - The hadronic cross-section in the $\Upsilon(nS)$ region $(1 \leq n \leq 4)$ as measured in e^+e^- interactions by the CLEO collaboration. Here the c.m. energy is represented by W. The W threshold for producing $B\overline{B}$ ia also indicated.

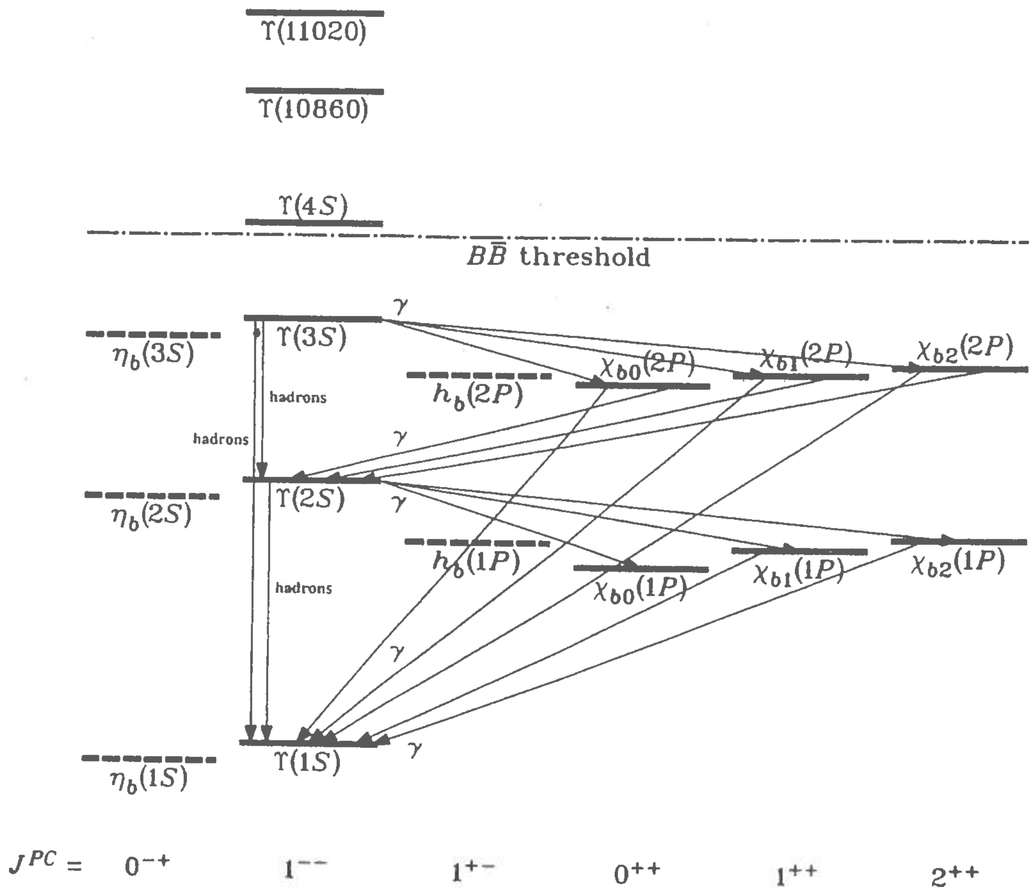

Fig. 1.4 - The energy-level scheme of the $b\bar{b}$ states taken from Phys. Rev D45, No 11 (1992). The singlet states are called η_b or h_b while triplets are denoted by Υ and P_{bJ}.

2 - The CKM matrix elements

2.1 - Generalities

The $SU(1) \times U(1)$ standard model[1] classifies the quarks and leptons into left-handed weak isodoublets, while right-handed quarks are considered to be isosinglets. In the six-quark model one has:

$$\begin{pmatrix} u \\ d' \end{pmatrix}_{left} , \quad \begin{pmatrix} c \\ s' \end{pmatrix}_{left} , \quad \begin{pmatrix} t \\ b' \end{pmatrix}_{left} . \tag{2.1}$$

where the up quarks have a charge 2/3 and the down ones the charge of -1/3. Charged current reactions relate transitions between quarks of charge 2/3 with those having -1/3 by emitting a W boson. Here the weak decay processes relate only, the quark fields within one isodoublet. The number of isodoublets is not determined by the standard model (SM). However, this model predicts that the number of quark isodoublets should be equal to the number of lepton doublets[2]. The actual experiments are in favor of three lepton doublets, namely

$$\begin{pmatrix} e \\ \nu_e \end{pmatrix} , \quad \begin{pmatrix} \mu \\ \nu_\mu \end{pmatrix} , \quad \begin{pmatrix} \tau \\ \nu_\tau \end{pmatrix} .$$

We will, therefore, consider first the three quark isodoublets. In fact, the d', s' and b' can be expressed in terms of the quark mass eigenstates by means of a mixing unitary matrix (V), the so-called mixing or Cabibbo-Kobayashi-Maskawa (CKM) matrix[3]

$$\begin{pmatrix} d' \\ s' \\ b' \end{pmatrix} = (V) \begin{pmatrix} d \\ s \\ b \end{pmatrix} . \tag{2.2}$$

The $V - A$ weak current responsible for these processes is given by

$$J_\mu = (u, \quad c, \quad t)_{\;left}\, \gamma_\mu \, (V) \begin{pmatrix} d \\ s \\ b \end{pmatrix} \tag{2.3}$$

where the CKM matrix elements of (V) describe the coupling of the intermediate $W^\pm$ bosons to quarks. Thus each element in the 3×3 matrix V relates a transition between a quark of charge 2/3 with one of charge -1/3. Such an element is denoted by $V_{qq'}$ where q and q' are the quarks between which the transition takes place. The transition itself is (usually) proportional to the $|V_{qq'}|^2$ participating in the decay processes. By considering the six-quark model the V matrix is represented by:

$$(V) = \begin{pmatrix} V_{ud} & V_{us} & V_{ub} \\ V_{cd} & V_{cs} & V_{cb} \\ V_{td} & V_{ts} & V_{tb} \end{pmatrix} . \tag{2.4}$$

Sometimes one presents the weak isodoublets in the form of generations (or families). In the six- quark model for instance we have three quark generations, namely:

$$\begin{pmatrix} u \\ d \end{pmatrix}, \quad \begin{pmatrix} c \\ s \end{pmatrix}, \quad \begin{pmatrix} t \\ b \end{pmatrix} . \tag{2.5}$$

In this picture the charged current reactions will relate elements within one generation (with the largest transition rate) or elements from different generations.

The values of the CKM matrix elements (real and imaginary parts) should be obtained from measurements of decay processes (see below). One could, however, evaluate the number of independant real and imaginary parameters in a unitary $N \times N$ matrix[4]. For conveniance one introduces the imaginary parameters in the matrix through $e^{i\delta_k}$, while it is customary to use the angles θ_k (through $\cos\theta_k$ or $\sin\theta_k$) for the real parameters. The unitarity condition $VV^+ = V^+V = 1$ and the fact that the physics will not be changed if the quark fields transform as

$$| q_j > \rightarrow e^{i\phi(q_j)} \, | q_j > \tag{2.6}$$

(gauge transformation of the first kind), allowing one to determine the number of independant parameters in a $N \times N$ matrix[4,5] (see Appendix 2.A). For simplicity we will also represent equation (2.6) by $q_j \rightarrow e^{i\phi(q_j)} q_j$. Note that the phase $\phi(q_j)$ related to the q_j quark could have any value.

Let us only comment here how the transformation (2.6) allows the removal of $2N - 1$ phases from the matrix elements (hence $2N - 1$ imaginary parts from the V_{ij} elements). This can be seen by writing formula (2.2) for three generations in the following way:

$$| d' > = V_{ud} \, | d > + V_{us} \, | s > + V_{ub} \, | b > \tag{2.7a}$$

$$| s' > = V_{cd} \mid d > + V_{cs} \mid s > + V_{cb} \mid b > \tag{2.7b}$$
$$| b' > = V_{td} \mid d > + V_{ts} \mid s > + V_{tb} \mid b > \ . \tag{2.7c}$$

One can then use formula (2.6) in order to transform the $| d >$, $| s >$ and $| b >$ fields in such a way that all the V_{ij} elements in the first row will be real. A phase on $| s' >$ could then be added for introducing an additional V_{ij} real element in equation (2.7b). A similar transformation on $| b' >$ will also render a CKM matrix element real in the last row. In the present example we have reduced the number of imaginary parts in the elements of the considered matrix by 5, corresponding precisely to $2N - 1$.

The number of real (θ_k) and imaginary (δ_k) parameters of an $N \times N$ unitar matrix are derived in Appendix 2.A. One finds that the $N \times N$ matrix depends on[4]

$$\begin{aligned} &(N^2 - 3N + 2)/2 \ \text{ phases}, \\ &(N^2 - N)/2 \ \text{ angles} \ . \end{aligned} \tag{2.8}$$

The number of parameters for the following N (generation) values are then given by:

	$N=2$	$N=3$	$N=4$
$(N^2 - N)/2$ angles	1	3	5
$(N^2 - 3N + 2)/2$ phases	0	1	3

For $N = 2$, only one angle is needed (the Cabibbo type of mixing) whereas for $N > 2$, at least one phase is present. The presence of phases that render some CKM matrix elements complex is of great importance. As seen below this will be a possible source of CP violation for the B decays in the framework of the usual standard model.

2.2 - The three-generation case

In the three-generation case a representation for the mixing matrix can be obtained in the following way. Since the 3×3 matrix depends on three angles one can consider (V) as a rotation matrix with the Euler type of angles in which one has to incorporate the required phase. A possible choice would be[5]

$$(V) = \begin{pmatrix} 1 & 0 & 0 \\ 0 & c_2 & -s_2 \\ 0 & s_2 & c_2 \end{pmatrix} \begin{pmatrix} c_1 & s_1 & 0 \\ -s_1 & c_1 & 0 \\ 0 & 0 & 1 \end{pmatrix} \begin{pmatrix} 1 & 0 & 0 \\ 0 & 1 & 0 \\ 0 & 0 & -e^{i\delta} \end{pmatrix} \begin{pmatrix} 1 & 0 & 0 \\ 0 & c_3 & s_3 \\ 0 & -s_3 & c_3 \end{pmatrix}$$

($c_i \equiv \cos\theta_i,\ s_i \equiv \sin\theta_i$) where rotations are performed around three axes. With this choice one obtains precisely the mixing matrix proposed by Kobayashi and Maskawa (Ref.3), which we write in the following way:

$$(V) = \begin{pmatrix} V_{ud} = c_1 & V_{us} = s_1c_3 & V_{ub} = s_1s_3 \\ V_{cd} = -s_1c_2 & V_{cs} = c_1c_2c_3 - s_2s_3e^{i\delta} & V_{cb} = c_1c_2s_3 + s_2c_3e^{i\delta} \\ V_{td} = -s_1s_2 & V_{ts} = c_1s_2c_3 + c_2s_3e^{i\delta} & V_{tb} = c_1s_2s_3 - c_2c_3e^{i\delta} \end{pmatrix} . \quad (2.9)$$

Even here there are cases where the phase can be removed and therefore cannot generate CP violation effects. The conditions for which this can happen have been studied in detail[6] and correspond in fact to (at least) one matrix element that vanish ($V_{ij} = 0$) and/or to one of the following conditions:

1) one isospin doublet decouples from the others
2) the quark masses within one isodoublet are equal (yieldig $V_{ij} = 0$ elements)
3) two masses of the top (or bottom) quarks are equal.
4) one angle in the (V) matrix is such that $\cos\theta_i$ or $\sin\theta_i = 0$

Depending on the way we present the items, some of them are inter-dependant. Nevertheless, they give a rather clear description of the present discussion. Some examples of theses cases are discussed in Appendix 2.B while a more complete description can be found in reference (6).

It is also very conveniant to use the parametrization of Wolfenstein for the mixing matrix[7] (V). By expanding the CKM matrix to the order λ^3 where $\lambda = \sin\theta_c \sim 0.22$, θ_c being the Cabibbo angle, one has:

$$(V) = \begin{pmatrix} 1 - \frac{\lambda^2}{2} & \lambda & \lambda^3 A(\rho - i\eta) \\ -\lambda & 1 - \frac{\lambda^2}{2} & A\lambda^2 \\ \lambda^3 A(1 - \rho - i\eta) & -A\lambda^2 & 1 \end{pmatrix} + O(\lambda^4) . \quad (2.10)$$

In this approach only the V_{ub} and V_{td} elements are complex. By studying the features of the beauty hadron decay, one also uses the following crude approximation for the mixing matrix:

$$(V) = \begin{pmatrix} \sim 1 & \lambda & \sim \lambda^3 \\ -\lambda & \sim 1 & \lambda^2 \\ \sim \lambda^3 & -\lambda^2 & \sim 1 \end{pmatrix} \tag{2.11}$$

thus depending only on the parameter λ. Although approximate, this form contains some of the essential features of the mixing matrix. Indeed the transitions within one generation are dominant as

$$V_{tb} \sim V_{cs} \sim V_{ud} \sim 1 \tag{2.12a}$$

whereas the jumps between generations are described by:

$$\mid V_{cd} \mid = \mid V_{us} \mid \sim \lambda; \quad \mid V_{cb} \mid = \mid V_{ts} \mid \sim \lambda^2; \quad \mid V_{td} \mid = \mid V_{ub} \mid \sim \lambda^3. \tag{2.12b}$$

as visualized by Fig. 2.1. The fact that some jumps between generations are more probable than others is in agreement with the experimental data. We will often use this simplified form for the matrix elements whenever we discuss the tendancies of quark decays and mixing phenomena (Chapter 3).

2.3 - Some physics properties due to the CKM matrix

As we already mentioned above, the physics will not change if the quark field $q_j \rightarrow e^{i\phi(q_j)} q_j$. This means that the up (u, c, t) and down (d, s, b) quark fields can be transformed as

$$\begin{pmatrix} u \\ c \\ t \end{pmatrix} \Longrightarrow \begin{pmatrix} e^{i\phi(u)} & 0 & 0 \\ 0 & e^{i\phi(c)} & 0 \\ 0 & 0 & e^{i\phi(d)} \end{pmatrix} \begin{pmatrix} u \\ c \\ t \end{pmatrix} \tag{2.13a}$$

and

$$\begin{pmatrix} d \\ s \\ b \end{pmatrix} \Longrightarrow \begin{pmatrix} e^{i\phi(d)} & 0 & 0 \\ 0 & e^{i\phi(s)} & 0 \\ 0 & 0 & e^{i\phi(b)} \end{pmatrix} \begin{pmatrix} d \\ s \\ b \end{pmatrix} . \tag{2.13b}$$

In the weak current J_μ, responsible of the decay process [formula (2.3)], the above transformations of the quark field would be equivalent to the change of the CKM matrix, $(V) \Longrightarrow (V')$ where

$$(V') = \begin{pmatrix} e^{-i\phi(u)} & 0 & 0 \\ 0 & e^{-i\phi(c)} & 0 \\ 0 & 0 & e^{-i\phi(t)} \end{pmatrix} \begin{pmatrix} V_{ud} & V_{us} & V_{ub} \\ V_{cd} & V_{cs} & V_{cb} \\ V_{td} & Vts & V_{tb} \end{pmatrix} \begin{pmatrix} e^{i\phi(d)} & 0 & 0 \\ 0 & e^{i\phi(s)} & 0 \\ 0 & 0 & e^{i\phi(b)} \end{pmatrix}$$

yield

$$(V') = \begin{pmatrix} U_u^* V_{ud} D_d & U_u^* V_{us} D_s & U_u^* V_{ub} D_b \\ U_c^* V_{cd} D_d & U_c^* V_{cs} D_s & U_c^* V_{cb} D_b \\ U_t^* V_{td} D_d & U_t^* Vts D_s & U_t^* V_{tb} D_b \end{pmatrix} . \tag{2.14}$$

Here $U_k = e^{i\phi(k)}$ with $k = u, c, t$ and $D_j = e^{i\phi(j)}$ with $j = d, s, b$ represent the contributions of the phases on the up and down quark fields, respectively.

Based on our previous statement, the physics should be identical by using the (V) or $(V') = (U^+ V D)$ matrices. What then are the expressions containing V_{ij} elements which can obey this rule? In fact, there are essentially two possibilities,

- any expression containing modulus of CKM matrix elements as $|U_i^* V_{ik} D_k| = |V_{ik}|$
- any expression containing four matrix elements in the following way, $(V_{ai} V_{aj}^* V_{bj} V_{bi}^*)$ for $a \neq b$ and $i \neq j$.

In the latter case, the expression has a combination of four elements forming a square or a rectangle in the matrix as shown in Fig. 2.2. This cancels the phases due to the U_j^* and D_k functions in the expression $(V'_{ai} V'^*_{aj} V'_{bj} V'^*_{bi})$, hence

$$V'_{ai} V'^*_{aj} V'_{bj} V'^*_{bi} = V_{ai} V^*_{aj} V_{bj} V^*_{bi} .$$

For three generations the expression $Im(V_{ai} V^*_{aj} V_{bj} V^*_{bi})$ has an additionnal property. This can be seen by using the unitary properties of (V) yielding

$$\sum_{k=1}^{3} V_{ik} V^*_{jk} = 0 , \quad \sum_{k=1}^{3} V_{ki} V^*_{kj} = 0 \quad \text{with } i \neq j .$$

These equations represent the product of one row (column) with another complex conjugated row (column) of the CKM matrix. Each of these six expressions can be represented by a triangle in the complex plane where each side of the triangle is given by $V_{ik} V^*_{jk}$ (or $V_{ki} V^*_{kj}$). Two examples are shown in Fig. 2.3.

In order to define the property arising from the three-generation case, let us take the example,

$$V_{ud}\ V_{ub}^* + V_{cd}\ V_{cb}^* + V_{td}\ V_{tb}^* = 0 \tag{2.15}$$

corresponding to the product of the first and third column of the CKM matrix (the lowest triangle in Fig. 2.3). By taking the imaginary part of this expression, previously multiplied by $V_{ud}^* V_{uc}$ [the complex conjugate of the first term of (2.15)], one obtains

$$\begin{aligned} Im\ [V_{ub}V_{ud}^*V_{cd}V_{cb}^*] &= -Im\ [V_{ub}V_{ud}^*V_{td}V_{tb}^*] \\ &= Im\ [V_{ud}V_{ub}^*V_{tb}V_{td}^*]\ . \end{aligned}$$

In the same way, one can multiply expression (2.15) by the complex conjugate of the second (or third) term, subsequently taking the imaginary part of the equation. One then finds that $|Im(V_{i1}V_{j3}^*V_{j1}^*V_{i3}^*|$ has the same value for any square or rectangle constucted from elements of the two considered rows in the way indicated in Fig. 2.4 [the multiplication of (2.15) by $V_{tb}V_{td}^*$ gives the same result but is not shown in the figure].

As a square or a rectangle of four elements can occur by a product of columns or rows, one easily obtain the general relation[8]:

$$Im\ [V_{Ai}V_{Aj}^*V_{Bj}V_{Bi}^*] = \pm K \tag{2.16}$$

where K simply denotes the absolute value of these products. This absolute value represents twice the area (A) of a triangle. To clarify this point, let us continue to consider the triangle described by (2.15) shown in Fig. 2.3. In this case one has

$$\begin{aligned} |Im\ [V_{ub}V_{ud}^*\ V_{cd}V_{cb}^*| &= |V_{ub}V_{ud}^*| \times |V_{cd}V_{cb}^*|\ \sin\phi_3 \\ &= 2A \end{aligned} \tag{2.17}$$

ϕ_3 being the angle between the $|V_{ub}V_{ud}^*|$ and $|V_{cd}V_{cb}^*|$ sides of the triangle (Fig. 2.3). Therefore, $|Im\ [V_{ub}V_{ud}^*\ V_{cd}V_{cb}^*|$ represents twice the area A of this triangle. Because of formula (2.16), one concludes that all six triangles built because of the unitarity of the (V) matrix will have the same area. Clearly, if the CKM matrix elements are all real the triangles will collapse into straight lines in the complex plane.

Let us now write the equations defining the six triangles in the complex planes explicitely. Below each side we indicate its length by using the crude approximation of the matrix elements given by formula (2.11). One has then:

$$V_{ud}V_{us}^* + V_{cd}V_{cs}^* + V_{td}V_{ts}^* = 0 \qquad (2.18a)$$
$$\sim\lambda \qquad \sim\lambda \qquad \sim\lambda^5$$
$$V_{ud}V_{ub}^* + V_{cd}V_{cb}^* + V_{td}V_{tb}^* = 0 \qquad (2.18b)$$
$$\sim\lambda^3 \qquad \sim\lambda^3 \qquad \sim\lambda^3$$
$$V_{us}V_{ub}^* + V_{cs}V_{cb}^* + V_{ts}V_{tb}^* = 0 \qquad (2.18c)$$
$$\sim\lambda^4 \qquad \sim\lambda^2 \qquad \sim\lambda^2$$
$$V_{ud}V_{cd}^* + V_{us}V_{cs}^* + V_{ub}V_{cb}^* = 0 \qquad (2.18d)$$
$$\sim\lambda \qquad \sim\lambda \qquad \sim\lambda^5$$
$$V_{ud}V_{td}^* + V_{us}V_{ts}^* + V_{ub}V_{tb}^* = 0 \qquad (2.18e)$$
$$\sim\lambda^3 \qquad \sim\lambda^3 \qquad \sim\lambda^3$$
$$V_{cd}V_{td}^* + V_{cs}V_{ts}^* + V_{cb}V_{tb}^* = 0 \qquad (2.18f)$$
$$\sim\lambda^4 \qquad \sim\lambda^2 \qquad \sim\lambda^2$$

One sees that the sides of two triangles [(2.18b) and (2.18e)] have comparable lengths while the others have one side much shorter that the two other lengths. The latter cases could not be used easily for proving the existence of such triangles as the modulus of some CKM matrix elements would have to be known with great accuracy. On the other hand the determination of CKM matrix elements from experimental data may be model dependent. The verification of equation (2.18e), yielding sides of comparable size requires the knowledge about the decays of hadrons containing a t quark. The triangle defined by equation (2.18b), however, could be investigated with the actual or near-future experiments (Chapter 4). In this case one will try to measure the angles between the sides of the triangle in order to prove the complex part of some V_{ij} elements.

Additional comments

Hereafter, we will very often use the Wolfenstein parametrization, where only V_{ub} and V_{td} are complex. Other choices of complex elements are possible, as only products of the $[V_{Ai}V_{Bj}V_{Aj}^*V_{Bi}^*]$ type can enter in the description of the decay mechanism. Note, however, that there must be more than two complex elements (at least three appearing in different columns and rows) in the CKM matrix (even if the imaginary part of some of them is negligible) in order to build the triangles in the complex plane so that they have the same area.

2.4 - B meson decays

The quark decay diagrams which may contribute to the B decay are shown in Fig. 2.5. Clearly additional $q\bar{q}$ pairs can be extracted from the sea in such a way that several hadrons will be present in the final state. The first graph is the so called spectator or tree diagram, in which the lighter quark does not participate in the decay process. Lepton-neutrino pairs and hadrons (semileptonic decays) or only hadrons can be produced by this graph. It is believed to give the largest contribution to the B decay process[9–11]. The graph (b) contributes to the production of $q\overline{q}$. Graph (c) with W exchange in the t channel (and the emission of a gluon) can only operate for neutral B, whereas W exchange in the s-channel, graph (d), applies only to charged B. Finally, the penguin type of diagram, graph (e), can contribute to both charged and neutral B decays.

Although the spectator diagram is supposed to give the dominant contribution for the B decay the presence of the other graphs is important in the context of CP violation. As we will see in Chapter 4, interferences between different decay mechanisms can genereate CP violation effects. Nevertheless, for comparing or estimating decay widths we will use the spectator model. In this approach the various b decay widths are given by[10,11]:

$$\Gamma(b \rightarrow q, l^- \nu) = \frac{G_F^2 m_b^5}{192\pi^3} |V_{bq}|^2 F_l \tag{2.19a}$$

$$\Gamma(b \rightarrow q, q_j \overline{q}'_j) = \frac{G_F^2 m_b^5}{192\pi^3} |V_{bq}|^2 F_j \times 3 |V_{q_j q'_j}|^2 \tag{2.19b}$$

where G_F is the Fermi coupling constant and m_b is the b quark mass. Here $F_{j,l}$ is a phase space factor depending on the ratios of the masses involved in the decay[12]. Note that the factor 3 appearing in the second expression is due to the fact that the qq' color singlet appearing in the $W \rightarrow qq'$ can be formed by quarks of three colors. The essential result which we will use in the following is that the total width of the B meson can be approximated by the sum of (2.19a) and (2.19b) and represented by:

$$\Gamma_t(b) = \Sigma_q \Gamma(b \rightarrow qW) \tag{2.20}$$

taking into account the $b \rightarrow cW$ and $b \rightarrow uW$ processes. This relation (which is proportional to $m_b^5 |V_{bq}|^2$) would lead to the same lifetime for the B mesons (B^+, B_d^0, B_s^0). Recent experimental data indicate that the lifetime of B_d^0 and B_s^0 are close to each other ($\sim$ 1.5 ps) thus justifying the above approximation.

For the semileptonic decay of the B mesons, the spectator diagram is considered to be responsible for this process [formula (2.19a)]. This leads to the equality of the semileptonic widths of the b and $\overline{b}$ quarks,

$$\Gamma(b \rightarrow q, l^- \nu) = \overline{\Gamma}(\overline{b} \rightarrow \overline{q}, l^+ \nu) \ . \tag{2.21}$$

meaning that no CP violation effects are expected in the B semileptonic decay.

This fact is of great importance for the tagging procedure needed to search for CP violation in the (non-semileptonic) B decay which will be discussed in Chapters 4 and 5.

Remarks about CKM values

Before discussing some features of the B decay related to the CKM matrix elements, let us recall some of the estimated values of CKM matrix elements obtained from the studies of decay processes. From the β decays, it was found that

$$|V_{ud}| \simeq 1 - \frac{\lambda^2}{2} = 0.9744 \pm 0.0010$$

while the hyperon and $K \to \pi e \nu$ decays give[13]

$$|V_{us}| = \lambda = 0.2205 \pm 0.0018 \ .$$

The information about V_{ub} and V_{cb} was obtained from the B decays. The study of the semileptonic decay of the B mesons can give estimates of the $|V_{ub}/V_{cb}|$ ratio, for instance, from the lepton momentum distribution due due to $b \to cl\nu$ and $b \to ul\nu$ processes. Although these estimates are model-dependent, the various analyses give $|V_{ub}/V_{cb}| = 0.08 \pm 0.02$ (Ref. 13). The parameter A in the Wolfenstein parametrization can be obtained from $|V_{cb}|^2$, that is related to the B lifetime yielding[13,14]

$$|V_{cb}| = 0.044 \pm 0.06, \quad \text{hence} \quad A = 0.90 \pm 0.12 \ .$$

The estimate of the $|V_{ub}/V_{bc}|$ ratio gives

$$\sqrt{\rho^2 + \eta^2} = 0.36 \pm 0.09$$

[see expression (2.10)]. The values of ρ and η depend on several parameters (for instance the mass of the top quark) as discussed in reference (14).

Summarizing this chapter, we can say that we have briefly discussed some properties related to the CKM matrix elements and hence to the weak decay of the B mesons. The features presented in Sections 2.1 to 2.3 are some of the ingredients required for the next chapters. We are now able to discuss the $B^0 \leftrightarrow \overline{B}^0$ mixing and CP violations in the the decay of the B system.

Appendix 2.A

Number of parameters in the CKM matrix

Let us consider an $N \times N$ unitarity matrix (N generations) and determine the number of parameter this matrix can depend on. In principle, a complex $N \times N$ matrix depends on $2 \times N^2$ parameters. The unitary condition

$$V\,V^{+} = V^{+}\,V = \begin{pmatrix} 1 & & & 0 \\ & \cdot & & \\ & & \cdot & \\ 0 & & & 1 \end{pmatrix}$$

introduces constraint yielding to a decrease in the number of parameters. Above and below the diagonal of this matrix the elements vanish whereas the diagonal elements are equal to one. Therefore, there are $(N^2 - N)/2$ independant non-diagonal elements where the real and imaginary parts have to equal zero. One has then

$$2\,[\frac{N^2 - N}{2}] \; + N = \; N^2 \quad \text{constraints}$$

from which one finds that a unitar matrix has $2N^2 \; - \; N^2 \; = \; N^2$ independant parameters.

The number of imaginary parameters is simply given by the difference between the total number of parameters of an unitary matrix and an orthogonal $N \times N$ matrix (having only real parameters). In the same manner as above, one finds that an orthogonal matrix will have

$$\frac{N^2 - N}{2} + N = \frac{N^2 + N}{2} \quad \text{constraints and}$$

$$N^2 - \frac{(N^2 + N)}{2} = \frac{N^2 - N}{2} \quad \text{real parameters} \; .$$

The number of imaginary parameters in the unitary matrix will then be given by

$$N^2 - \frac{N^2 - N}{2} = \frac{N^2 + N}{2} \; .$$

The physics will not be changed if the quark fields transform as $q_j \to exp(i\phi_j)q_j$. By redefining the phases of the quark fields, one can remove $2N - 1$ phases (an overall phase remains). One thus finally obtain an unitary $N \times N$ matrix depending on

$$\frac{N^2+N}{2} - (2N-1) = \frac{1}{2}\left(N^2 - 3N + 2\right) \text{ phases} \tag{2.A1}$$

$$\text{and } \frac{N^2-N}{2} \text{ angles} \tag{2.A2}$$

Appendix 2.B

Examples of the phase elimination in the CKM matrix
a) Decoupling of a quark isodoublet

Let us first give a simple example where we assume that one family decouples from the other two (no transition between the members of one family and those of the other two). In this case only two families communicate, we should be in the Cabibbo mixing case (no phase).

Let us show this explicitely by assuming for instance that the (u, d) generation decouples from the other ones. Then one has ($c_1 = 1$):

$$\begin{pmatrix} d' \\ s' \\ b' \end{pmatrix} = \begin{pmatrix} 1 & 0 & 0 \\ 0 & c_2c_3 - s_2s_3e^{i\delta} & c_2s_3 + s_2c_3e^{i\delta} \\ 0 & s_2c_3 + c_2s_3e^{i\delta} & s_2s_3 - c_2c_3e^{i\delta} \end{pmatrix} \begin{pmatrix} d \\ s \\ b \end{pmatrix}$$

which can also be written in the following form:

$$\begin{aligned} &\mid d' > = \mid d > \\ &\mid s' > = (c_2c_3 - s_2s_3e^{i\delta}) \mid s > + (c_2s_3 + s_2c_3e^{i\delta}) \mid b > \\ &\mid b' > = (s_2c_3 + c_2s_3e^{i\delta}) \mid s > + (s_2s_3 - c_2c_3e^{i\delta}) \mid b > \ . \end{aligned}$$

Let us now change the phase of $\mid s >$ in the following way:

$$\mid s > \rightarrow \mid s > e^{-i\delta}$$

and define

$$A = c_2 c_3 e^{-i\delta} - s_2 s_3$$
$$B = c_2 s_3 + s_2 s_3 e^{i\delta}$$

their moduli being denoted by $\overline{A}$ and $\overline{B}$. One then obtains

$$| s' > = A \mid s > + B \mid b >$$
$$| b' > = B^* \mid s > - A^* \mid b >$$

Defining the phases of A and B by φ_1 and φ_2, one can write the last two expressions as

$$e^{-i\varphi_2} \mid s' > = \overline{A} e^{i(\varphi_1 - \varphi_2)} \mid s > + \overline{B} \mid b >$$
$$e^{+i\varphi_1} \mid b' > = \overline{B} e^{i(\varphi_1 - \varphi_2)} \mid s > - \overline{A} \mid b > \quad .$$

Further phase transformations

$$| s > \rightarrow e^{i(\varphi_1 - \varphi_2)} \mid s >$$
$$| s' > \rightarrow e^{-i\varphi_2} \mid s' >$$
$$| b' > \rightarrow e^{+i\varphi_1} \mid b' >$$

finally yield

$$| s' > = \overline{A} \mid s > + \overline{B} \mid b >$$
$$| b' > = \overline{B} \mid s > - \overline{A} \mid b >$$

which is indeed a Cabibbo type of mixing (no phase).

In a more general approach it has been shown[5] that the phase can be be removed in the three-generation case if a pair of quarks of the same charge have identical masses (the quarks will then be indistinguishable as far as weak interactions are concerned or if a $V_{qq'}$ matrix element vanishes). For the CKM matrix all the conditions required for CP violation through the phase δ can be put into one equation in the following way[5]:

$$D = s_1^2 \; s_2 \; s_3 \; c_1 \; c_2 \; c_3 \; \sin\delta \; J \neq 0$$

with

$$J = (m_u - m_c)(m_c - m_t)(m_u - m_t)(m_d - m_s)(m_s - m_b)(m_b - m_d)$$

(m_q denoting the mass of the quark q). This equation covers 14 different conditions.

b) Example of a vanishing cosine value

Let us now take the example of an angle leading to a zero value of its cosine, for instance $\theta_2 = \pi/2$ yielding $\cos\theta_2 \equiv c_2 = 0$ and $\sin\theta_2 = 1$. In this case the relations between the d', s', b' and the s, d, b quarks will be given by

$$\begin{pmatrix} d' \\ s' \\ b' \end{pmatrix} = \begin{pmatrix} c_1 & s_1 c_3 & s_1 s_3 \\ 0 & -s_3 e^{i\delta} & c_3 e^{i\delta} \\ -s_1 & c_1 c_3 & c_1 s_3 \end{pmatrix} \begin{pmatrix} d \\ s \\ b \end{pmatrix}$$

or by the expressions

$$\begin{aligned} | d' > &= c_1 \mid d > + s_1 c_3 \mid s > + s_1 s_3 \mid b > \\ | s' > &= -s_3 e^{i\delta} \mid s > + c_3 e^{i\delta} \mid b > \\ | b' > &= -s_1 \mid d > + c_1 c_3 \mid s > + c_1 s_3 \mid b > \ . \end{aligned}$$

The phase δ will diseappear by doing the transformation

$$| s' > \rightarrow | s' > \ e^{-i\delta} \ .$$

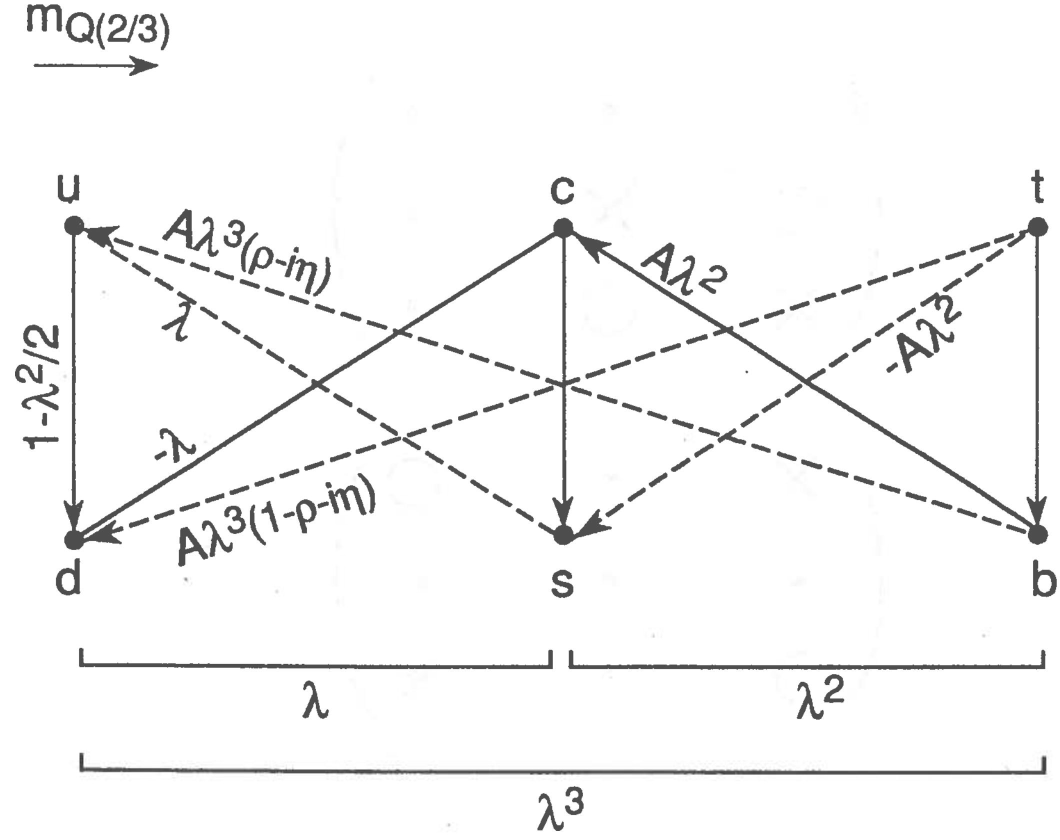

Fig. 2.1 - Various transitions between the three quark generations with the corresponding CKM matrix elements in the Wolfenstein parametrization. In our simplified version, the transitions depend essentially on one parameter λ.

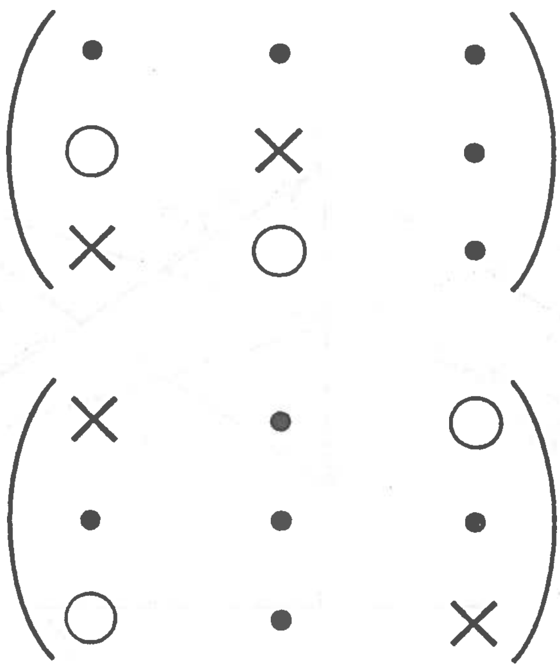

Fig. 2.2 - The $\circ$ and the $\times$ represent the matrix elements entering into the $V_{ai}V_{bj}V^*_{aj}V^*_{bi}$ products. These terms are independant of the $q_j \rightarrow exp[i\phi(q_j)]q_j$ transformation. The circle sign represents a matrix element while the cross indicates the complex conjugate of the considered element.

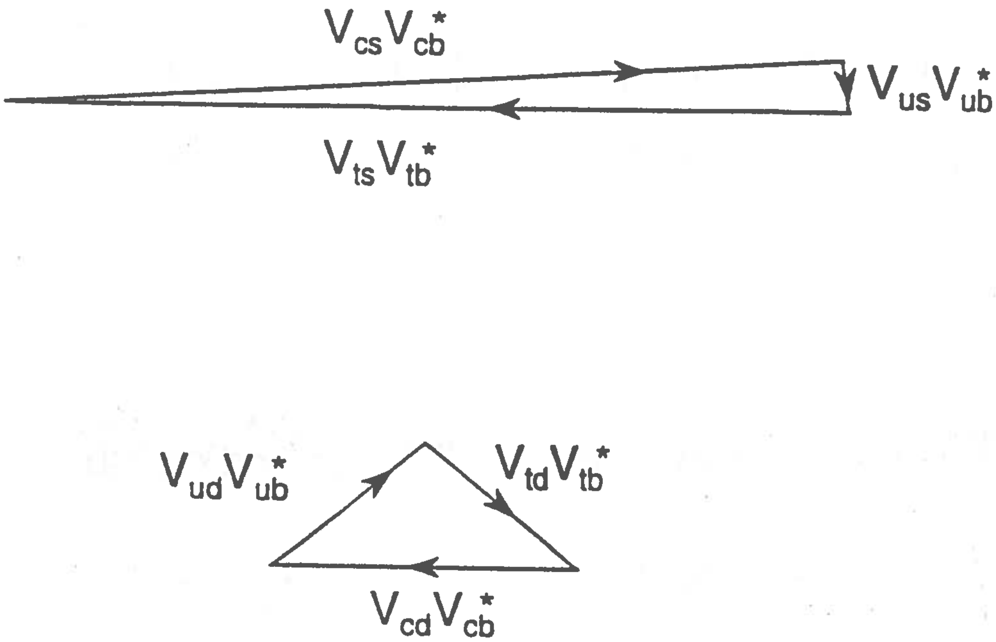

Fig. 2.3 - Examples of two triangles in the complex planes and having the same areas. The top triangle represents equation (2.18c) and the bottom one equation (2.18b).

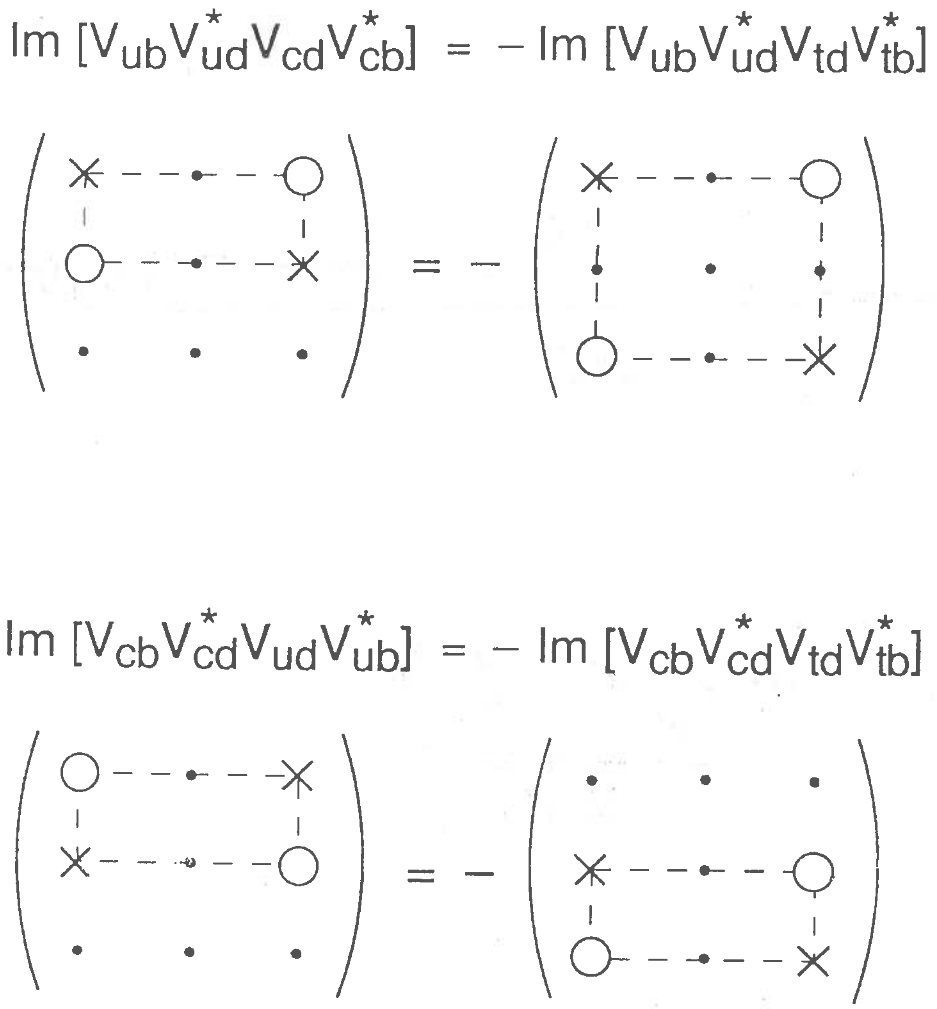

Fig. 2.4 - CKM elements forming a square or a rectangle in the matrix and obtained by multiplying the first and the third column as explained in the text. The $\circ$ and the $\times$ represent elements or complex ones, respectively. The expression $|Im(V_{ai}V_{bj}V^*_{aj}V^*_{bi})|$ has the same value in all cases (Section 2.3).

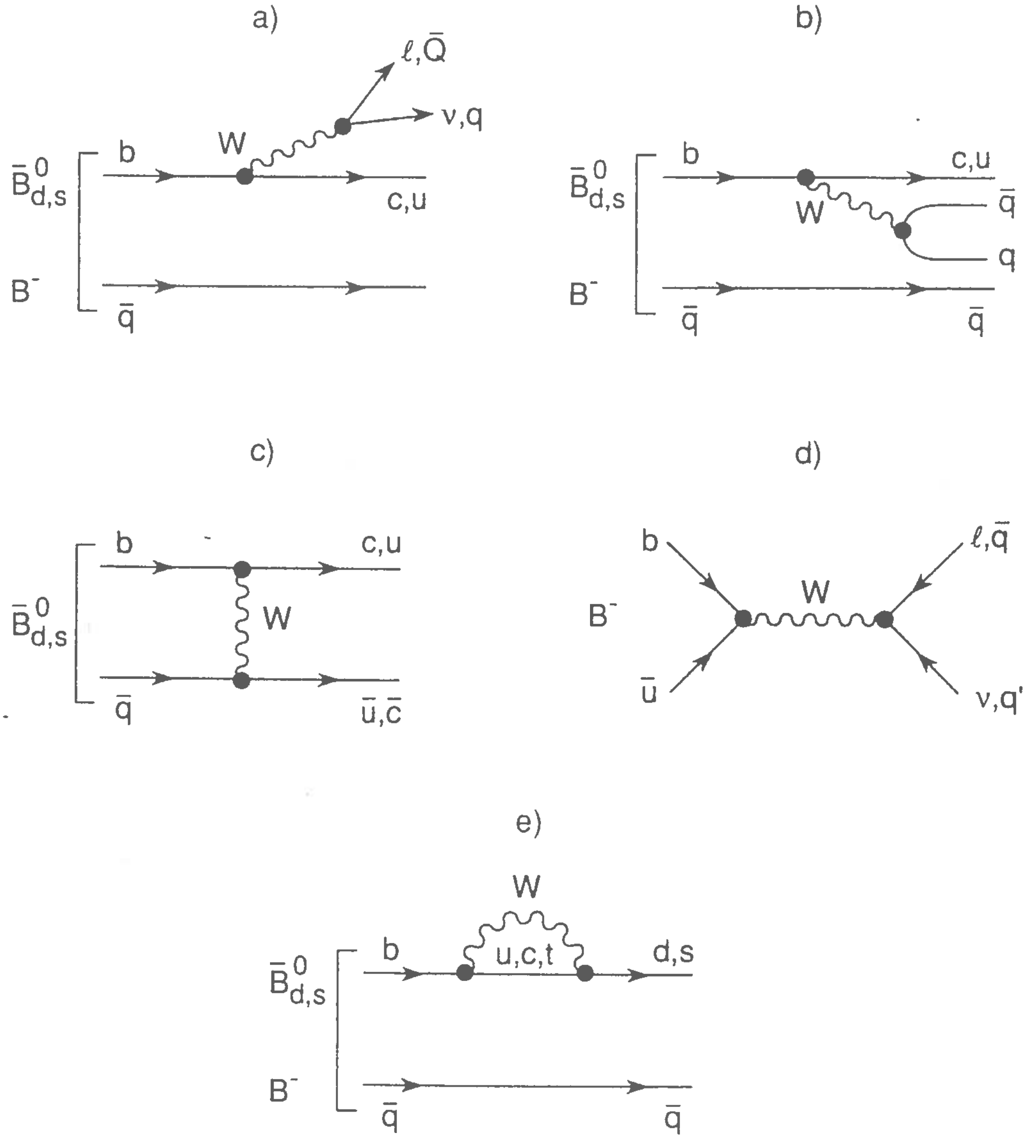

Fig. 2.5 - The quark diagrams contributing to the decay of the $\overline{B}$ mesons (B are not shown). Additionnal $q\bar{q}$ can be extracted from the sea leading to final states with several hadrons.

3 - Meson mixing

3.1 - Introduction

As in the case of $K^0, \overline{K}^0$, mixing is expected to manifest itself for the $B^0, \overline{B}^0$ mesons. In fact, the $B_d^0 \leftrightarrow B_d^0$ mixing (or oscillations) has been observed in producing the B_d^0 and $\overline{B}_d^0$ mesons in different ways,

$$\begin{aligned} e^+e^- &\rightarrow \Upsilon(4S) \rightarrow B_d^0\overline{B}_d^0 \\ pN &\rightarrow B_d^0(\overline{B}_d^0)X \\ e^+e^- &\rightarrow Z^0 \rightarrow B_d^0(\overline{B}_d^0)X \ . \end{aligned}$$

The study of the mixing in the first case is different from the other ones. In the $\Upsilon(4S)$ decay the c.m. energy is just enough to produce a $B\overline{B}$ pair (no additionnal π). Therefore, to fullfil the $J^{PC} = 1^{--}$ conditions due to the $\Upsilon(4S)$, the relative orbital momentum between the two outgoing mesons has to be $l = 1$. As already mentioned in Section 1.1, such a value will not be compatible with the Bose-Einstein statistics requirement for a $B_d^0 B_d^0$ or a $\overline{B}_d^0\overline{B}_d^0$ system (as the wave function describing the final state cannot be even under the permutation of the two mesons). Thus, a mixing procedure only occurs in the first case if the associated meson has decayed first. Note that the observation of the $B_d^0 \rightarrow f$ ($\overline{B}_d^0 \rightarrow \overline{f}$) decay does not give any information about the type of meson produced at time $t = 0$ that was responsible for the observed decay. The tagging of the associated beauty hadron is then necessary and is treated in more detail below.

In the other two cases the situation is somewhat different. The associated beauty hadron could be a neutral or a charged meson or even a beauty baryon. As above, the information about the type of the associated meson produced in the same event is necessary and will be obtained by the tagging procedure.

Before discussing the methods used to measure mixing, we will give a brief description of the formalism used to describe the mixing phenomenon in the B system (Section 3.2 and 3.3). Next we will briefly discuss some results obtained from theoretical investigations and their impact on the analysis of experimental results (Section 3.4). Then we will consider the measurement possibilities of the mixing process, with the observation of time oscilattions (Section 3.5) and B^0 semileptonic decay (Section 3.6). Furthermore, we will discuss the case of the beauty hadrons produced in pN interactions. For comparison we will also present some features related to the $e^+e^- \rightarrow \Upsilon(nS) \rightarrow B^0\overline{B}^0$ ($n = 4,5$). taking into account the correlation introduced by the Bose-Einstein statistics requirement.

3.2 - Basic formalism

Let us recall that by mixing or oscillations we mean transitions of the type of $B^0 \leftrightarrow \overline{B}^0$. These transitions have been widely discussed[1-3] and result from flavor non-conservation in weak interactions. Fig. 3.1 presents the box diagrams which are believed to be responsible for the mixing in the B^0 system. Whenever we use B^0 ($\overline{B}^0$), we mean that the expressions and formula can be used for the B^0_d ($\overline{B}^0_d$) or B^0_s ($\overline{B}^0_s$) mesons.

Because of the $B^0 \leftrightarrow \overline{B}^0$ transitions, the $\mid B^0 >$ and $\mid \overline{B}^0 >$ states are no longer the physical states. Thus they are not the eigenvectors of the Hamiltonian (H) considered to be made from a strong and a weak interaction part. This phenomenological Hamiltonian will be represented by a 2×2 matrix in the $\mid B^0 >$ and $\mid \overline{B}^0 >$ space (the flavor space).

In order to describe the decay of particles one writes[4]:

$$(H) = (M) - \frac{i}{2}(\Gamma)$$

where (M) and (Γ) are the mass and the decay matrices, respectively. Note that here (H) is not hermitian, the eigenvalues are not real and the eigenvectors do not need to be orthogonal, in contrast to (M) and (Γ), which are associated with measurable quantities. The hermiticity of (M) and (Γ) leads to the following relations between the matrix elements: $H_{12} = M_{12} - i\Gamma_{12}/2$ and $H_{21} = M_{21} - i\Gamma_{21}/2$ namely

$$H_{21} = M^*_{12} - \frac{i}{2}\Gamma^*_{12}$$

Moreover, the CPT theorem yields $H_{11} = H_{22}$. One can thus write:

$$(H) = \begin{pmatrix} M - i\Gamma/2 & M_{12} - i\Gamma_{12}/2 \\ M^*_{12} - i\Gamma^*_{12}/2 & M - i\Gamma/2 \end{pmatrix} .$$

The matrix elements represent transition amplitudes and are given by[2,5]:

$$< B^0 \mid H \mid B^0 > = < \overline{B}^0 \mid H \mid \overline{B}^0 > = M - i\Gamma/2 \tag{3.1a}$$
$$< \overline{B}^0 \mid H \mid B^0 > = M_{12}^* - i\Gamma_{12}^*/2 \tag{3.1b}$$
$$< B^0 \mid H \mid \overline{B}^0 > = M_{12} - i\Gamma_{12}/2 \ . \tag{3.1c}$$

The last two equations relate the $B^0 \leftrightarrow \overline{B}^0$ transitions (the mixing phenomenon) to the elements of the mass and the decay matrices. One already sees that CP violation can occur in the $B^0 \leftrightarrow \overline{B}^0$ mixing if the the non diagonal elements are complex quantities (a necessary but not a sufficiant condition) or more precisely if:

$$|< B^0 \mid H \mid \overline{B}^0 >|^2 - |< \overline{B}^0 \mid H \mid B^0 >|^2 = 2Im(M_{12}^* \Gamma_{12}) \neq 0 \ . \tag{3.1d}$$

The physical states $\mid B_l > \equiv \mid B_1 >$ and $\mid B_h > \equiv \mid B_2 >$ where l (h) stands here for light (heavy) are obtained by diagonalizing (H). Eigenvalues $\mu_\pm$ are obtained from

$$Det \mid H - \mu I \mid = 0$$

(I is the unit 2×2 unit matrix) yielding:

$$(M - i\frac{\Gamma}{2} - \mu)^2 - (M_{12} - i\frac{\Gamma_{12}}{2})\ (M_{12}^* - i\frac{\Gamma_{12}^*}{2}) = 0$$

and

$$\mu_\pm = M - i\frac{\Gamma}{2} \pm Q$$
$$\Delta\mu = \mu_+ - \mu_- = 2Q$$

with

$$Q = \sqrt{(M_{12} - i\Gamma_{12}/2)(M_{12}^* - i\Gamma_{12}^*/2)} \ .$$

The masses $M_{l,h} \equiv M_{1,2}$ and widths $\Gamma_{l,h} \equiv \Gamma_{1,2}$ of the physical states $\mid B_{l,h} >$ are then given by:

$$M_{h,l} = Re\ \mu_\pm = M \pm Re\ Q$$
$$\Gamma_{h,l} = -2Im\ \mu_\pm = \Gamma \mp 2Im\ Q$$

One obtains thus the following relations which will be used throughout:

$$\boxed{\begin{aligned} &\Delta M = M_h - M_l = 2ReQ \\ &\Delta\mu = \mu_+ - \mu_- = 2Q \\ &\Delta\Gamma = \Gamma_h - \Gamma_l = -4ImQ \\ &Q = \sqrt{(M_{12}^* - i\Gamma_{12}^*/2)(M_{12} - i\Gamma_{12}/2)} \\ &Q = (\Delta M - i\Delta\Gamma/2)/2 \\ &\Gamma = (\Gamma_h + \Gamma_l)/2 \end{aligned}} \quad . \tag{3.2}$$

We will see later (Section 3.4) that for the B^0 mesons, $\Delta\mu = 2Q$ will practically be equal to $\Delta M = 2ReQ$, as Q can be approximated by $Q = |M_{12}|$. This will simplify the calculations of the B^0 mixing processes.

Using the $\mu_\pm$ eigenvalues, one finds that the eigenvectors can be expressed in the form (see Appendix 3.A):

$$\begin{aligned} &| B_1 >= p \mid B^0 > +q \mid \overline{B}^0 > \\ &| B_2 >= p \mid B^0 > -q \mid \overline{B}^0 > \quad . \end{aligned} \tag{3.3}$$

From the eigenvector equations

$$(H - \mu I) \begin{pmatrix} p \\ \pm q \end{pmatrix} = 0$$

one obtains

$$\frac{q}{p} \equiv \eta = \frac{-Q}{M_{12} - i\Gamma_{12}/2} = \pm \left| \frac{M_{12}^* - i\Gamma_{12}^*/2}{M_{12} - i\Gamma_{12}/2} \right|^{1/2} \tag{3.4}$$

where we will use the plus sign. One has also:

$$|\eta|^2 = \left| \frac{M_{12}^* - i\Gamma_{12}^*/2}{M_{12} - i\Gamma_{12}/2} \right| \tag{3.5}$$

where for conveniance we now use the symbol $\eta \equiv q/p$. Let us repeat here (see Section 3.4) that if M_{12} and Γ_{12} are real, or more precisely if $Im(M_{12}^*\Gamma_{12}) = 0$, there will be no CP violation in the $B^0 \leftrightarrow \overline{B}^0$ transitions [see equations (3.1b), (3.1c) and (3.1d)]. One has then $|\eta|^2 = 1$. Thus the departure of $|\eta|$ from 1 will indicate CP violations in the $B^0 \leftrightarrow \overline{B}^0$ transition.

As already stated above, the $| B_1 >$ and $| B_2 >$ states do not need to be orthogonal. A simple calculation gives :

$$< B_1 \mid B_2 > = \frac{1-|\eta|^2}{1+|\eta|^2} = \frac{2Im(M_{12}^*\Gamma_{12}/2)}{|M_{12}|^2 + |\Gamma_{12}/2|^2 + |Q|^2} .$$

Thus it is only in the absence of CP violation in the $B^0 \leftrightarrow \overline{B}^0$ mixing that the states $| B_1 >$ and $| B_2 >$ become orthogonal.

Even if $|\eta| = 1$, η can have a phase. In fact this phase is related to the particle phase δ defined in the following way. The $| B^0 >$ and $| \overline{B}^0 >$ states are related through CP transformation up to an arbitrary and non measurable phase[6,7] δ (usually called the particle phase). Thus one has

$$CP \mid B^0 >= e^{i\delta} \mid \overline{B}^0 >$$

and hence necessarily

$$CP \mid \overline{B}^0 >= e^{-i\delta} \mid B^0 >$$

as $(CP)^2 = 1$. Before choosing a convention for defining δ, let us give the relation between the phase of η and δ when there is no CP violation in the mixing process. Then the physical states $| B_{1,2} >$ must be eigenstates of CP. Using (3.3) one has[8]:

$$CP \mid B_1 > = pe^{i\delta} \mid \overline{B}^0 > + qe^{-i\delta} \mid B^0 >= \pm\Big(p \mid B^0 > + q \mid \overline{B}^0 >\Big)$$
$$CP \mid B_2 > = pe^{i\delta} \mid \overline{B}^0 > - qe^{-i\delta} \mid B^0 >= \mp\Big(p \mid B^0 > - q \mid \overline{B}^0 >\Big) .$$

This can only occur when

$$\frac{q}{p} \equiv \eta = \pm e^{i\delta} . \qquad (3.6)$$

If one choose a phase δ such that:

$$CP \mid B^0 >= - \mid \overline{B}^0 > \qquad (3.7a)$$

$$CP \mid \overline{B}^0 >= - \mid B^0 > \tag{3.7b}$$

one obtains that $\eta = q/p$ will then be real if there is no CP violation in the $B^0 \leftrightarrow \overline{B}^0$ mixing.

3.3 - Time dependence and mixing

Let us now investigate the time evolution of the state $\mid B^0(t) >$ (or $\mid \overline{B}^0(t) >$) where a pure $\mid B^0 >$ (or $\mid \overline{B}^0 >$) state has been produced at the time $t = 0$. To simplify our discussion we will first consider the (unrealistic) cases of having B^0 or $\overline{B}^0$ beams. We notice again that there are the physical states $|B_{1,2} >$, which have definite lifetimes. This means that the time evolution of the states $\mid B_{1,2}(t) >$ are simply given by:

$$\mid B_{1,2}(t) >=\mid B_{1,2} > e^{-i(M_{1,2}-i\Gamma_{1,2}/2)t}$$

With this expression and formula (3.3), one easily obtains (see the demonstrations in Appendix 3.A)

$$\boxed{\begin{aligned} &\mid B^0(t) >= f_+(t) \mid B^0 > +\eta f_-(t) \mid \overline{B}^0 > \\ &\mid \overline{B}^0(t) >= \frac{f_-(t)}{\eta} \mid B^0 > +f_+(t) \mid \overline{B}^0 > \end{aligned}} \tag{3.8}$$

where

$$f_\pm(t) = \frac{1}{2}\left(e^{-iM_1t-\frac{\Gamma_1 t}{2}} \pm e^{-iM_2t-\frac{\Gamma_2 t}{2}}\right) \tag{3.9a}$$

$$|f_\pm|^2 = \frac{1}{4}\left(e^{-\Gamma_1 t} + e^{-\Gamma_2 t} \pm 2e^{-\Gamma t}\cos \Delta M t\right) \; . \tag{3.9b}$$

Remember that $|B^0(t) >$ ($|\overline{B}^0(t) >$) means that a B^0 ($\overline{B}^0$) has been produced at time $t = 0$. Thus, clearly $f_+(0) = 1$ and $f_-(0) = 0$, as one produces pure states at $t = 0$.

Let us point out that we will often approximate these last expressions using $\Gamma_1 \simeq \Gamma_2$ (i.e. $\Gamma \simeq \Gamma_{1,2}$ or $\Delta\Gamma \simeq 0$, see the discussion in Section 3.4). Indeed, because of the large phase space available for the B decays one expects that the heavy and light $B_{h,l}$ mesons will have nearly the same lifetimes (hence $\Gamma_1 \simeq \Gamma_2$). Then, expressions (3.9) give the relations:

$$f_+(t) = e^{-\imath \overline{M}t/2} e^{-\Gamma t/2} \cos\left(\frac{\Delta M t}{2}\right) \tag{3.10a}$$

$$f_-(t) = \imath\ e^{-\imath \overline{M}t/2} e^{-\Gamma t/2} \sin\left(\frac{\Delta M t}{2}\right) \tag{3.10b}$$

$$|f_\pm(t)|^2 = \frac{e^{-\Gamma t}}{2}(1 \pm \cos \Delta M t) \tag{3.10c}$$

$$f_-(t) f_+^*(t) = \frac{i}{2}\ e^{-\Gamma t} \sin \Delta M t \tag{3.10d}$$

using the notation $\overline{M} = (M_1 + M_2)/2$.

With the help of formula (3.8) one can calculate the B^0 and the $\overline{B}^0$ content in $\mid B^0(t) >$, or in a beam decribed by $\mid \overline{B}^0(t) >$. They are given by

$$|< B^0 \mid B^0(t) >|^2 = |f_+(t)|^2$$

$$|< \overline{B}^0 \mid B^0(t) >|^2 = |f_-(t)|^2\ |\eta|^2$$

$$|< B^0 \mid \overline{B}^0(t) >|^2 = \frac{|f_-(t)|^2}{|\eta|^2}$$

$$|< \overline{B}^0 \mid \overline{B}^0(t) >|^2 = |f_+(t)|^2\ .$$

Using the approximations given by formulae (3.10), the B^0 and $\overline{B}^0$ contents in the considered beams can be expressed by:

$$|< B^0 \mid B^0(t) >|^2 \simeq \frac{e^{-\Gamma t}}{2}\ (1 + \cos \Delta M t) \tag{3.11a}$$

$$|< \overline{B}^0 \mid B^0(t) >|^2 \simeq \frac{e^{-\Gamma t}}{2}\ (1 - \cos \Delta M t)\ |\eta|^2 \tag{3.11b}$$

$$|< \overline{B}^0 \mid \overline{B}^0(t) >|^2 \simeq \frac{e^{-\Gamma t}}{2}\ (1 + \cos \Delta M t) \tag{3.11c}$$

$$|< B^0 \mid \overline{B}^0(t) >|^2 \simeq \frac{e^{-\Gamma t}}{2|\eta|^2}\ (1 - \cos \Delta M t)\ . \tag{3.11d}$$

These formulae show the oscillation character of the B^0 and $\overline{B}^0$ content in a given B^0 or $\overline{B}^0$ beam. The oscillations depend crucially on the ΔM or $x = \Delta M/\Gamma$

values, as can be seen from Fig. 3.2. This figure presents expressions (3.11a) and (3.11b) as a function of $\tau = t/\overline{\tau}$ for different x values ($\overline{\tau}$ is the lifetime of the B meson considered) assuming $|\eta|^2 = 1$. Thus, according to the value of $x = \Delta M/\Gamma$, there might be several oscillations before the B meson will decay.

One has to emphasize that the oscillation can only be observed if information about the type of the meson responsible for the decay is known at the production time $t = 0$. In a real experiment B^0 and $\overline{B}^0$ can be produced. If, for instance, one wants to observe a $\mid B^0 >$ state the lack of information about the parent type produced at $t = 0$ will lead to a time dependence given by the sum of equations (3.11a) and (3.11d). This leads to a purely time exponential behavior (assuming still $|\eta|^2 = 1$). We will later discuss the manner applied for observing the oscillation character in the decay time distribution.

Because of the difficulties in measuring the oscillations, one often consider the time-integrated rates

$$\int_0^\infty \mid < B^0 \mid B^0(t) > \mid^2 dt = \frac{1}{2}\Big(\frac{1}{\Gamma_1} + \frac{1}{\Gamma_2} + \frac{2\Gamma}{\Gamma^2 + \Delta M^2}\Big)$$

$$\int_0^\infty \mid < \overline{B}^0 \mid B^0(t) > \mid^2 dt = \frac{|\eta|^2}{2}\Big(\frac{1}{\Gamma_1} + \frac{1}{\Gamma_2} - \frac{2\Gamma}{\Gamma^2 + \Delta M^2}\Big)$$

where similar expressions can be obtained for a $\overline{B}^0$ "beam". In order to measure quantitatively the amount of mixing one can use the so-called Pais and Treiman parameters[9], r and $\overline{r}$ defined by

$$r = \frac{\int \mid < \overline{B}^0 \mid B^0(t) > \mid^2 dt}{\int \mid < B^0 \mid B^0(t) > \mid^2 dt} = \frac{B^0 \to \overline{B}^0}{B^0 \to B^0} \tag{3.12a}$$

$$\overline{r} = \frac{\int \mid < B^0 \mid \overline{B}^0(t) > \mid^2 dt}{\int \mid < \overline{B}^0 \mid \overline{B}^0(t) > \mid^2 dt} = \frac{\overline{B}^0 \to B^0}{\overline{B}^0 \to \overline{B}^0}\ . \tag{3.12b}$$

Thus r ($\overline{r}$) defines the ratio of $\overline{B}^0/B^0$ ($B^0/\overline{B}^0$) that one has at $t \to \infty$ when at $t = 0$ one has produced pure B^0 ($\overline{B}^0$) states. This is symbolized by the expressions in the right-hand side of formula (3.12). An elementary calculation then gives:

$$\boxed{\begin{aligned} r &= |\eta|^2 \frac{x^2+y^2}{2+x^2-y^2} \\ \overline{r} &= \frac{1}{|\eta|^2}\frac{x^2+y^2}{2+x^2-y^2} \end{aligned}} \tag{3.13}$$

using $x = \Delta M/\Gamma$ and $y = \Delta\Gamma/(2\Gamma)$. The mixing probabilities can be defined by

$$\chi = \frac{B^0 \to \overline{B}^0}{B^0 \to B^0 + B^0 \to \overline{B}^0} = \frac{r}{1+r} \tag{3.14a}$$

$$\overline{\chi} = \frac{\overline{B}^0 \to B^0}{\overline{B}^0 \to \overline{B}^0 + \overline{B}^0 \to B^0} = \frac{\overline{r}}{1+\overline{r}} \; . \tag{3.14b}$$

Note that the non-mixing probabilities will simply be expressed by $1-\chi$ and $1-\overline{\chi}$.

The maximum mixing occurs when $r \simeq 1$ (or $\overline{r} \simeq 1$ when $\overline{B}^0$ are produced at $t = 0$) which corresponds to a nearly equal amount of $| B^0 >$ and $| \overline{B}^0 >$ in the beam at $t \to \infty$. Let us note that this can occur in two different situations[6,8]:

1 - $|y| = |\Delta\Gamma/(2\Gamma)| \simeq 1$

Here one has $r \simeq |\eta|^2$ and $\overline{r} \simeq 1/|\eta|^2$ [formula (3.13)] which in the limit of non CP violation in the mixing process ($|\eta|^2 = 1$) leads to full mixing. The condition $|y| = |\Gamma_1 - \Gamma_2|/(\Gamma_1 + \Gamma_2) = 1$ will be fullfilled when $\Gamma_1 \gg \Gamma_2$ or $\Gamma_2 \gg \Gamma_1$, a situation similar to the K^0 case (see next Section).

2 - $x = \Delta M/\Gamma \gg 1$

In this case one also has $r = \overline{r} \simeq 1$ (with $|\eta|^2 = 1$). Let us now write x in the following form:

$$\frac{\Delta M}{\Gamma} = \frac{1/\Gamma}{1/\Delta M} = \frac{\overline{\tau}}{\tau_{\text{mixing}}} \gg 1$$

where τ_{mixing} is the average time between the $B^0 \leftrightarrow \overline{B}^0$ oscillations. The last equation means that the system will oscillate rapidly before decaying and will thus appear as a nearly equal mixing of B^0 and $\overline{B}^0$. This is a situation believed to occur for the $B_s^0 \leftrightarrow \overline{B}_s^0$ mixing.

3.4 - Implications of the box diagram

As yet we have not used any estimation for Γ, ΔM and $\Delta\Gamma$. The total width $\Gamma \sim 1/\overline{\tau}$ can be obtained from the lifetime ($\overline{\tau}$) measurements, determined as ~ 1.5 ps for the B mesons[10] (small differences between the lifetimes of the B_s^0 and B_d^0 have been observed). Theoretically the main contribution to Γ is due to the spectator diagram [graph (a) in Fig. 2.5]. The total width for the process $b \rightarrow qW$ is then given by formula (2.20). In contrast, ΔM and $\Delta\Gamma$ can be estimated from the box diagram shown in Fig. 3.1. In fact this diagram allows one to calculate M_{12} and Γ_{12}, from which one obtains ΔM and $\Delta\Gamma$ (formulae 3.2). The M_{12} value depends on the masses of the quark exchanged in the box and on the CKM matrix elements entering in each corner of the box diagram. In the leading order where we consider only the exchanges of the quark giving the largest contribution, corresponding to exchange of the heaviest quark, one obtains for the B system[1,2]:

$$M_{12} = -\frac{G_F^2}{12\pi^2}\, B_B f_B^2 m_B (V_{tb}V_{tp}^*)^2 m_t^2\, \eta_{QCD} \qquad (3.15a)$$

$$\Gamma_{12} = \frac{G_F^2}{8\pi}\, B_B f_B^2 m_B (V_{tb}V_{tp}^*)^2 m_b^2\, \eta'_{QCD} \qquad (3.15b)$$

where $\eta_{QCD} \sim 0.85$ (Ref. 2) and η'_{QCD} (Ref. 11 and 12) represent the QCD correction factors. Here m_t is the t quark mass, m_B is the B meson mass. The symbol $p \equiv d,\ s$ is used in order to allow the description of the $B_d^0 \leftrightarrow \overline{B}_d^0$ and the $B_s^0 \leftrightarrow \overline{B}_s^0$ mixing. As already mentioned above, we use the convention that the CKM matrix element is V_{ij}^* (V_{ij}) if the outgoing quark at the $q_i q_j W$ vertex is a *down* (*up*) like quark[6] (see Fig. 3.1). In non relativistic models the B meson decay constant f_B is given by[13]:

$$f_B^2 = \frac{12}{m_B^2}|\psi(0)|^2$$

which is estimated to be $f_B = 0.1 - 0.5\ GeV$ for the B system[13]. Here $\psi(0)$ is the B meson wave function at the origin. The B_B (bag) parameter in formulae (3.15) is usually considered to be in the range of 0.5-1.5 unit[2].

Despite the uncertainties for certain of these parameters, some conclusions can nevertheless be drawn from formula (3.15). We first note that M_{12} and Γ_{12} have the same phases within the present approximation and that

$$\frac{|\Gamma_{12}|}{|M_{12}|} \simeq 10^{-2} \qquad (3.16)$$

with $m_t \sim 150$ GeV [as recent experimental results indicate that $m_t \geq 150\ GeV/c^2$, Ref. 14]. The fact that $|\Gamma_{12}/M_{12}| \ll 1$ means that formula (3.5) leads to

$$\eta = \frac{q}{p} = \sqrt{\frac{M_{12}^* - i\Gamma_{12}^*/2}{M_{12} - i\Gamma_{12}/2}}$$
$$\simeq \sqrt{\frac{M_{12}^*}{M_{12}}} = \frac{V_{tb}^* V_{tp}}{V_{tb} V_{tp}^*} . \tag{3.17}$$

Remarks

Remember that η is used for discussing the $B^0, \overline{B}^0$ cases. Later on, we will consider the $B_d^0 \leftrightarrow \overline{B}_d^0$ and $B_s^0 \leftrightarrow \overline{B}_s^0$ mixing with the parameters η_d and η_s, respectively. In the framework of the present approximation, there will be no CP violation in the $B_d^0 \leftrightarrow \overline{B}_d^0$ and $B_s^0 \leftrightarrow \overline{B}_s^0$ mixing as $|\eta_{d,s}|^2 \simeq 1$. The phases of $\eta_{d,s}$, however, will be of great importance for the discussion of CP violation effects in the B decays (Chapter 4). With the example of the CKM matrix (2.10), one has from formula (3.17) that $\eta_s = 1$ and $\eta_d = exp(2\phi_1)$ (see the notation discussed in Section 4.6).

Another important consequence due to $|\Gamma_{12}/M_{12}| \ll 1$ is that one can obtain simple expressions for ΔM and $\Delta\Gamma$ and hence for the Pais and Treiman parameters r and $\overline{r}$. From the relation (3.2), one has

$$\Delta M = 2ReQ = 2Re\sqrt{(M_{12} - i\Gamma_{12}/2)(M_{12}^* - i\Gamma_{12}^*/2)}$$

leading to

$$\Delta M \simeq 2|M_{12}| \simeq \frac{G_F^2}{6\pi^2} B_B f_B^2 m_B \mid V_{tb} V_{tp}^* \mid^2 m_t^2 \, \eta_{QCD} . \tag{3.18}$$

For deriving an approximation for $\Delta\Gamma$ let us use one of the expressions (3.2) yielding

$$\frac{1}{4}(\Delta M - i\frac{\Delta\Gamma}{2})^2 = (M_{12}^* - i\frac{\Gamma_{12}^*}{2})(M_{12} - i\frac{\Gamma_{12}}{2}) .$$

By equating the imaginary parts one gets:

$$\frac{\Delta M \Delta\Gamma}{4} = Re(M_{12}\Gamma_{12}^*) \simeq |M_{12}| \, |\Gamma_{12}|$$

as M_{12} and Γ_{12} have the same phase in the framework of the approximations given by formulae (3.15a) and (3.15b). Finally, by using $\Delta M = 2|M_{12}|$ and formula

(3.18) one obtains

$$\Delta\Gamma \simeq 2|\Gamma_{12}| \simeq \frac{G_F^2}{4\pi} B_B f_B^2 m_B |V_{tb}V_{tp}^*|^2 m_b^2 \eta'_{QCD} \,. \tag{3.19}$$

Using the (3.18) and (3.19) approximations and formula (3.16) one sees that

$$\frac{\Delta M}{\Gamma} >> \frac{\Delta\Gamma}{2\Gamma}$$

which according to our previous definitions means that $x \gg y$. Therefore the Pais and Treiman parameter for the B system can be approximated by the following forms:

$$\boxed{\begin{aligned} r &= |\eta|^2 \frac{x^2}{2+x^2} \\ \overline{r} &= \frac{1}{|\eta|^2} \frac{x^2}{2+x^2} \end{aligned}} \tag{3.20}$$

whereas the probability forms with $|\eta|^2 = 1$ [formula (3.14)] become

$$\chi = \overline{\chi} = \frac{x^2}{2(1+x^2)} \tag{3.21a}$$

$$1-\chi = 1-\overline{\chi} = \frac{2+x^2}{2(1+x^2)} \,. \tag{3.21b}$$

Thus the mixing phenomenon for the B mesons is governed by only one parameter which we recall is $x = \Delta M/\Gamma$.

The larger x becomes, the larger the mixing measured by the r or $\overline{r}$ parameter will be, with the asymptotic values of $r, \overline{r} \to 1$. It is now easy to understand why the mixing is expected to be larger for the B_s^0 system than for B_d^0. This is simply a consequence of the fact that $x_d < x_s$, the indices indicating values associated to the B_d^0 or B_s^0 mesons respectively, as[10]

$$|V_{tb}V_{td}^*| < |V_{tb}V_{ts}^*|$$

[see also the CKM matix approximation given by (2.11)]. Strictly speaking, f_B, B_B (and of course m_B) can be different for the B_d^0 and B_s^0 mesons, although it is usually assumed that they are nearly equal. With this approximation, and assuming that $\Gamma_s \simeq \Gamma_d$, one would expect that $x_s/x_d \geq 15$ by utilizing the $|V_{ij}|$ estimates of Ref. 10. This means that the oscillations given by $\Delta M_{d,s}t$ will have a larger frequency for the B_s^0 than for the B_d^0 system.

By using formulae (3.15) one can also relate quantities entering in the mixing of the B_d^0 with those of the B_s^0. In particular one observes that:

$$\frac{\Delta M_s}{\Delta M_d}, \frac{\Delta\Gamma_s}{\Delta\Gamma_d} \simeq \frac{| V_{ts} |^2}{| V_{td} |^2} > 1$$

assuming that $V_{tb} \simeq 1$. Moreover, one also notices that because of $\Delta\Gamma_s > \Delta\Gamma_d$ it might be easier in principle to detect the two different lifetimes of the heavy and light B in B_s^0 than in B_d^0 case.

In a very qualitative way we are now able to understand why mixing is expected to be more important for the B^0 system than for the D^0. The argument we will use is not an exact one as we will only compare those quantities giving the largest contribution to $x \propto |V_{ij}V_{ik}^*|^2 m_Q^2 m_M/\Gamma$ for various cases [using formula (3.18)]. Here, m_Q is the quark mass that can be exchanged in the box diagram, whereas m_M is the mass of the considered (B or D) meson. We thus ignore the f_M and B_M dependence of the various cases and we assume that $y = \Delta\Gamma/(2\Gamma) \simeq 0$ is valid for all cases, a fact not necessarily true for the D meson[15]. In addition, let us use the simplified form for the CKM matrix inspired from the Wolfenstein parametrization and discussed in Chapter 1. In this approach one has

$$V_{tb} \sim V_{cs} \sim V_{ud} \sim 1$$
$$V_{cd} = V_{us} = \lambda; \quad V_{cb} = V_{ts} = \lambda^2; \quad V_{td} = V_{bu} = \lambda^3 .$$

Fig. 3.3 presents the different box diagrams for the D^0 and $B_{d,s}^0$ cases. In the figure are also given indications for the $x \propto |V_{ij}V_{ik}^*|m_Q^2 m_M/\Gamma$ quantities, where for Γ we use the dominant spectator model prediction $\Gamma \propto m_q^5|V_{qq'}|^2$. Thus $\Gamma(B) \propto |V_{bc}|^2 \simeq \lambda^4$, which appears in the denominator of the studied ratio, will cancel part of the λ dependance appearing in the numerator. For the B_s^0 this cancellation is complete within this rough approximation, as $\Delta M_s/\Gamma \simeq m_t^2/m_b^4$ does not depend in the leading order on λ.

3.5 - Mixing measurements with the time oscillations

We will discuss now the measurement possibilities of the B^0 mixing through the observation of the decay time-oscillation. We consider this approach for simplicity, although the first observation of the B_d^0 mixing were made through their semileptonic decays (see below) and not with the time oscillation process. At the begining we consider the general case where the B^0 are produced in hadron-hadron interactions at c.m. energies where all types of beauty-hadron pairs can be produced. Note that the same method can also be used for e^+e^- interactions at large c.m. energies (for instance, $e^+e^- \to Z \to X$) although some differences might appear between pN and e^+e^- interactions (see Section 5). We will also comment on the relatively simple case for the B^0 mesons produced by the $e^+e^- \to \Upsilon(nS) \to B^0\overline{B}^0$ channels (with $n = 4, 5$).

a) hadron-hadron collisions

Let us consider a $B_d^0 \to f$ decay where the experimental reconstruction of the daughter f state signs the type of the parent meson at the decay time. For instance, one could consider the $B_d^0 \to D_s^+\pi^-$ that could not come from the $\overline{B}_d^0$ decay. As already discussed above (Section 3.3), information about the type of the B meson produced at $t = 0$ and responsible for the decay into the f state could be partly obtained by tagging the associated beauty hadron through its semileptonic decay. This is because the charge of the lepton indicates the quark responsible of the decay ($b \to l^-X$, $\bar{b} \to l^+X$, X meaning anything). In the present example we consider the final l^-fX state that can be produced by the following beauty-hadron combination:

(1) $B^-B_d^0$

(2) $N_bB_d^0$

(3) $\overline{B}_s^0B_d^0$ and $B_s^0\overline{B}_d^0$ (coherent mixture)

(4) $\overline{B}_d^0B_d^0$

where the particles are those appearing at the production time ($t = 0$). Let us now consider these cases[8].

Cases (1) and (2)

These cases are trivial, as the beauty hadrons decay in an event independently from each other. For case 1, the initial vector state is given by

$$|\phi >= |B^-(t_-) > |B_d^0(t_d) > \qquad (3.22)$$

where t_- (t_d) corresponds to the proper time of the B^- (B_d^0) state in its rest frame.

The amplitude of the considered processes is then given by:

$$A(l^-f) \equiv < l^-f \mid \phi > = < l^-X|B^-(t_-) > < f|B_d^0(t_d) > \ .$$

Using

$$| < l^-X|B^-(t_-) > |^2 = | < l^-X|B^- > |^2 \ e^{-\Gamma_- t_-}$$

and formula (3.11a) one obtains successively

$$|A(l^-f)|^2 \equiv \frac{d\sigma_1}{dt_-dt_d} = \frac{|T|^2}{2} \ e^{-(\Gamma_- t_- + \Gamma_d t_d)} \ (1 + \cos \Delta M_d t_d) \qquad (3.23a)$$

$$\frac{d\sigma_1}{dt_d} = \frac{|T|^2}{2\Gamma_-} \ e^{-\Gamma_d t_d} \ (1 + \cos \Delta M_d t_d) \qquad (3.23b)$$

where $T = < l^-X|B^- >< f|B_d^0 >$, while Γ_i represents the decay width of the beauty hadron considered (the indice being self-explanatory). For point 2, one has the same formula with the transformation of $\Gamma_- \rightarrow \Gamma_N$ and $T \rightarrow T'$ as the $< l^-X|B^- >$ part of the amplitude might be different from the $< l^-X|N_b >$ part (see the discussion below).

Case (3)

This case is more complicated, as each neutral meson can be subject to mixing. Because of these procedures, the l^-f state can arise from systems that at time $t = 0$ were either $B_s^0\overline{B}_d^0$ or $\overline{B}_s^0 B_d^0$. The initial state vector is now given by

$$|\phi > = |B_s(t_s) > |\overline{B}_d(t_d) > + |\overline{B}_s(t_s > |B_d(t_d) > \qquad (3.24a)$$

where $t_{d,s}$ represent the proper times in the B_d^0 and B_s^0, respectively. If we now consider the final state in which the strange meson decays into l^-X at time t_s and the non-strange one into f at time t_d, one can write the amplitude for this process as

$$A(l^-f) = < l^-X|B_s(t_s) >< f|\overline{B}_d(t_d) > + < l^-X|\overline{B}_s(t_s) >< f|B_d(t_d) > \ .$$

By using formula (3.8) giving the time evolution of $|B^0(t) >$ and $|\overline{B}^0(t) >$ one has

$$A(l^-f) = T\Big[\frac{\eta_s}{\eta_d} \ f_-(t_s)f_-(t_d) + f_+(t_s)f_+(t_d)\Big] \qquad (3.24b)$$

where, as usual, $T = < l^-X|\overline{B}^0 >< f|B^0 >$. With this amplitude, one obtains the following time dependence expressions (Appendix 3.B using $\eta_s = 1$):

$$\frac{d\sigma_3}{dt_s dt_d} = \frac{|T|^2}{2} e^{-(\Gamma_s t_s - + \Gamma_d t_d)} [1 + \cos(\Delta M_s t_s + \Delta M_d t_d) +$$
$$+ \sin \Delta M_s t_s \sin \Delta M_d t_d \times (1 - \mathrm{Re}\eta_d)] \qquad (3.25a)$$
$$\frac{d\sigma_3}{dt_d} = \frac{|T|^2}{2\Gamma_s} e^{-\Gamma_d t_d} \left[1 + \frac{1}{1+x_s^2} \left(\cos \Delta M_d t_d - x_s \mathrm{Re}\eta_d \sin \Delta M_d t_d \right) \right], \qquad (3.25b)$$

the last expression being the t_d time dependence for case 3. Because of the large expected x_s value (Section 3.4), the $d\sigma_3/dt_d$ distribution will essentially have an exponential behaviour (a situation which would be different for $d\sigma_3/dt_s$).

Case (4)

For the $B_d^0 \overline{B}_d^0$ case, we must take into account the charge conjugation of the two meson system defined by $\eta_c = \pm 1$. The state vector of such a system is then given by

$$| \phi >=| B(t), p_1 >| \overline{B}(t), p_2 > + \eta_c | \overline{B}(t), p_1 >| B(t), p_2 > \qquad (3.26)$$

where $p_{1,2}$ are the meson momenta defined, for instance, in the production c.m. system and where $C|\phi >= \eta_c|\phi >$. Let us now consider the final state in which one meson decays into $l^- X$ at time t_1 while the other one is decaying into f at time t_2 (t_1 and t_2, as usual, are defined in the corresponding meson rest frame). The amplitude for this process will then be given by:

$$A(l^- f) =< l^- X \mid B^0(t_1) >< f \mid \overline{B}^0(t_2) > + \eta_c < l^- X \mid \overline{B}^0(t_1) >< f \mid B^0(t_2) >$$

where we label yet the B mesons by their disintegration time t_1 and t_2. Still using formula (3.8) one gets

$$A(l^- f) = T \left[f_-(t_1) f_-(t_2) + \eta_c f_+(t_1) f_+(t_2) \right]$$

with $T =< l^- X|\overline{B}_s^0 >< f|B_d^0 >$. One thus easily gets the double differential cross section

$$\frac{d\sigma_4(l^- f)}{dt_1 dt_2} = \frac{|T|^2}{2} e^{-\Gamma(t_1+t_2)} \left[1 + \cos \Delta M (t_1 + \eta_c t_2) \right] . \qquad (3.27a)$$

Integrating over t_1, the time related to the semileptonic decay, one obtains the following t_2 dependance (t_2 being replaced by t_d):

$$\frac{d\sigma_4(l^- f)}{dt_d} = \frac{|T|^2}{2\Gamma_-} e^{-\Gamma t_d} \left[1 + \frac{1}{1+x_d^2} \left(\cos\ \Delta M_d t_d - \eta_c x_d \sin \Delta M_d t_d \right. \right] . \qquad (3.27b)$$

For c.m. energies above the $B\overline{B}$ threshold, the two charge-conjugated states of the

$B_d^0\overline{B}_d^0$ system ($\eta_c = \pm 1$) have equal probability. Then the third term in the right part of the last equation vanishes.

Finally, the four cases can be summarized as follow:

$$\begin{aligned}
\frac{d\sigma_1(l^-f)}{d\tau_d} &= \frac{|T|^2}{2\Gamma_-\Gamma_d}\, e^{-\tau_d}\, (1+\cos x_d\tau_d) \\
\frac{d\sigma_2(l^-f)}{d\tau_d} &= \frac{|T'|^2}{2\Gamma_N\Gamma_d}\, e^{-\tau_d}\, (1+\cos x_d\tau_d) \\
\frac{d\sigma_3(l^-f)}{d\tau_d} &= \frac{|T|^2}{2\Gamma_s\Gamma_d}\, e^{-\tau_d} \left[1+\frac{1}{1+x_s^2}\left(\cos x_d\tau_d - x_s \mathrm{Re}\eta_d \sin x_d\tau_d\right)\right] \\
\frac{d\sigma_4(l^-f)}{d\tau_d} &= \frac{|T|^2}{2\Gamma_d\Gamma_d}\, e^{-\tau_d} \left[1+\frac{1}{1+x_d^2}\, cos x_d\tau_d\right]
\end{aligned} \tag{3.28}$$

using $\tau_d = t_d/\overline{\tau}_d \equiv t_d\Gamma_d$ ($\overline{\tau}_d$ being the B_d^0 lifetime). The $d\sigma(l^-f)/d\tau_d$ cross-section will then by obtained by adding incoherently the different $d\sigma_i(l^-f)/d\tau_d$ distributions, each of them being weighted by the production values of the B_d^0 (p_d) and of the associated beauty hadron ($p_\pm, p_s, p_d$ or p_N), i.e.

$$\frac{d\sigma(l^-f)}{d\tau_d} = \sum_{j=1}^{4} p_d\; p_j\; \frac{d\sigma_j(l^-f)}{d\tau_d}\ . \tag{3.29}$$

The amplitudes $|<l^-X|\overline{B}><f|B_d^0>| = |T|$ and $|<l^-X|N_b><f|B_d^0>| = |T'|$ will be taken as being the same in all cases, as we assume that the semileptonic decays of beauty hadrons are dominated by the spectator model (Section 2.4). This simply means that the widths of the semileptonic decays of the beauty hadrons are nearly equal. For estimates of the distributions due to formula (3.28), we will also assume that the beauty meson decays are essentialy due to the $b \to qW$ or $\overline{b} \to \overline{q}W$ processes (the spectator model) yielding equal lifetimes for the various B mesons, and hence that

$$\Gamma_+ = \Gamma_d = \Gamma_s\ .$$

The binding energy of the light quarks in the beauty baryon are expected to be smaller than in the B meson. Therefore, the beauty-baryon lifetimes should be shorter than those of the B mesons, yielding $\Gamma_N > \Gamma_i$. From the actual observation of the beauty-hadron lifetimes, one has $\Gamma_N \simeq \epsilon\,\Gamma_i$ with $\epsilon \simeq 1.3$ (Ref. 16).

The p_j probabilities depend on the c.m. energy where the beauty-hadron pairs are produced. At large c.m. energy ($\sqrt{s} > 1$ TeV), one generally uses the values of:

$$p_{\pm} : p_d : p_s : p_N \simeq 0.38 : 0.38 : 0.14 : 0.10 \ . \tag{3.30}$$

obtained from Monte Carlo calculations[17]. Note that the sum of the equations in (3.28) leads to a distribution of

$$\frac{d\sigma}{d\tau_d} \propto e^{-\tau_d} \left[1 + A \cos x_d \tau_d - B \sin x_d \tau_d\right] \tag{3.31}$$

where the A and B parameters depend essentially on $x_{s,d}$, the probabilities p_j and the values of the $\Gamma_{\pm}$, Γ_d, Γ_s and Γ_N widths. The coefficient A is sometimes considered as the dilution factor as $A < 1$, despite the small sine term appearing in (3.31).

The expressions given by formulae (3.28) can be utilized for the B_s^0 oscillations by transforming the subscripts $d \leftrightarrow s$. As an example, we present in Fig. 3.4 a decay time distribution for a $B_s^0 \to f$ decay with $x_s = 15$, $\mathrm{Re}\eta_d = 1$, $\Gamma_N/\Gamma_- = 1$ [formula (3.31) with $s \leftrightarrow d$] assuming that the amplitudes ($|T|$) in the four cases are nearly equal. The calculated distribution is not very sensitive to the $\Gamma_N/\Gamma_- = \epsilon$ value, in the $1-2$ range. One also sees from this figure that the calculated distribution is not too far from the $| < B^0 \mid B^0(t) > |^2 \simeq e^{-\Gamma t}\ (1 + \cos \Delta M t)/2$ distribution [formula (3.11a)] when the backround has an exponantial form.

b) The $e^+e^- \to \Upsilon(nS)$ reactions

The situation is simpler for the $e^+e^- \to \Upsilon(4S) \to B_d^0 \overline{B}_d^0$ process where the relative orbital momentum between the two mesons has to be $l = 1$ [in order to have the $J^{PC} = 1^{--}$ quantum numbers of the $\Upsilon(4S)$]. Then the oscillation forms will be given by formulae (3.27) with $\eta_c = -1$, namely:

$$\frac{d\sigma_4(l^- f)}{dt_1 dt_2} = \frac{|T|^2}{2} e^{-\Gamma(t_1+t_2)} \Big[1 + \cos \Delta M(t_1 - t_2)\Big] \tag{3.32a}$$

$$\frac{d\sigma_4}{dt_d} = \frac{|T|^2}{2\Gamma_d}\ e^{-\Gamma_d t_d} \left[1 + \frac{1}{1 + x_d^2}\ \Big(\cos \Delta M_d t_d + x_d\ \sin \Delta M_d t_d\Big)\right] \ . \tag{3.32b}$$

The same relation could be used for the $\Upsilon(5S) \to B_s^0 \overline{B}_s^0$ decay replacing $d \to s$.

One has to notice that formulae (3.27) can also be applied for the process

$$e^+e^- \to B_s^0\overline{B}_s^{*0}, \overline{B}_s^0 B_s^{*0} \to B_s^0\overline{B}_s^0\gamma$$

where no additionnal π being produced. This time one has $\eta_c = 1$ (and $d \to s$) in formula (3.27b).

The formula (3.32b) has not really been used as yet for measuring the B^0 mixing. This analysis would have some problems for the $e^+e^- \to \Upsilon \to B\overline{B}$ case because of the difficulty of reconstructing the interaction point, thus complicating the proper time measurement. In this respect, the oscillation observation could be more powerful for measuring the x_s parameter related to the B_s^0 mixing in the case of pp interactions.

3.6 - Mixing measurements with semileptonic decays

The method that we now comment on was in fact used for observing and measuring the $B_d^0 \leftrightarrow \overline{B}_d^0$ mixing. In this approach, one measure in a given experiment the number of events (denoted by N) having BB (or $\overline{N}_bB$), $\overline{B}\overline{B}$ (or $N_b\overline{B}$) and $\overline{B}B$ (N_bB or $\overline{N}_b\overline{B}$) in the observed final states. Note that $N(BB)$, for example, does not mean that one has necessarily two B (or $\overline{B}$) at the same time defined, for instance, in the production c.m. system (which is not be allowed in some cases as in the $e^+e^- \to \Upsilon(4S) \to B\overline{B}$ process). Here $N(BB)$ simply means that the observed final states are due to two B decays. As the identification of a beauty hadron through its reconstruction is difficult, one usually uses the semileptonic decay $B \to l^+\nu X$ ($\overline{N}_b \to l^+\nu X$) and $\overline{B} \to l^-\nu X$ ($N_b \to l^-\nu X$). Mixing could then be observed by measuring the following ratios[18]:

$$R' = \frac{N(l^+l^+) + N(l^-l^-)}{N(l^+l^-)} \tag{3.33}$$

$$R = \frac{N(l^+l^+) + N(l^-l^-)}{N(l^+l^+) + N(l^-l^-) + N(l^+l^-)} \; .$$

Here $N(l^\pm l^\pm)$ denotes the number of events having two leptons of the same charge in the final state arising from the mixing process and the subsequent semileptonic decays of the beauty-hadron pair. The number of events with two leptons of different charge and resulting fróm beauty-hadron decays is denoted by $N(l^+l^-)$. Non-zero values of the above ratios indicate the occurence of mixing in the B^0 system.

a) hadron-hadron collisions

Although the $B_d^0 \leftrightarrow \overline{B}_d^0$ mixing was discovered in the $e^+e^- \to \Upsilon(4S) \to B\overline{B}$ process let us begin to consider the general case in pp interactions. At large c.m. energy (for instance, $\sqrt{s} > 1$ TeV), several types of beauty-hadron pairs can lead to the production of $l^\pm l^\pm$ due to the semileptonic decays of the b quarks. Let us, for example, consider the l^-l^- case. The pairs of beauty hadrons at the production time ($t = 0$) that may be responsible of l^-l^- are:

$$B^-B_d^0,\ B^-B_s^0,\ B_s^0\overline{B}_d^0 + \overline{B}_s^0 B_d^0,\ \overline{B}_d^0 B_d^0,\ \overline{B}_s^0 B_s^0$$
$$N_b B_d^0,\ N_b B_s^0\ .$$

The amplitudes and the cross-sections $\sigma(l^-l^-) \propto N(l^-l^-)$ expressions are derived in the Appendix 3.C for the $B\overline{B}$ cases. Let us give here only the obtained expressions:

$$B^-B_d^0 \Rightarrow \quad \sigma_a(l^-l^-) = \frac{|T|^2}{2\Gamma_-\Gamma_d}\,\frac{x_d^2}{1+x_d^2}\,p_\pm p_d \tag{3.34a}$$

$$B^-B_s^0 \Rightarrow \quad \sigma_b(l^-l^-) = \frac{|T|^2}{2\Gamma_-\Gamma_d}\,\frac{x_s^2}{1+x_s^2}\,p_\pm p_s \tag{3.34b}$$

$$\overline{B}_s^0 B_d^0 \Rightarrow \quad \sigma_c(l^-l^-) = \frac{|T|^2}{2\Gamma_s\Gamma_d}\,\frac{x_s^2 + x_d^2 + x_s^2 x_d^2 + x_s x_d \mathrm{Re}\eta_d}{(1+x_s)\,(1+x_d^2)}\,p_s p_d \tag{3.34c}$$

$$\overline{B}_d^0 B_d^0 \Rightarrow \quad \sigma_d(l^-l^-) = \frac{|T|^2}{2\Gamma_d\Gamma_d}\left[\frac{x_d^2(2+x_d^2)}{(1+x_d^2)^2}\right] p_d^2 \tag{3.34d}$$

$$\overline{B}_s^0 B_s^0 \Rightarrow \quad \sigma_e(l^-l^-) = \frac{|T|^2}{2\Gamma_s\Gamma_s}\left[\frac{x_s^2(2+x_s^2)}{(1+x_s^2)^2}\right] p_s^2 \tag{3.34e}$$

where, as usual, $\Gamma_{i,j}$ are the total widths of the various beauty hadrons and T is the amplitude part taken equal for these cases (see Appendix 3.C). The $N_b B_d^0$ or $N_b B_s^0$ cases can simply obtained by replacing $\Gamma_- \to \Gamma_N$ and $p_\pm \to p_N$ in equations (3.34a) and (3.34b) using the same (or a different) T amplitude. Here $\sigma(l^-l^-) \neq 0$ will indicate mixing although an estimate of x_s (x_d is known) is not evident.

b) The $e^+e^- \to \Upsilon(nS)$ reactions

The study of the $e^+e^- \to \Upsilon(4S) \to B_d^0\overline{B}_d^0$ about mixing has been done without difficulty as one can produce only one pair of neutral mesons $B^0\overline{B}^0$ in the final state, which will be responsible on two outgoing leptons having the same charge.

In the general case, odd or even orbital momentum l between the outgoing mesons, one has[8]

$$\boxed{\begin{aligned} N(l^+l^+) &= K^2\left[1-\frac{1-\eta_c x^2}{(1+x^2)^2}\right]|\eta|^2 \\ N(l^-l^-) &= K^2\left[1-\frac{1-\eta_c x^2}{(1+x^2)^2}\right]\frac{1}{|\eta|^2} \\ N(l^+l^-) &= K^2\left[1++\frac{1-\eta_c x^2}{(1+x^2)^2}\right]\times 2 \end{aligned}} \tag{3.35}$$

where $K^2 = |<l^-X|B^0>|^2/(2\Gamma^2_{d,s})$ and $\eta_c = \pm 1$. Here $N(l^+l^-)$ represents only the number of events with l^+l^- due to the $B^0\overline{B}^0$ pair. For the $e^+e^- \to \Upsilon(4S) \to B^0_d\overline{B}^0_d$ process one has $\eta_c = -1$. Using in addition $|\eta|^2 = 1$, one obtains

$$N(l^\pm l^\pm)_{\rm odd} = K^2\left(1-\frac{1}{1+x_d^2}\right) = K^2\frac{x_d^2}{1+x_d^2} \tag{3.36a}$$

$$N(l^+l^-)_{\rm odd} = 2K^2\left(1+\frac{1}{1+x_d^2}\right) = 2K^2\frac{2+x_d^2}{1+x_d^2} \tag{3.36b}$$

the symbol odd denoting that we are dealing with an odd l value. This leads to:

$$\boxed{R'_{\rm odd} = \frac{N(l^+l^+)_{\rm odd}+N(l^-l^-)_{\rm odd}}{N(l^+l^-)_{\rm odd}} = \frac{x_d^2}{2+x_d^2} = r_d\ .} \tag{3.37}$$

The same expression will be obtained for the $e^+e^- \to \Upsilon(5S) \to B^0_s\overline{B}^0_s$ but where $d \to s$.

Remarks

If the events have outgoing mesons produced with relative odd and even orbital momentum in equal amounts, one would then obtain

$$R'_{\rm odd+even} = \frac{x^2(2+x^2)}{2+2x^2+x^4} = \frac{2r}{1+r^2}\ ,$$

using now x, r instead of $x_{d,s}, r_{d,s}$. The influence of the relative orbital momentum on R' is shown in Fig. 3.5. where $R'_{\rm odd}$, $R'_{\rm even}$ and $R'_{\rm odd+even}$ are expressed as a function of x. As expected, the Bose-Einstein statistics requirement leads to a smaller mixing than in the uncorrelated case for $x < 5$.

Appendix 3.A

Mixing formulae

As seen in Section 3.2 the eigenvalues $\mu_\pm$ are obtained from

$$Det \mid H - \mu I \mid = 0$$

yielding

$$\mu_\pm = M - i\frac{\Gamma}{2} \pm Q$$

with

$$Q = \sqrt{(M_{12} - i\frac{\Gamma_{12}}{2})(M_{12}^* - i\frac{\Gamma_{12}^*}{2})}$$

The eigenvectors $\mid B_1 >$ and $\mid B_2 >$ will be expressed as a linear combination of $\mid B^0 >$ and $\mid \overline{B}^0 >$, namely

$$\mid B_1 > = p \mid B^0 > + q \mid \overline{B}^0 >$$
$$\mid B_2 > = p' \mid B^0 > + q' \mid \overline{B}^0 >$$

where we associate $\mid B_1 >$ to the light state ($M_1 = Re\ \mu_- = M - Re\ Q$) and $\mid B_2 >$ to the heavy one ($M_2 = Re\ \mu_+ = M + Re\ Q$). The p, q and p', q' values will be obtained from the equations:

$$(M - \mu_- I) \begin{pmatrix} p \\ q \end{pmatrix} = 0; \quad (M - \mu_+ I) \begin{pmatrix} p' \\ q' \end{pmatrix} = 0 .$$

These matrix equations give

$$\frac{q}{p} = \frac{-Q}{M_{12} - i\Gamma_{12}/2} = \pm\sqrt{\frac{M_{12}^* - i\Gamma_{12}^*/2}{M_{12} - i\Gamma 12}}$$
$$\frac{q'}{p'} = \frac{Q}{M_{12} - i\Gamma_{12}/2} = \mp\sqrt{\frac{M_{12}^* - i\Gamma_{12}^*/2}{M_{12} - i\Gamma 12}}$$

and therefore

$$\frac{q}{p} = -\frac{q'}{p'}$$

One can thus write the eigenstates in the following form

$$\boxed{\begin{array}{l} | B_1 > = p \mid B^0 > +q \mid \overline{B}^0 > \\ | B_2 > = p \mid B^0 > -q \mid \overline{B}^0 > \end{array}} \qquad (3.3)$$

which are the formula (3.3) given in the text.

Let us now give the time dependance of the B^0 and $\overline{B}^0$ states, namely $| B^0(t) >$ and $| \overline{B}^0(t) >$. As the the physical states $| B_1 >$ and $| B_2 >$ have definite lifetimes one merely has

$$| B_{1,2} > = | B_{1,2} > e^{-i(M_{1,2} - i\Gamma_{1,2}/2)t}$$

Now using equations (3.3) one obtains

$$| B^0 > = \frac{1}{2p}\Big(| B_1 > + | B_2 > \Big)$$
$$| \overline{B}^0 > = \frac{1}{2q}\Big(| B_1 > - | B_2 > \Big)$$

which expresses at time $t = 0$, $| B^0 >$ and $| \overline{B}^0 >$ as a function of the physical states $| B_{1,2} >$. As we know how the physical states behave as a function of time, the time evolution of the B^0 and $\overline{B}^0$ states are simply given by:

$$| B^0(t) > = \frac{1}{2p}\Big(| B_1 > e^{-iM_1 t - \Gamma_1 t/2} + | B_2 > e^{-iM_2 t - \Gamma_2 t/2}\Big)$$
$$| \overline{B}^0(t) > = \frac{1}{2q}\Big(| B_1 > e^{-iM_1 t - \Gamma_1 t/2} - | B_2 > e^{-iM_2 t - \Gamma_2 t/2}\Big)$$

Let us now replace $| B_{1,2} >$ (the physical states at $t = 0$) in these last equations with the help of formula (3.3). One obtains thus

$$\boxed{\begin{aligned} \mid B^0(t) > &= f_+(t) \mid B^0 > + \eta f_-(t) \mid \overline{B}^0 > \\ \mid \overline{B}^0(t) > &= f_+(t) \mid \overline{B}^0 > + \frac{f_-(t)}{\eta} \mid B^0 > \end{aligned}} \tag{3.8}$$

with

$$f_\pm(t) = \frac{1}{2}\Big(e^{-iM_1t - \Gamma_1 t/2} \pm e^{-iM_2 t - \Gamma_2 t/2}\Big) \tag{3.9a}$$

which are the wanted expressions, namely formula (3.8) and (3.9a) from the text. Sometime this last formula is also written in the following forms:

$$\begin{aligned} f_+(t) &= e^{-i(M_1+M_2)t/2} e^{-\Gamma t/2} \cos\Big(\frac{\Delta\mu t}{2}\Big) \\ f_-(t) &= i\ e^{-i(M_1+M_2)t/2} e^{-\Gamma t/2} \sin\Big(\frac{\Delta\mu t}{2}\Big) \end{aligned}$$

where

$$\begin{aligned} \Delta\mu &= \mu_+ - \mu_- = 2Q \\ &= \Delta M - i\Delta\Gamma/2 \end{aligned}$$

is a complex number but with a very small imaginary part as $\Delta\Gamma/\Delta M \ll 1$. As already mentioned in Sections 3.2 and 3.3, the widths (or the lifetimes) of the heavy and light B^0 mesons are nearly equal, yielding $\Delta\mu \simeq \Delta M$ and

$$\begin{aligned} f_+(t) &= e^{-i(M_1+M_2)t/2} e^{-\Gamma t/2} \cos\Big(\frac{\Delta M t}{2}\Big) \\ f_-(t) &= i\ e^{-i(M_1+M_2)t/2} e^{-\Gamma t/2} \sin\Big(\frac{\Delta M t}{2}\Big) \end{aligned}$$

where this time, the arguments of the cosine and sine terms are real. These expressions are given in Section 3.3 [formula (3.10a) and (3.10b)].

Appendix 3.B

Time dependence for case (3) in Section 3.5

Using the amplitude (3.24b),

$$A(l^- f) = T\left[\frac{\eta_s}{\eta_d}\ f_-(t_s)f_-(t_d) + f_+(t_s)f_+(t_d)\right]$$

and $\eta_s = 1$, one obtains

$$\frac{d\sigma_3}{dt_s dt_d} \equiv |A(l^- f)|^2 = |T|^2\Big[|f_+(t_s)|^2|f_+(t_d)|^2 + |f_-(t_s)|^2|f_-(t_d)|^2 +$$
$$2\mathrm{Re}\Big(f_-(t_s)f_+^*(t_s)f_-(t_d)f_+^*(t_d)\eta_d\Big)\Big]$$

By using now formulae (3.8) and (3.10), the last expression becomes

$$\frac{d\sigma_3}{dt_s dt_d} = \frac{|T|^2}{2}\ e^{-(\Gamma s t s - + \Gamma_d t_d)}\ [1 + \cos(\Delta M_s t_s + \Delta M_d t_d)]$$
$$+ \sin(\Delta M_s t_s)\sin(\Delta M_d t_d) \times (1 - \mathrm{Re}\eta_d)\ . \qquad (3.25a)$$

To integrate this expression over t_s we use the following integrals:

$$\int_0^\infty e^{-\tau}\cos(x\tau + q)d\tau = \frac{1}{1+x^2}\ [\cos q - x\sin q] \qquad (3.B1)$$

$$\int_0^\infty e^{-\tau}\sin(x\tau + q)d\tau = \frac{1}{1+x^2}\ [x\cos q - \sin q]\ , \qquad (3.B2)$$

yielding

$$\frac{d\sigma_3}{dt_d} = \frac{|T|^2}{2\Gamma_s}\ e^{-\Gamma_d t_d}\left[1 + \frac{1}{1+x_s^2}\ \big(\cos\Delta M_d t_d - x_s \mathrm{Re}\eta_d \sin\Delta M_d t_d\big)\right]\ . \qquad (3.25b)$$

Appendix 3.C

Formulae for pN interactions

As a simple exercice, let us derive equations (3.34a) to (3.34e). These expressions give the $\sigma_j(l^-l^-)$ cross-sections ($j = a ... e$) obtained from the following pairs of beauty meson produced at $t = 0$:

$$B^-B_d^0,\ B^-B_s^0,\ B_s^0\overline{B}_d^0 + \overline{B}_s^0 B_d^0,\ \overline{B}_d^0 B_d^0,\ \overline{B}_s^0 B_s^0\ .$$

The first two cases are simple. Let us, for example, consider the $B^-B_d^0$ production at $t = 0$ described by the state vector $|B^-(t) > |B_d^0(t) >$ yielding the amplitude

$$\begin{aligned} A(l^-l^-) &=< l^-|B^-(t) >< l^-|B_d^0(t) > \\ &= T\ e^{-\Gamma_- t_-/2}\ \eta f_-(t_d) \end{aligned}$$

with $T =< l^-|B^- >< l^-|\overline{B}_d^0 >$. The last term was obtained by using essentially formula 3.8. By integrating the square of the above expression over t_- and t_d one obtains

$$\sigma_a(l^-l^-) = \frac{|T|^2}{2\Gamma_-\Gamma_d}\ \frac{x_d^2}{1 + x_d^2}\ p_\pm p_d\ . \tag{3.34a}$$

where p_j represents the probability of producing a B_j (or $\overline{B}_j$) meson. The $B^-B_s^0$ case is simply obtained by replacing the d symbol by the s one yielding,

$$\sigma_b(l^-l^-) = \frac{|T|^2}{2\Gamma_-\Gamma_s}\ \frac{x_s^2}{1 + x_s^2}\ p_\pm p_s\ . \tag{3.34b}$$

Let us now consider the third case where the state vector is given by

$$|\phi >= |B_s(t_s) > |\overline{B}_d(t_d) > + |\overline{B}_s(t_s > |B_d(t_d) > \tag{3.24}$$

leading to the amplitude

$$A(l^-l^-) = T\ \Big[\eta_s f_-(t_s) f_+(t_d) + \eta_d f_+(t_s) f_-(t_d)\Big]$$

using still equations 3.8. The integrations of $|A(l^-l^-)|^2$ over t_s and t_d give now with $\eta_s = 1$:

$$\sigma_c(l^-l^-) = \frac{|T|^2}{2\Gamma_s\Gamma_d} \; \frac{x_s^2 + x_d^2 + x_s^2 x_d^2 + x_s x_d \mathrm{Re}\eta_d}{(1+x_s^2)\;(1+x_d^2)} \; p_s p_d \qquad (3.34c)$$

which, of course, should be symmetric in the x_s and x_d parameters.

By using the state vector

$$| \, \phi >=| \, B(t), p_1 >| \, \overline{B}(t), p_2 > +\eta_c \, | \, \overline{B}(t), p_1 >| \, B(t), p_2 > \qquad (3.26)$$

(see the definitions in Section 3.5) one obtains the amplitude for the $B_d^0 \overline{B}_d^0$ system

$$A(l^-l^-) = T \; \eta_d \left[f_-(t_1) f_+(t_2) + f_+(t_1) f_-(t_2) \; \eta_c \right] .$$

By integrating this expression over t_1 and t_2, one has the total cross-section:

$$\sigma_d(l^-l^-) = \frac{|T|^2}{2\Gamma_d\Gamma_d} \left[1 - \frac{1 - \eta_c x_d^2}{(1+x_d^2)^2} \right] p_d^2 \, .$$

As already explained above the term containing η_c can be cancelled as the number of events with odd and even orbital momentum between the outgoing mesons are equal. One obtains then

$$\sigma_d(l^-l^-) = \frac{|T|^2}{2\Gamma_d\Gamma_d} \left[\frac{x_d^2(2+x_d^2)}{(1+x_d^2)^2} \right] p_d^2 \, . \qquad (3.34d)$$

By changing in this last expression $d \rightarrow s$, one has the cross-section σ_e related to the $B_s^0 \overline{B}_s^0$ system.

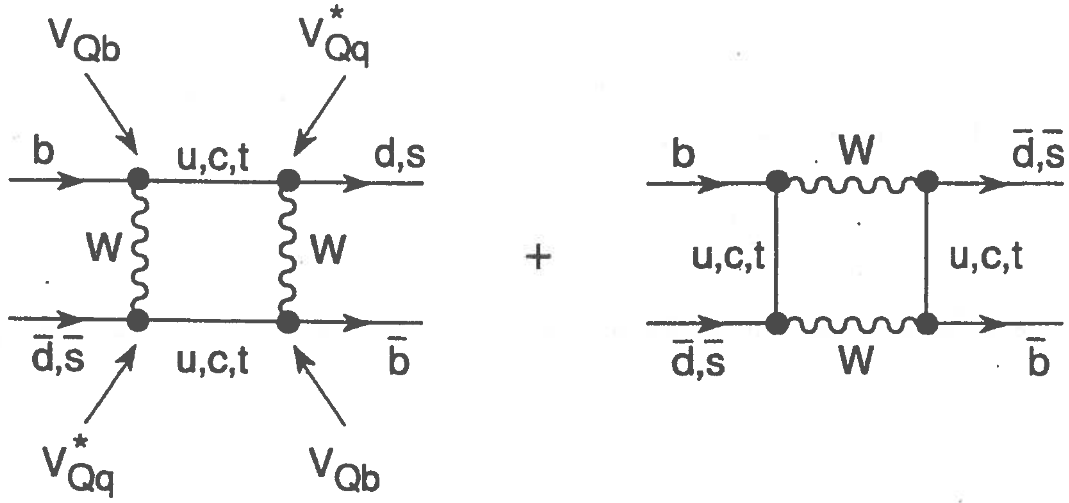

Fig. 3.1 - The box diagrams assumed to be responsible for the $\overline{B}_d^0 \to B_d^0$ mixing. The left-handed graph indicates also the manner in which the CKM matrix elements are defined. If the outgoing quark at a $q_1 q_2 W$ vertex is a down (up) quark, the matrix element is V_{ij}^* (V_{ij}). Note that Q (q) denotes a heavy (light) quark.

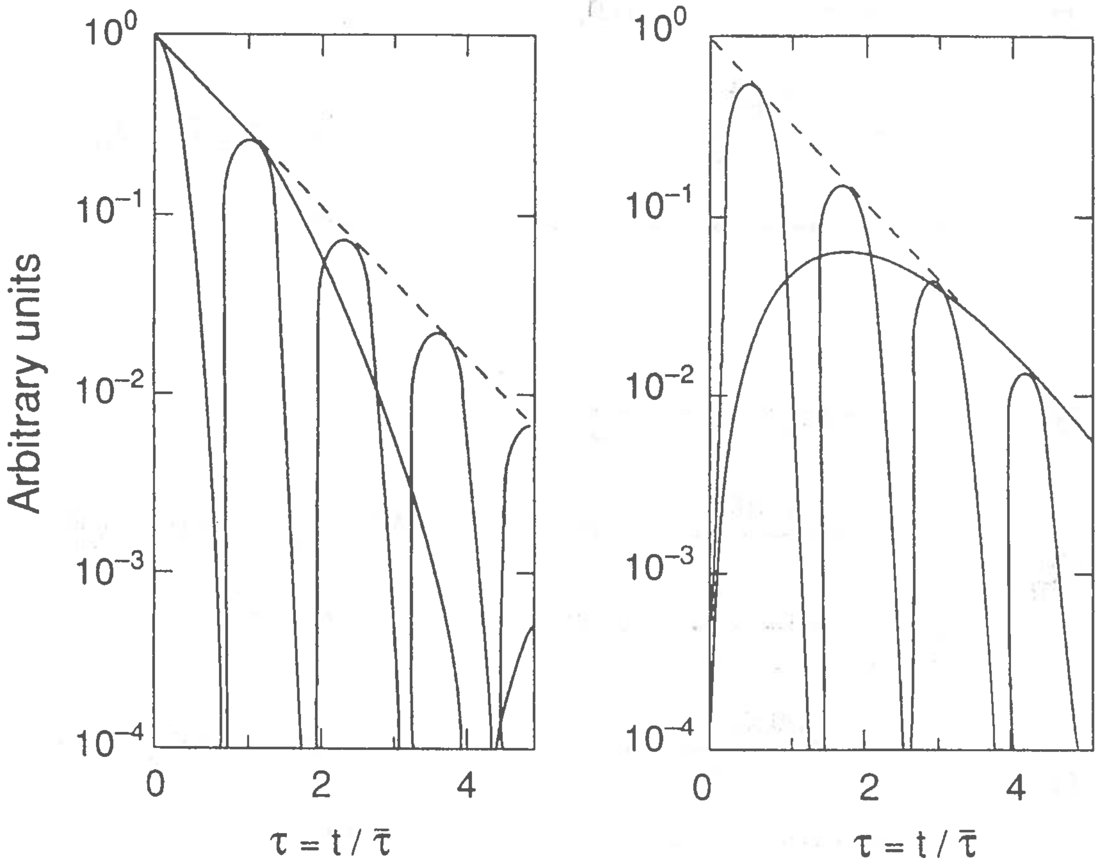

Fig. 3.2 - The time dependence of the B^0 and $\overline{B}^0$ mesons when pure B^0 have been produced at time $t = 0$. The curves (full lines) are calculated with x values of 0.75 and 5.

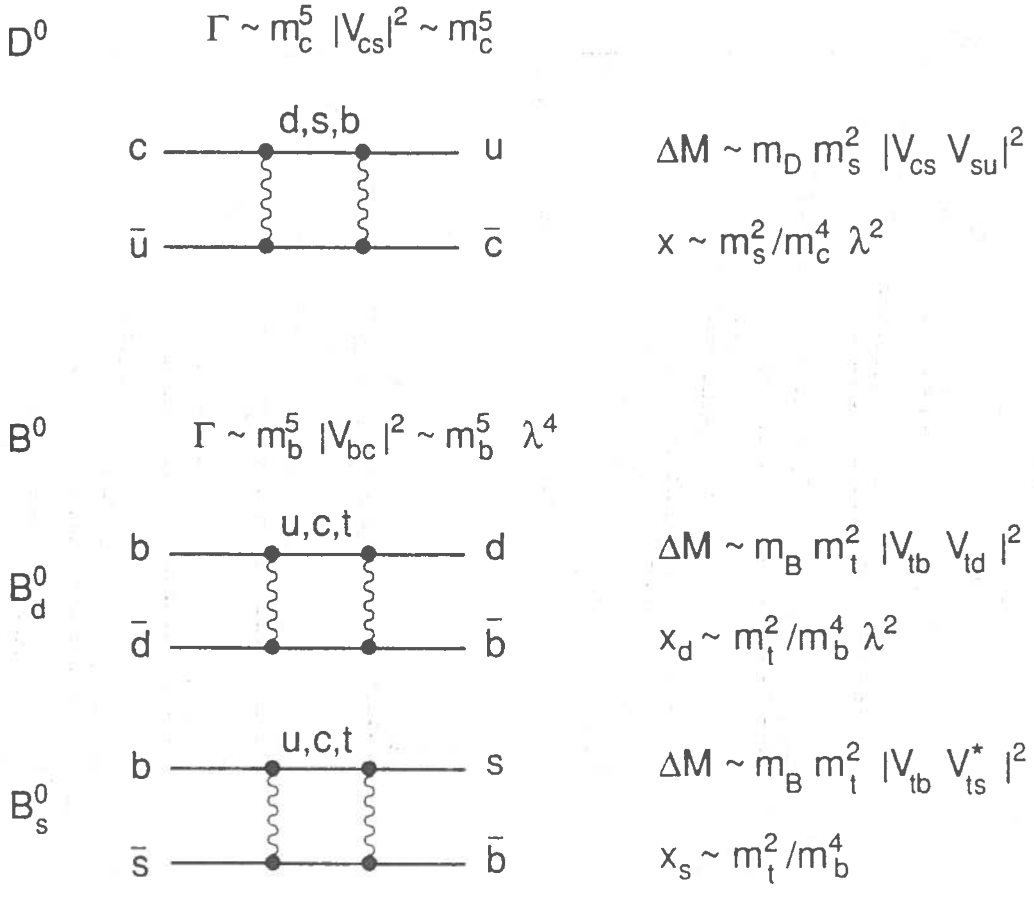

Fig. 3.3 - The various box diagrams which may contribute to the D^0 and $B^0_{d,s}$ mixing. In each case the dependance of x and Γ on the quark masses and on λ are indicated.

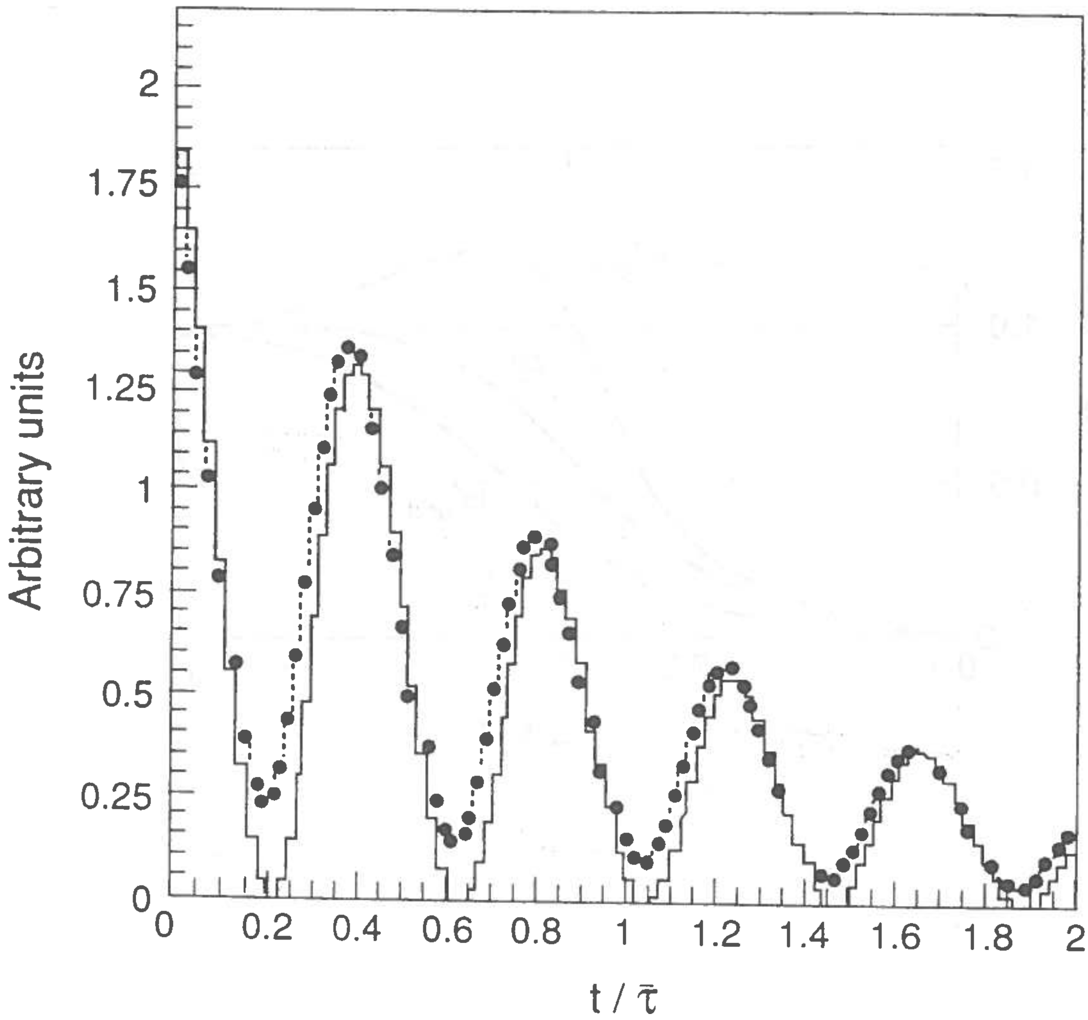

Fig. 3.4 - Comparison between the time-dependant decay distribution of the B_s^0 obtained with the B^- for the tagging process (full line) or with any beauty hadron (dash in the figure). The value of $x_s = 15$ and $\Gamma_N/\Gamma_- = 1$ have been taken for this example.

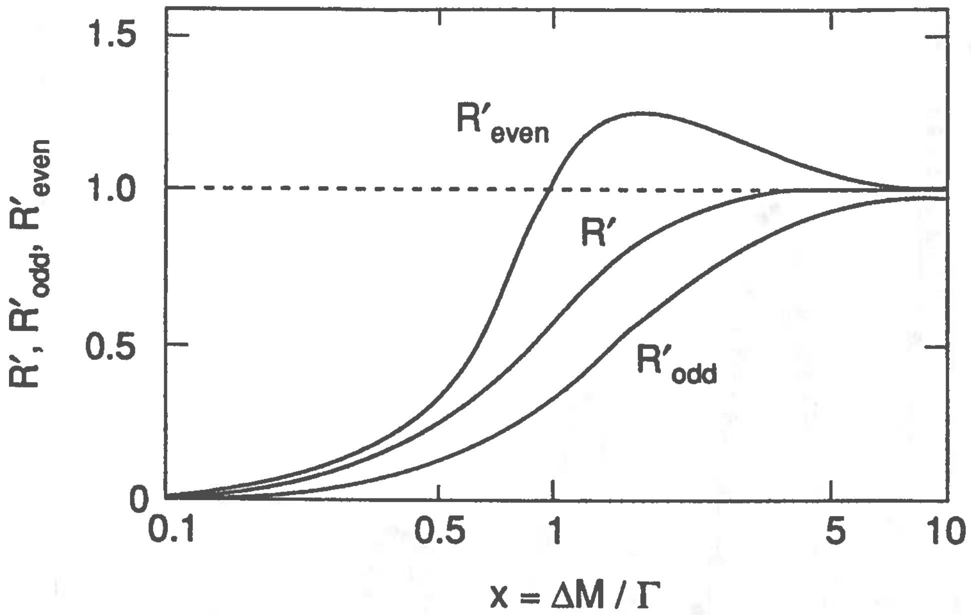

Fig. 3.5 - The $R' = [N(l^+l^+) + N(l^-l^-)]/N(l^+l^-)$ ratio as a function of x. The curves are obtained when the relative orbital momentum between the B and $\overline{B}$ is even ($R'_{\rm even}$), odd ($R'_{\rm odd}$), or when the number of odd and even parial waves are equal ($R' \equiv R'_{\rm odd+even}$).

4 - Generalities on CP violation in the B decays

4.1 - Introduction

In the following we will discuss the comparison of $B \to f$ with $\overline{B} \to \overline{f}$ decay in order to search for CP violation effects in the weak B meson decay. Here f representing a given final state while P and C denote the parity and the charge conjugate operators. We know from experiments that the parity is not conserved in the weak decay. This means that, if CP is violated, the charge conjugate can be conserved or violated. Our question now is how to learn from B decays the validity or not of CP conservation in these processes.

The search for CP violation in the B decay, can be advantageous by using decay channels which do not depend on the parity operation. Then the CP violation can simply by tested by comparing the $B \to f$ with its charged conjugated channel $\overline{B} \to \overline{f}$. In fact the $B \to f$ and $\overline{B} \to \overline{f}$ transition rates will not be influenced by the parity violation of the weak decays if the final state is a parity eigenstate.

As an example, let us consider the B decaying into two particles. Only one relative orbital momentum will then appear in the final state if the outgoing particles are spinless or if only one of them has a spin value different from zero. This leads to a parity eigenvalue of the final state. For instance, the $B^+ \to f^+$ (or $B^0 \to f$) could be compared with its charge conjugated states if, for instance, one uses $f^+ = D^0K^+, D^+\overline{D}^0, \ldots$ (or $f = J/\psi K_s^0, \pi^+\pi^-, \overline{D}^0\pi^0, \ldots$). In contrast, such an operation will not be applicable to the decay of $B_d^0 \to J/\psi K^{*0}, D^{*+}D^{*-}$ where the spin of the outgoing particle will allow even and odd orbital momentum between the outgoing particle (and hence even and odd parity contribution in the final state).

The detection of, or the possibility of setting limits on, CP violation is certainly one of the key reasons for collecting large $B\overline{B}$ data samples. In the framework of the standard model, the CP violation in the B and $\overline{B}$ decay will arise because of the complex CKM matrix elements. Therefore, any process where only $|V_{ij}|$ terms enter in the decay mechanism cannot be sensitive to these effects, in contrast to processes containing products of CKM elements with at least one complex element. As discussed in Chapter 2, the product will be of the form $V_{ai}V_{ak}^*V_{bj}V_{bk}^*$, which could lead to a difference between $B \to f$ and $\overline{B} \to \overline{f}$ as $V_{i,j} \leftrightarrow V_{i,j}^*$ when the

$B \to f$ amplitude is transformed to describe the charged conjugated $\overline{B} \to \overline{f}$ process (hereafter we always assume that the final state is a parity eigenstate apart from some specified exceptions). This means that the search for CP violation can only be applied when interference phenomena contribute to the decay process. We will see below that essentially either of the following methods or both can contribute to interferences:

- difference in the modulus of the decay amplitudes, namely $| < f \mid B > | \neq | < \overline{f} \mid \overline{B} > |$,
- mixing influence in the $B^0_{d,s}$ decay.

Thus, by choosing specific B decays having a definite parity eigenvalue in the final state, the CP violation effects can be searched for by detecting differences in the partial decay rates of $B \to f$ and $\overline{B} \to \overline{f}$. One defines the time-dependent $A(t)$ and the time-integrated A asymmetry parameters by

$$A(t) = \frac{\Gamma(B(t) \to f) - \Gamma(\overline{B}(t) \to \overline{f})}{\Gamma(B(t) \to f) + \Gamma(\overline{B}(t) \to \overline{f})} \tag{4.1}$$

$$A = \frac{\Gamma(B \to f) - \Gamma(\overline{B} \to \overline{f})}{\Gamma(B) \to f) + \Gamma(\overline{B} \to \overline{f})} \tag{4.2}$$

For example, $\Gamma(B(t) \to f) = | < f|B(t) > |^2$ denotes the time-dependent rate (argument t), while

$$\Gamma(B \to f) = \int \Gamma(B(t) \to f) dt$$

is the integrated decay rate (partial decay width). Non-vanishing values for $A(t)$ or A will, in principle, demonstrate the existence of CP violation in the B decay.

The interference arising from the amplitudes will be considered in some detail in Sections 4.2. In Section 4.3 we will examine the influence of the mixing, while the formalism will be described in Section 4.4. Expressions of the asymmetry parameters will then be given (Section 4.5) as well as some approaches about the measurement of CP violation parameters (Section 4.6). In Section 4.7 another possibilitiy for measuring one of the CP violation parameters will be discussed.

4.2 - CP violation due to decay amplitudes

Let us consider the simplest CP violation effect occurring through the decay amplitudes, namely when

$$|< f \mid B >| \neq |< \overline{f} \mid \overline{B} >| . \tag{4.3}$$

Let us recall that the above amplitudes represent those appearing at the production time $t = 0$. In the most general case one can always write[1]

$$< f \mid B >= \Sigma_j g_j M_j e^{i\delta_j} \tag{4.4}$$

where each term in the sum represents a mechanism (shown by a graph in the example given by Fig. 4.1) contributing to the $B \rightarrow f$ decay. Here g_j are the weak decay parameters containing products of CKM matrices involved in the considered graph, M_j are real quantities depending on each graph, and δ_j are phases due to final state interactions (strong or electromagnetic interactions). Under the transformation $< f \mid B > \rightarrow < \overline{f} \mid \overline{B} >$ the g_j becomes complex conjugate[2], while the phases due to final state interactions remain the same. Indeed, final state interactions among outgoing particles are not changed when all the outgoing particles are transformed into their antiparticles. One has then:

$$< \overline{f} \mid \overline{B} >= \Sigma_j g_j^* M_j e^{i\delta_j} . \tag{4.5}$$

If the same combination of CKM matrice elements enters into each term of the sum given by formula (4.4) [or (4.5)], they can be factorized out and

$$|< f \mid B >| = |< \overline{f} \mid \overline{B} >| .$$

The same equality could, of course, also occur if only real CKM elements enter in formula (4.4) and (4.5). If this were not the case, CP violation could occur, as the transition rates might be different.

To simplify our discussion, let us consider an example where only two graphs contribute essentially to the $B \rightarrow f$ and $\overline{B} \rightarrow \overline{f}$ amplitudes. One has then

$$< f \mid B > = g_1 M_1 e^{i\delta_1} + g_2 M_2 e^{i\delta_2}$$
$$< \overline{f} \mid \overline{B} > = g_1^* M_1 e^{i\delta_1} + g_2^* M_2 e^{i\delta_2} .$$

A simple calculation with formula (4.2) then gives the asymmetry parameter:

$$A = \frac{4\mathrm{Im}(g_1^* g_2)\ \sin(\delta_1 - \delta_2)\ M_1 M_2}{2 \mid g_1 \mid^2 M_1^2 + 2 \mid g_2 \mid^2 M_2^2 + 4\mathrm{Re}(g_1 g_2^*)\ \cos(\delta_1 - \delta_2)\ M_1 M_2} . \tag{4.6}$$

We notice again that we obtain our previous result, namely that for the same set of CKM matrix elements for each graph ($g_1 = g_2$) or with only real CKM elements, one has $A = 0$. Clearly, $A \neq 0$ when in addition to the fact that $g_1^* g_2$ has a non-vanishing imaginary part one also has $\delta_1 \neq \delta_2$. This last point is a crucial condition for searching CP violation effects in the case discussed here. The choice of investigating specific decay channels is difficult, as any estimate of the importance of final state interactions suffers from large uncertainties (model dependance).

a) **CP violation in the $B^{\pm}$decays**

A CP violation effect in the $B^{\pm} \to f^{\pm}$ decay can only occur through the decay amplitudes, as mixing does not influence the $B^{\pm}$ decays. Examples are shown in Fig. 4.2 as well as in Table 4.1. Let us now take the examples $B^- \to D^{*0} D^-$ and $B^+ \to \overline{D}^{*0} D^+$, yielding

$$< D^{*0} D^- \mid B^- > = V_{cb} V_{cd}^* A_1 + V_{ub} V_{ud}^* A_2$$
$$< \overline{D}^{*0} D^+ \mid B^- > = V_{cb}^* V_{cd} A_1 + V_{ub}^* V_{ud} A_2$$

where we used now $A_j = M_j e^{i\delta_j}$. Formula (4.6) becomes now

$$A = \frac{4\text{Im}(V_{cb} V_{cd}^* V_{ub} V_{ud}^*)\ M_1 M_2 \sin(\delta_1 - \delta_2)}{|< D^{*0} D^- \mid B^- >|^2 + |< \overline{D}^{*0} D^+ \mid B^+ >|^2} \ . \quad (4.7)$$

The CP violation parameter is given by $\text{Im}(V_{cb} V_{cd}^* V_{ub} V_{ud}^*)$. As seen in Chapter 2, the absolute value of this quantity is independant of the CKM matrix elements in the framework of the standard model with three generations. This means that the CP violation effect due to the inequality of the amplitude modulus is identical for all the $B^{\pm}$ channels (as well as for B^0). The measurement of the asymmetry parameters, however, will not be identical, as they will depend on the M_j parameters and on the final state interactions. One has also to note that in the case of two different decay mechanisms, one of them very often gives a small contribution to the decay process (in, for instance, the examples indicated in Fig. 4.2) leading thus to interference effects wich will be small with respect to the background. Therefore, it would be rather worthwile to use decay channels where the two graphs contributing to the decay mechanism have a similar order of magnitude.

Note that the time dependance $\Gamma(B^+(t) \to f^+)$ and $\Gamma(B^-(t) \to f^-)$ will not be very useful as they have nearly the same exponential behavior, a situation different for CP violation in the B^0 decay where mixing contributes to the decay

Table 4.1 - Example of $B, \overline{B}$ decays where no tagging is necessary and where CP violation effects could only arise from the decay amplitudes. $BR(tot)$ represents the measurements or rough estimates of the branching ratio leading to the final state indicated. Here we consider only charged particles in the final state.

Decay channel	Final state	$BR(tot)$
$B^+ \to \overline{D}^0 \pi^+$ $\overline{D}^0 \to K^+\pi^-$	$K^+\pi^+\pi^-$	$\sim 10^{-4}$
$B^+ \to J/\psi K^+$ $J/\psi \to \mu^+\mu^-$	$K^+\mu^+\mu^-$	$\sim 4\ 10^{-5}$
$B^+ \to \rho K^+$	$K^+\pi^+\pi^-$	$\sim 10^{-7}$
$B^0_d \to J/\psi \overline{K}^{*0}$ $J/\psi \to \mu^+\mu^-$ $\overline{K}^{*0} \to K^-\pi^+$	$K^-\pi^+\mu^+\mu^-$	$\sim 2\ 10^{-4}$
$B^0_s \to D^-_s \pi^+$ $D^-_s \to K^+K^-\pi^-$	$K^+K^-\pi^+\pi^-$	$\sim 3\ 10^{-5}$
$B^0_s \to \overline{D}^0 \overline{K}^{*0}$ $\overline{D}^0 \to K^+\pi^-$ $\overline{K}^{*0} \to K^-\pi^+$	$K^+K^-\pi^+\pi^-$	$\sim 10^{-4}$

processes (see Section 4.3). In the case discussed here the time behavior is determined by the B lifetime that is identical to its charged conjugated particle $\overline{B}$. Therefore, CP violation will be searched by measuring the A parameter [rather than $A(t)$].

b) CP violation in the B^0 decays

The CP violation due to the decay amplitudes can also occur for B^0 decays. The observation of such effects is more delicate because of the mixing processes (see Section 4.3). There are, however, B^0 decays where the observation of the final state identifies the type of the parent B meson. This happens when $f \neq \overline{f}$ can only be produced by the B^0 ($\overline{B}^0$) decay and not from the $\overline{B}^0$ (B^0) one. In such cases, difference between the B^0 and the $\overline{B}^0$ decays could only be due to the influence of the decay amplitudes. Table 4.1 gives some examples where specific B^0 decays allow one to identify the parent meson. However, in the standard model with three generations, no CP violation effects (or only negligible ones) are expected for the B^0 examples given in Table 4.1 (see also the discussion in Section 5.1 about the contribution of penguin diagrams when a J/ψ appear in the final state).

c) Measurement informations

Let us now assume that a difference between the $B^+ \to f^+$ and $B^- \to f^-$ decay widths (Γ^+ and Γ^-, respectively) has been observed. Information about the complex part of some CKM matrix elements could then be attempted. Let us now represent the amplitudes by

$$\begin{aligned} < f^- \mid B^- > &= A_1 e^{i\phi_1} e^{i\delta_1} + A_2 e^{i\phi_2} e^{i\delta_2} \\ < f^- \mid B^- > &= A_1 e^{-i\phi_1} e^{i\delta_1} + A_2 e^{-i\phi_2} e^{i\delta_2} \end{aligned} \tag{4.8}$$

for a two-graph contribution to the decay mechanism. The A_j now contain the M_j term and the modulus of the V_{ij} elements. The complex part of the CKM matrix elements is represented by the ϕ_j phases. One then obtains

$$\begin{aligned} \Gamma^- &= A_1^2 + A_2^2 + 2A_1A_2 \ \cos(\phi_W + \phi_F) \\ \Gamma^+ &= A_1^2 + A_2^2 + 2A_1A_2 \ \cos(-\phi_W + \phi_F) \end{aligned} \tag{4.9}$$

using $\phi_W = \phi_1 - \phi_2$ and $\phi_F = \delta_1 - \delta_2$. Models allow one to have estimates of A_1 and A_2 using the known estimates of the modulus of the CKM matrix elements entering in the decay channels considered[3]. This leads to estimates of

$$\begin{aligned} c_+ &= \cos(\phi_W + \phi_F) \\ c_- &= \cos(-\phi_W + \phi_F) \end{aligned}$$

yielding

$$\begin{aligned} c_+ + c_- &= 2\cos\phi_W \ \cos\phi_F \\ c_+ - c_- &= 2\sin\phi_W \ \sin\phi_F \ . \end{aligned}$$

One then has a twofold ambiguity for $\sin^2\phi_W$ given by

$$\sin^2\phi_W = \frac{1 - c_+c_- \pm \sqrt{(1-c_+^2)\,(1-c_-^2)}}{2} \ . \tag{4.10}$$

When only one complex CKM matrix element contributes to the considered decay process, one can obtain from the last equation some information about its weak phase[3]. The discussed method is, however, very uncertain as the estimate will depend on the models used to evaluate $A_{1,2}$. Furthermore, the precision of the $\sin^2\phi_W$ estimate will strongly depend on the phases due to final state interactions.

4.3 - Mixing and CP violation

It was recognized some years ago[4,5] that if the B^0 and the $\overline{B}^0$ mesons are able to decay into the same final state f (and hence necessarily into $\overline{f}$), CP violation could be observed as a result of the interplay between mixing and decay amplitudes. Thus the final state f (or $\overline{f}$) can be reached directly from the B^0 or $\overline{B}^0$ decay or through a $B^0 \leftrightarrow \overline{B}^0$ mixing with a subsequent decay (see the sketch presented in Fig. 4.3 and the example shown in Fig. 4.4). It is the interference between the different routes which can lead to CP violation effects in the framework of the standard model.

Two cases can be considered: namely where f is self-conjugate, $f = \overline{f}$ (as for instance ψK_s, $D\overline{D}$, $D^*\overline{D^*}$) and where $f \neq \overline{f}$ (see the example shown in Figs. 4.4). Let us first consider the simple case $f = \overline{f}$, which is usually expected to be the most important for CP violation effects.

a) Case where $f = \overline{f}$

The routes leading to the production of the f state are shown in Fig. 4.3a, which also indicate the meson produced at time $t = 0$ and responsible for the tagging procedure. Clearly, the observation of the final state does not give any information about the production at $t = 0$. The knowledge about the type of beauty quark (b or $\overline{b}$) contained in the associated beauty hadron produced at $t = 0$ could indicate if the production of a B^0 or $\overline{B}^0$ was responsible of the observed f state. This could, in principle, be obtained by observing the lepton charge ($l^\pm$) in semileptonic decay of the associated beauty hadron (tagging procedure) produced in the event ($b \rightarrow l^- X$ and $\overline{b} \rightarrow l^+ X$). In practice, however, the semileptonic decay occurs at a time $t \neq 0$. Therefore, in a similar fashon to the discussion we had in the measurement of the mixing process (Chapter 3), mixing has also to be taken into account for the $B^0, \overline{B}^0 \rightarrow lX$ decays.

To simplify the present discussion, let us consider only $B^\pm$ or the beauty baryons (where no mixing is present) for tagging. Then, the decay of $B^-, N_b \rightarrow l^- X$ or $B^+, \overline{N}_b \rightarrow l^+ X$ allows one the identification of the neutral B at birth (B^0 or $\overline{B}^0$). Let us remember that no CP violation is expected in the semileptonic decays, which should essentially occur through the tree diagram where the lighter quark will not participate in the decay mechanism (only $|V_{cb}|$ and $|V_{ub}|$ will then contribute to the decay).

A measured assymmetry parameter (A_m) can then be obtained by comparing the number of events [$N(l^+ f)$] having $l^+ f X$ in their final state with the number of

$l^- fX$ events $[N(l^- f)]$. A CP violation effect will then be observed if

$$A_m = \frac{N(l^+ f) - N(l^- f)}{N(l^+ f) + N(l^- f)} \neq 0 \,. \tag{4.11}$$

In Chapter 5 we will describe the formalism needed to take into account the production of the various type of beauty-hadron pairs in pN interactions.

b) Case where $f \neq \overline{f}$

As discussed above, the search for CP violation can be made by comparing the decays of

$$B^0 \to f \text{ with } \overline{B}^0 \to \overline{f} \quad \text{or}$$
$$B^0 \to \overline{f} \text{ with } \overline{B}^0 \to f \,.$$

The tagging procedure with the $B^\pm$, will correspond to the comparison of the following number of events (see Fig, 4.3b):

$$N(l^- f) \;\text{ with }\; N(l^+ \overline{f}) \quad \text{or} \tag{4.12a}$$
$$N(l^- \overline{f}) \;\text{ with }\; N(l^+ f) \,. \tag{4.12b}$$

The two methods are similar but not really equal (see next section). Also here, the search for the CP violation effect will be efficient if the two decay ways to the f or $\overline{f}$ state (Fig. 4.3b) have comparable magnitude.

4.4 - Formalism for the neutral B decays

Let us now express the transition rates of the $B^0 \to f$ and $\overline{B}^0 \to \overline{f}$ decays assuming a tagging that allows one to compare the $l^- fX$ and the $l^+ \overline{f} X$ number of events in a given experiment. Here we also implicitely assume that the tagging is only applied with $B^\pm$ mesons (or beauty baryons), the more complicated situation being discussed in Chapter 5. The expressions for $A(t)$ and A will be obtained by evaluating

$$\Gamma(B^0(t) \to f) = |< f \mid B^0(t) >|^2 \tag{4.13}$$
$$\Gamma(\overline{B}^0(t) \to \overline{f}) = |< \overline{f} \mid \overline{B}^0(t) >|^2 \,.$$

In the present notation, A_m represents the measured asymmetry parameter while A [and $A(t)$] denotes the expected value. Using expressions (3.8), namely

$$\boxed{\begin{aligned} &| B^0(t) >= f_+(t) \mid B^0 > +\eta f_-(t) \mid \overline{B}^0 > \\ &| \overline{B}^0(t) >= \frac{f_-(t)}{\eta} \mid B^0 > +f_+(t) \mid \overline{B}^0 > \end{aligned}} \tag{3.8}$$

from which we obtain

$$\begin{aligned} &< f \mid B^0(t) > = f_+(t) < f \mid B^0 > +\eta f_-(t) < f \mid \overline{B}^0 > \\ &< \overline{f} \mid \overline{B}^0(t) > = f_+(t) < \overline{f} \mid \overline{B}^0 > +\frac{f_-(t)}{\eta} < \overline{f} \mid B^0 > \ . \end{aligned}$$

We write these expressions as

$$\begin{aligned} < f \mid B^0(t) > &= < f \mid B^0 > (f_+(t) + \lambda f_-(t)) \\ < \overline{f} \mid \overline{B}^0(t) > &= < \overline{f} \mid \overline{B}^0 > (f_+(t) + \overline{\lambda} f_-(t)) \end{aligned}$$

using

$$\boxed{\lambda = \eta \frac{< f \mid \overline{B}^0 >}{< f \mid B^0 >} \quad , \quad \overline{\lambda} = \frac{1}{\eta} \frac{< \overline{f} \mid B^0 >}{< \overline{f} \mid \overline{B}^0 >} \ .} \tag{4.14}$$

The time-dependent rates are then obtained from formula (4.13) giving

$$\Gamma(B^0(t) \to f) = |T|^2 \Big(|f_+(t)|^2 + |\lambda|^2 |f_-(t)\mid^2 + 2\mathrm{Re}[\lambda f_-(t) f_+^*(t)] \Big) \tag{4.15a}$$

$$\Gamma(\overline{B}^0(t) \to \overline{f}) = |\overline{T}|^2 \Big(|f_+(t)|^2 + |\overline{\lambda}\mid^2 |f_-(t)|^2 + 2\mathrm{Re}[\overline{\lambda} f_-(t) f_+^*(t)] \Big) \tag{4.15b}$$

where $T =< f \mid B >$ and $\overline{T} =< \overline{f} \mid \overline{B}^0 >$. The approximations of $\Gamma_1 \simeq \Gamma_2$ (see formulae 3.10) leading to

$$\begin{aligned} |f_\pm|^2 &\simeq \frac{e^{-\Gamma t}}{2} (1 \pm \cos \Delta M t) \\ f_+^*(t) f_-(t) &\simeq i \frac{e^{-\Gamma t}}{2} \sin \Delta M t \end{aligned}$$

then give the transition rates:

$$\Gamma(B^0(t) \to f) = |T|^2 \frac{e^{-\Gamma t}}{2}(1 + \cos \Delta M t + \qquad (4.16a)$$
$$+|\lambda|^2(1 - \cos \Delta M t) - 2\text{Im}\lambda \ \sin \Delta M t)$$
$$\Gamma(\overline{B}^0(t) \to \overline{f}) = |\overline{T}|^2 \frac{e^{-\Gamma t}}{2}(1 + \cos \Delta M t + \qquad (4.16b)$$
$$+ |\overline{\lambda}|^2(1 - \cos \Delta M t) - 2\text{Im}\overline{\lambda} \ \sin \Delta M t) \ .$$

From the above formulae one sees that $A(t) \neq 0$ can arise from the CP violation due to the decay amplitudes, $|T| \neq |\overline{T}|$, or from the fact that $\lambda \neq \overline{\lambda}$. Note that in the latter case an eventual CP violation effect in the $B^0 \leftrightarrow \overline{B}^0$ mixing could also influence CP violation in the B^0 decay. This is because η enters in the definition of λ and $\overline{\lambda}$ [equations (4.14)]. The time integration of (4.16) yields

$$\Gamma(B^0 \to f) = |T|^2 \ \frac{1}{2\Gamma}(1 + a + |\lambda|^2(1 - a) - 2xa\text{Im}\lambda) \qquad (4.17a)$$
$$\Gamma(\overline{B}^0 \to \overline{f}) = |\overline{T}|^2 \frac{1}{2\Gamma}(1 + a + |\overline{\lambda}|^2(1 - a) - 2xa\text{Im}\overline{\lambda}) \qquad (4.17b)$$

from which we obtain A. Here $a = 1/(1 + x^2)$ where $x = \Delta M/\Gamma$ is the mixing parameter of the considered B^0 meson (x_d or x_s for the B^0_d or B^0_s, respectively). Once T, $\overline{T}$, λ and $\overline{\lambda}$ are estimate one can evaluate $A(t)$ and A. The expresions given above for estimating $N(l^- f)$ and $N(l^+ \overline{f})$ can also be used for the $N(l^- \overline{f})$ and $N(l^+ f)$ cases simply by replacing f ($\overline{f}$) by $\overline{f}$ (f). By using formula (4.14), one sees that this would correspond to the transformation of $\lambda \to 1/\overline{\lambda}$ and $\overline{\lambda} \to 1/\lambda$. Let us now express the asymmetry parameters for some specific decay processes.

Further comments

In the formulae (4.15) and (4.16), the parts due to the semileptonic decay were not included in the T and $\overline{T}$ expressions. This is because the decay of the $B^\pm$ and the B^0 (or $\overline{B}^0$) in an event are independent of each other in the considered examples. The constants introduced by the time integration of the $B^\pm$ decays have, therefore, no importance in the expressions of $A(t)$ and A.

4.5 - The asymmetry parameters in some simple cases

In the following we express the CP asymmetry parameters in some simple cases[6]. As above, we assume that the event tagging is made with the semileptonic decay of charged B mesons or beauty baryons.

1) No CP violation in the amplitudes

This assumption means that one has

$$|< f \mid B^0 >| = |< \overline{f} \mid \overline{B}^0 >|$$
$$|< \overline{f} \mid B^0 >| = |< f \mid \overline{B}^0 >|$$

as both B^0 and $\overline{B}^0$ are decaying into f and $\overline{f}$. Formulae (4.16) and (4.17) then lead to

$$A(t) = \frac{(|\lambda|^2 - |\overline{\lambda}|^2)\ (1 - \cos \Delta M t) - 2 \sin \Delta M t\ \mathrm{Im}(\lambda - \overline{\lambda})}{2 + |\lambda|^2 + |\overline{\lambda}|^2 + (2 - |\lambda|^2) - |\overline{\lambda}|^2)\ \cos \Delta M t - 2 \sin \Delta M t\ \mathrm{Im}(\lambda + \overline{\lambda})}$$

and

$$A = \frac{(1-a)\ (|\lambda|^2 - |\overline{\lambda}|^2) - 2xa\ \mathrm{Im}(\lambda - \overline{\lambda})}{2(1+a) + (1-a)\ (\mid \lambda \mid^2 + \mid \overline{\lambda} \mid^2) - 2xa\ \mathrm{Im}(\lambda + \overline{\lambda})} \tag{4.18}$$

still using $a = 1/(1 + x^2)$.

2) And no CP violation in the mixing process

In addition to the absence of CP violation in the amplitude we also assume that there is no CP violation in the mixing process ($|\eta|^2 = 1$). Then one has

$$\boxed{|\lambda| = |\overline{\lambda}|} \tag{4.19}$$

yielding

$$A(t) = \frac{-\sin \Delta M t\ \mathrm{Im}(\lambda - \overline{\lambda})}{1 + \cos \Delta M t + |\lambda|^2(1 - \cos \Delta M t) - \sin \Delta M t\ \mathrm{Im}(\lambda + \overline{\lambda})}$$

$$A = \frac{-x\mathrm{Im}(\lambda - \overline{\lambda})}{2 + x^2(1 + |\lambda|^2) - x\mathrm{Im}(\lambda + \overline{\lambda})}\ . \tag{4.20}$$

3) And weak phases due only to the CKM matrix elements

If we now use the conditions of the former cases and assume in addition that the phases in the amplitudes are entirely given by the CKM matrix elements, one has the relations

$$< f \mid B^0 > = < \overline{f} \mid \overline{B}^0 >^*$$
$$< \overline{f} \mid B^0 > = < f \mid \overline{B}^0 >^*$$

from which one obtains $\lambda = \overline{\lambda}^*$. The conditions

$$\boxed{\begin{aligned} |\lambda| &= |\overline{\lambda}| \\ \lambda &= \overline{\lambda}^* \end{aligned}} \tag{4.21}$$

now lead to

$$A(t) = \frac{-2 \sin \Delta M t \ \mathrm{Im}\lambda}{1 + \cos \Delta M t + |\lambda|^2 \ (1 - \cos \Delta M t)}$$

$$A = \frac{-2x \ \mathrm{Im}\lambda}{2 + x^2(1 + \mid \lambda \mid^2)} \ . \tag{4.22}$$

4) Case where in addition $f = \overline{f}$

The fact that f is selfconjugate means that the state vectors obey the relation $\mid f >= \pm \mid \overline{f} >$. Let us show that in this case one has $|\overline{\lambda}| = |\lambda| = 1$ and also $\overline{\lambda} = \lambda^*$ by still assuming that there is no CP violation in the amplitudes and that $|\eta|^2 = 1$. Defining φ as being the phase of η and φ_1 (φ_2), the phase of the $< f \mid B^0 >$ ($< \overline{f} \mid \overline{B}^0 >$) amplitude, one has

$$\eta = e^{i\varphi}$$
$$< f \mid B^0 > \ = |< f \mid B^0 >| \ e^{i\varphi_1}$$
$$< \overline{f} \mid \overline{B}^0 > \ = |< f \mid B^0 >| \ e^{i\varphi_2} \ .$$

One then obtains

$$\lambda = e^{i\varphi} \frac{< f \mid \overline{B}^0 >}{< f \mid B^0 >} = \pm e^{i\varphi} \frac{< \overline{f} \mid \overline{B}^0 >}{< f \mid B^0 >} = \pm e^{i\varphi} e^{i(\varphi_2 - \varphi_1)}$$
$$\overline{\lambda} = e^{-i\varphi} \frac{< \overline{f} \mid B^0 >}{< \overline{f} \mid \overline{B}^0 >} = \pm e^{-i\varphi} \frac{< f \mid B^0 >}{< \overline{f} \mid \overline{B}^0 >} = \pm e^{-i\varphi} e^{-i(\varphi_2 - \varphi_1)}$$

yielding

$$\boxed{\begin{array}{c}\overline{\lambda} = \lambda^* \\ |\,\overline{\lambda}\,| \;=|\,\lambda\,| = 1\end{array}} \tag{4.23}$$

The time-dependent rates take now a very simple form, i.e.

$$\begin{aligned}\Gamma(B^0(t) \to f) &= |< f \mid B^0 >|^2 \; e^{-\Gamma t}\Big(1 - \mathrm{Im}\lambda \;\; \sin \Delta M t\Big) \\ \Gamma(\overline{B}^0(t) \to f) &= |< f \mid B^0 >|^2 \; e^{-\Gamma t}\Big(1 + \mathrm{Im}\lambda \;\; \sin \Delta M t\Big) \; .\end{aligned} \tag{4.24}$$

The asymmetry parameters are again given by:

$$A(t) = -\sin \Delta M t \;\, \mathrm{Im}\lambda \tag{4.25a}$$

$$A = -\,\frac{x}{1+x^2}\;\mathrm{Im}\lambda \tag{4.25b}$$

5) <u>Case where $f = \overline{f}$, $|\eta|^2 = 1$, and $| < f|B > | \neq | < f|\overline{B} >$</u>

To calculate the $A(t)$ asymmetry parameter, we will use again the $|B^0(t)>$ and $|\overline{B}^0(t)>$ expressions given by formula (3.8) and using for simplicity:

$$f_+(t) = e^{-i\overline{M}t}\; e^{-\Gamma t/2}\;\cos\left(\frac{\Delta M t}{2}\right) \tag{3.10a}$$

$$f_-(t) = i\; e^{-i\overline{M}t}\; e^{-\Gamma t/2}\sin\;\left(\frac{\Delta M t}{2}\right) \; . \tag{3.10b}$$

Let us remember that $\overline{M} = (M_1 + M_2)/2$ is the average mass of the heavy and light B^0 mass. With these formulae one obtains the transition rates

$$\begin{aligned}\Gamma(B^0(t) \to f) = |< f|B^0 >|^2 e^{-\Gamma t}\Big[\cos^2\left(\frac{\Delta M}{2}\right) + \\ +|\lambda|^2\sin^2\left(\frac{\Delta M}{2}\right) - \mathrm{Im}\lambda \;\; \sin\Delta M t\Big] \\ \Gamma(\overline{B}^0(t) \to f) = |< f|B^0 >|^2 e^{-\Gamma t}\Big[\cos^2\;\left(\frac{\Delta M}{2}\right) + \\ +|\lambda|^2\sin^2\left(\frac{\Delta M}{2}\right) - \mathrm{Im}\lambda \;\; \sin\Delta M t\Big] \; .\end{aligned}$$

Here the same term $| < f \mid B^0 > |^2$ was taken out from the right part of the above expressions. The asymmetry parameter now becomes

$$A(t) = \frac{(1 - |\lambda|^2)\cos \Delta mt - 2\mathrm{Im}\ \lambda \sin \Delta Mt}{1 + |\lambda|^2} \tag{4.26}$$

with a $\cos \Delta Mt$ term appearing in the numerator of the $A(t)$ expression. Clearly, (4.26) becomes equivalent to (4.25a) if $|\lambda|^2 = 1$.

Additional comments

The case 4 (where $f = \overline{f}$) corresponding to the asymmetry parameters given by formula (4.25) is usually used for the discussion about the search for CP violation effects (as the CP violation parameter is expected to be important in that case). Equation (4.25b) cannot be used easily for the B_s^0 decay as the mixing parameter is expected to be large ($x_s/x_d \geq 15$, Section 3.4). This will reduce the asymmetry parameter $|A_s|$ for the B_s^0 decays as

$$A_s = -\frac{x_s}{1 + x_s^2}\ \mathrm{Im}\lambda \simeq -\frac{\mathrm{Im}\lambda}{x_s}\ .$$

The measurement of

$$A_s(t_s) = -\sin \Delta M_s t_s\ \mathrm{Im}\lambda = -\sin x_s \tau_s\ \mathrm{Im}\lambda$$

could then be more powerful, although strong oscillations require the measurement of the time τ_s (given here in B_s^0 lifetime units) with good precision.

4.6 - Measurement of the CP violation parameter

Let us again consider the case 4 of the previous section, namely when $f = \overline{f}$, $|\eta|^2 = 1$, $| < f|B > | = | < f|\overline{B} > |$ and when the imaginary part of the amplitudes are assumed to come only from the CKM matrix elements. As seen in Section 4.5, the asymmetry parameters will then depend only on one parameter $\mathrm{Im}\lambda$ obtained from the relation

$$\lambda = \eta \frac{< f \mid \overline{B}^0 >}{< f \mid B^0 >}\ . \tag{4.27}$$

For the present discussion, we utilize the standard model with three generations and the Wolfenstein approximation of the CKM matrix. In this approach only the V_{td} and V_{ub} elements will be complex (Chapter 2), and hence responsible for the possible CP violation effect. In order to represent the complexity of these elements we show in Fig. 4.5 one of the unitar triangles discussed in Chapter 2 [equation (2.18b)], where both V_{ub} and V_{td} appear namely,

$$V_{ud}V_{ub}^* \; + \; V_{cd}V_{cb}^* \; + \; V_{td}V_{tb}^* = 0 \; .$$

The ϕ_j angles appearing in this figure are then related to the CKM matrix elements by

$$\begin{aligned} Arg\; [V_{cd}V_{cb}^*V_{td}V_{tb}^*] \; &\Rightarrow \; \phi_1 \\ Arg\; [V_{ud}V_{ub}^*V_{td}V_{tb}^*] \; &\Rightarrow \; \phi_2 \\ Arg\; [V_{ud}V_{ub}^*V_{cd}V_{cb}^*] \; &\Rightarrow \; \phi_3 \; . \end{aligned}$$

To verify the validity of this approach, one could, for instance, measure the sides of this triangle or the relative angles $\phi_{1,2,3}$ shown in Fig. 4.5. The first method would be complicated from the experimental point of view, as one would have difficulties of determining with accuracy (today) the modulus of the V_{ub} and V_{td} elements. The measurements of $\phi_{1,2,3}$ will be simpler as they are related directly to Imλ obtained from the measurements of the asymmetry parameters $A(t)$ and A.

Let us now show the relation between λ and the ϕ_i angles shown in Fig. 4.5 using formula (4.27). The coefficient η is due to the B^0 mixing (η_d for $B_d^0 \leftrightarrow \overline{B}_d^0$ and η_s for $B_s^0 \leftrightarrow \overline{B}_s^0$) and is given by (see Chapter 3)

$$\eta_d \simeq \frac{V_{tb}^* \; V_{td}}{V_{tb} \; V_{td}^*} \simeq \frac{V_{td}}{V_{td}^*} = e^{2i\phi_1} \qquad (4.28a)$$

$$\eta_s \simeq \frac{V_{tb}^* \; V_{ts}}{V_{tb} \; V_{ts}^*} \simeq \frac{V_{ts}}{V_{ts}^*} = 1 \; . \qquad (4.28b)$$

From equation (4.28a), one sees that for any B_d^0 decay where no other complex $V_{i,j}$ element contributes to this process, one obtain ϕ_1 by measuring the CP violation parameter Im$\lambda \equiv \sin 2\phi_1$ [see equation (4.27) and Fig. 4.5]. At the quark level, the following decays

$$\begin{aligned} b \longrightarrow \; & c+\bar{c}d \qquad (4.29) \\ & c+\bar{c}s \\ & c+\bar{u}s \\ & c+\bar{u}d \end{aligned}$$

with their c.c., lead to the measurement of ϕ_1 assuming that the spectator (tree) model is predominant[7] (no penguin contributions).

One has to emphasize that processes of this kind at the quark level and appearing in the B_s^0 decay will give real values of λ as $\eta_s \simeq 1$ (for instance, the $B_s^0, \overline{B}_s^0 \to D_s^+ D_s^-, J/\phi\psi$ reactions). No CP violation effects should then be observed in the framework of the standard model assuming, in addition, that no difference appears in the decay amplitudes. Other cases of B_s^0 decay may lead to CP violation effects (for instance when $b \to uW$). Clearly, the $B_s^0, \overline{B}_s^0$ decay have to be investigated in order to see if our present approach concerning CP violation effects in B decay is really the right one.

There are some typical decay channels proposed for measuring the ϕ_i. They are[6,7]:

- $B_d^0 \to J/\psi K_s^0 \quad \Rightarrow \quad \text{Im}\lambda = \sin 2\phi_1$
- $B_s^0 \to \rho^0 K_s^0 \quad \Rightarrow \quad \text{Im}\lambda = \sin 2\phi_3$
- $B_d^0 \to \pi^+\pi^- \quad \Rightarrow \quad \text{Im}\lambda = \sin 2(\phi_1 + \phi_3)$

as shown in Fig. 4.5. In the last case, one does not measure directly ϕ_2. However, with the unitar triangle assumption one has $\phi_2 = \pi - \phi_1 - \phi_3$. Discussions about other decay channels allowing one to measure ϕ_{1-3} can be found in reference 7. Before presenting in the next section another method for measuring ϕ_3, let us add some comments about decay of B^0 channels where the final states are not CP eigenstates.

Let us consider the cases where the states are charge conjugate ($f = \overline{f}$) but not parity eigenstates. As already noted above, this can occur when a mixture of partial waves with different orbital momentum might be present in the final state due to the spins of outgoing particles. For example, this could happen for the $B^0 \to J/\psi K^{*0}, \psi' K^{0*}, D^{*+}D^{*-}$ decays (where $K^{*0} \to K_s^0 +$ pions in such a way that $f = \overline{f}$). To clarify our present discussion, let us first consider a final state having a CP eigenstate with an even or odd CP eigenvalue (+1 or -1). In this case, one could also write the $B^0, \overline{B}^0 \to f$ decay widths in the following forms

$$\Gamma(B^0 \to f) \equiv \Gamma_{CP}\,[1 - \epsilon]\ , \qquad \Gamma(\overline{B}^0 \to f) \equiv \Gamma_{CP}\,[1 + \epsilon]\ . \qquad (4.30)$$

The CP violation parameter A can then be written with the help of formulae (4.2) and (4.25b),

$$A = -\epsilon \equiv -\frac{x}{1 + x^2}\,\text{Im}\lambda\ . \qquad (4.31)$$

The form of equation (4.30) is evident. Without tagging the final f state obtained from $B^0 \to f$ and $\overline{B}^0 \to f$ processes will have a decay width of $2\Gamma_{CP}$, which, as expected, cannot depend of CP violation effects.

If the final f state will have an even (odd) CP eigenvalue, we will denote this decay by $B^0_+, \overline{B}^0_+ \to f$ ($B^0_-, \overline{B}^0_- \to f$). Then the decay widths can be expressed in the following ways:

$$\Gamma(B^0_+ \to f) \equiv \Gamma_+(1+\epsilon) , \quad \Gamma(\overline{B}^0_+ \to f) \equiv \Gamma_+(1-\epsilon)$$
$$\Gamma(B^0_- \to f) \equiv \Gamma_-(1-\epsilon) , \quad \Gamma(\overline{B}^0_- \to f) \equiv \Gamma_-(1+\epsilon) .$$

Here again $\Gamma(B^0_\pm \to f) + \Gamma(\overline{B}^0_\pm \to f)$ will not depend on a CP violation influence, as no tagging is present. Moreover, the asymmetry parameter is now reduced, as by calculating the asymmetry parameter A one obtains that

$$\mathrm{Im}\lambda \quad \to \quad \mathrm{Im}\lambda \, \frac{\Gamma_- - \Gamma_+}{\Gamma_- + \Gamma_+} . \tag{4.32}$$

Cuts on the angular distributions of the outgoing particles could allow one to separate the events having even and odd CP eigenvalues. Then both samples could be fitted simultanously to obtain $\mathrm{Im}\lambda$ using, however, opposite signs for $Im\lambda$ in the two samples.

4.7 - Further measurement possibilities for ϕ_3

The measurement of ϕ_3 with the $B^0_s \to \rho^0 K^0_s$ channel will be difficult as its branching ratio with charged particles in the final states is expected to be small ($\sim 10^{-6}$). Moreover, the detection efficiency of this reaction is further decreaed by detecting the semileptonic decay of the associated beauty hadron for the tagging procedure, as the branching ratio of the semileptonic decay is $BR(B \to \mu X, eX) \simeq 0.12$.

A new method for measuring ϕ_3 was proposed[8] with self-tagging channels. It was suggested that the $B^\pm \to D^0 K^\pm, \overline{D}^0 K^\pm$ decay be measured as well as the $B^\pm \to D^0_{1,2} K^\pm$. Here D^0_1 (D^0_2) is the CP even (odd) state of the charmed neutral mesons. For example, the decay of charmed mesons into $\pi^+\pi^-, K^+K^-$, etc., will identify D^0_1, whereas the $K^0_s\rho^0, K^0_s\phi$ etc., will indicate the D^0_2 . The flavor of the $B^\pm$ is tagged by $K^\pm$ ($B^\pm \to K^\pm X$), while the D^0 or $\overline{D}^0$ are identified by the $D^0 \to K^- X$ or $\overline{D}^0 \to K^+ X$ processes (one implicitely assumes that there is no CP violation in the $D^0/\overline{D}^0$ decay).

As an example we present in Fig. 4.6 the spectator diagrams contributing to the $B^+ \to \overline{D}^0(D^0)K^+$ decay. One spectator diagram contributes to the $B^+ \to D^0 K^+$, in contrast to the $B^+ \to \overline{D}^0 K^+$ channel. The two diagrams in the last case have, however, the same set of CKM matrix elements (no interferences will then appear between these two graphs). Therefore, the independent decay widths for describing the $B^\pm \to D^0(\overline{D}^0)K^\pm, D_{1,2}K^\pm$ are then:

$$\Gamma(B^+ \to D^0 K^+) = \Gamma(B^- \to \overline{D}^0 K^-) \tag{4.33a}$$

$$\Gamma(B^+ \to \overline{D}^0 K^+) = \Gamma(B^- \to D^0 K^-) \tag{4.33b}$$

$$\Gamma(B^+ \to \overline{D}_1^0 K^+)\ ,\quad \Gamma(B^- \to D_1^0 K^-)\ . \tag{4.33c}$$

Let us now use the above relations in order to express the amplitudes corresponding to $B^\pm \to D_{1,2}^0 K^\pm$, i.e.

$$A(B^+ \to D_{1,2}^0 K^+) = \frac{1}{\sqrt{2}}[A(B^+ \to \overline{D}^0 K^+) \pm A(B^+ \to D^0 K^+)] \tag{4.34a}$$

$$A(B^- \to D_{1,2}^0 K^-) = \frac{1}{\sqrt{2}}[A(B^- \to \overline{D}^0 K^-) \pm A(B^- \to D^0 K^-)] \tag{4.34b}$$

in a simple form (the notation being self-explanatory). Remember, that because of equations (4.33a) and (4.33.b), one has the following relations between the modulus of the amplitudes:

$$|A(B^+ \to \overline{D}^0 K^+)| = |A(B^- \to D^0 K^-)| \equiv |A_1|$$

$$|A(B^+ \to D^0 K^+)| = |A(B^- \to \overline{D}^0 K^-)| \equiv |A_2|$$

For simplicity, let us consider now the D_1^0 production. Relations (4.34) then become

$$A(B^+ \to D_1^0 K^+) = \frac{1}{\sqrt{2}}[|A_1|e^{i\delta_1} + |A_2|e^{i\phi_3}e^{i\delta_2}] \tag{4.35a}$$

$$A(B^- \to D_1^0 K^-) = \frac{1}{\sqrt{2}}[|A_1|e^{i\delta_1} + |A_2|e^{-i\phi_3}e^{i\delta_2}] \tag{4.35b}$$

taking the Wolfenstein parametrization where only V_{ub} is complex in the diagrams shown in Fig. 4.6. Here also $\delta_{1,2}$ represents the phases introduced by the final state interactions. The formula (4.34) with D_1 is represented in Fig. 4.7 showing the two-fold ambiguity of $2\phi_3$, the angle between the $A(B^+ \to D^0 K^+)$ and $A(B^- \to \overline{D}^0 K^-)$ amplitudes. One of the two solutions shown in the figure coressponds to

$2\phi_3$, whereas the second one is due to the difference $\Delta = \delta_2 - \delta_1$ between the phases of the final state interactions. Mathematically, this ambiguity can be seen by taking the modulus of expressions (4.35). One then has

$$|A(B^+ \to D_1^0 K^+)|^2| = \frac{1}{2}\left[|A_1|^2 + |A_2|^2 + 2|A_1|\ |A_2|\cos(\phi_3 - \Delta)\right]$$
$$|A(B^- \to D_1^0 K^-)|^2| = \frac{1}{2}\left[|A_1|^2 + |A_2|^2 + 2|A_1|\ |A_2|\cos(\phi_3 + \Delta)\right] .$$

By measuring the various decay widths one obtains estimates of

$$c_- = \cos(\phi_3 - \Delta) \quad \text{and} \quad c_+ = \cos(\phi_3 + \Delta)$$

indicating the two-fold ambiguity of ϕ_3 and Δ, as $\phi_3 \leftrightarrow \Delta$ do not change $c_\mp$.

The ambiguity can be resolved by choosing several reactions $B^\pm \to D^0(\overline{D}^0)X^\pm$ where $X^\pm = K^\pm, K^\pm\pi^0, K^\pm\pi^+\pi^-$ etc,. One could then find a solution where the weak phase is common to all the processes, while the phase due to the final state interactions will be different in each channel.

In this chapter, we have mainly discussed the possibilities for searching CP violation effects in the $B^\pm$ and $B^0, \overline{B}^0$ decays. For the last cases we consider the tagging procedure with semileptonic decays of $B^\pm$ (or beauty baryons). In practice, the tagging is somewhat more complicated, as no attempt is usually made to reconstruct the associated beauty hadrons. Only the charge of the lepton due to the semileptonic decay of the beauty hadrons is identified. One has, therefore, to also take into account the tagging due to the $B^0_{d,s}, \overline{B}^0_{d,s}$ decays. These important features for the case of pN interactions will be discussed in the next chapter.

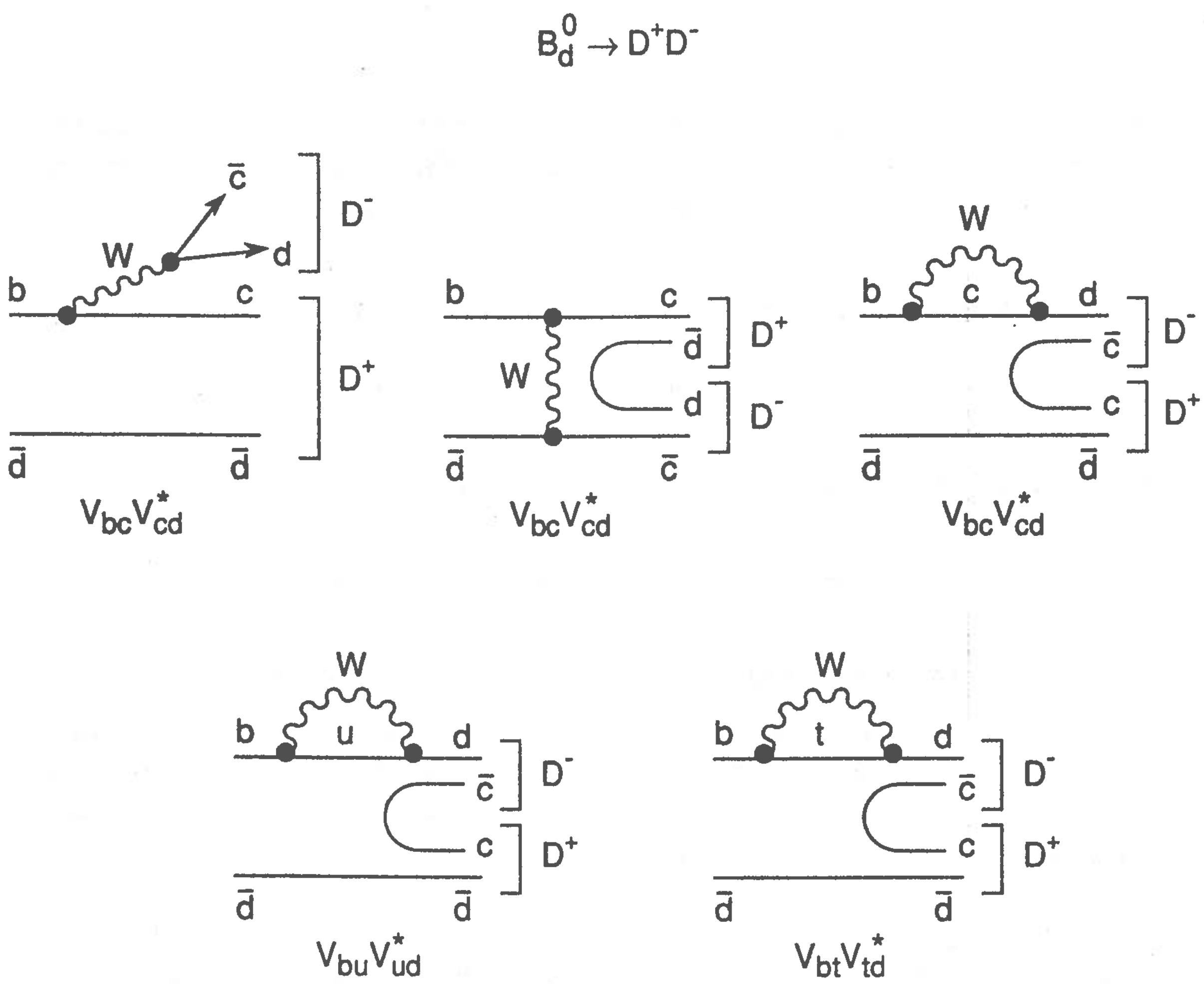

Fig. 4.1 - Graphs contributing to the $B_d^0 \rightarrow D^+D^-$ decay. Under each diagram the corresponding set of CKM matrix elements entering in the decay is indicated.

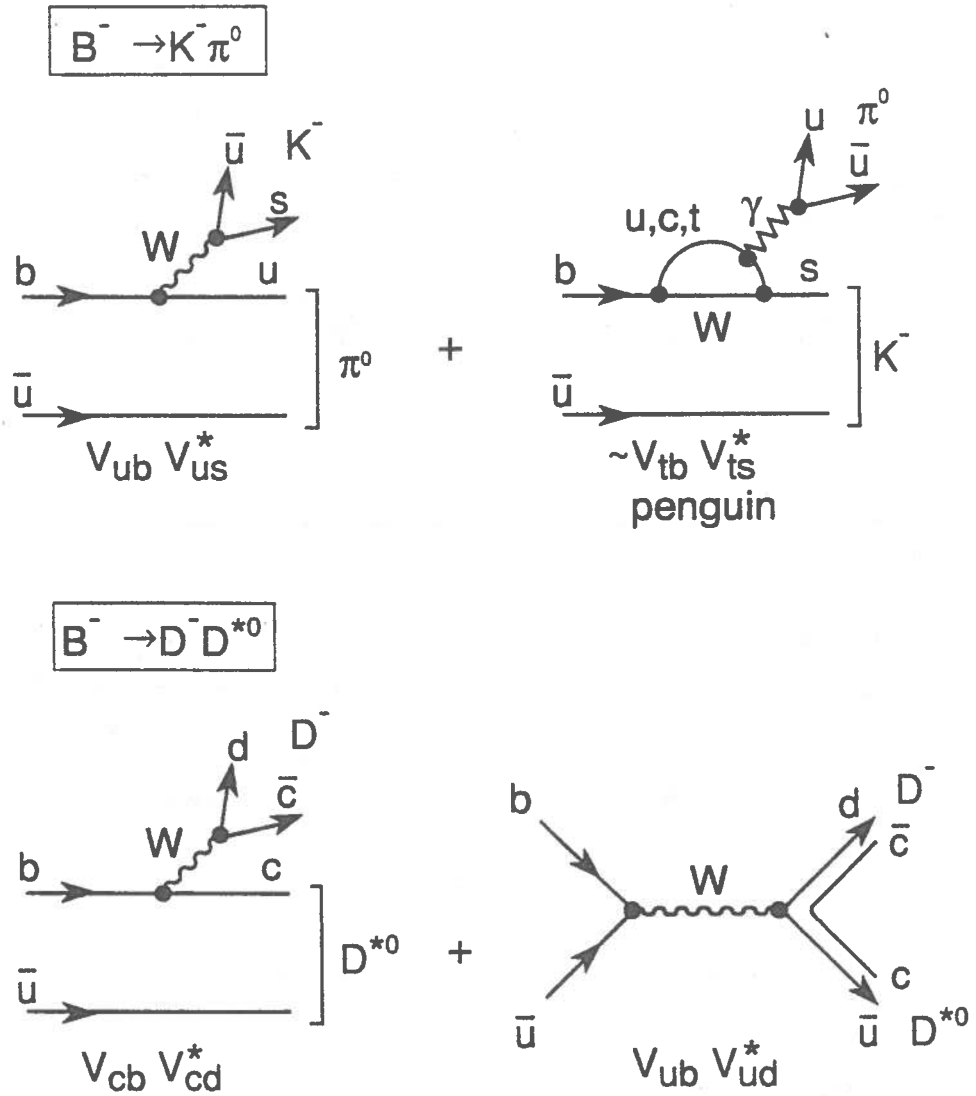

Fig. 4.2 - Examples of charged B decays which may proceed via two decay decay mechanisms involving different sets of CKM matrix elements.

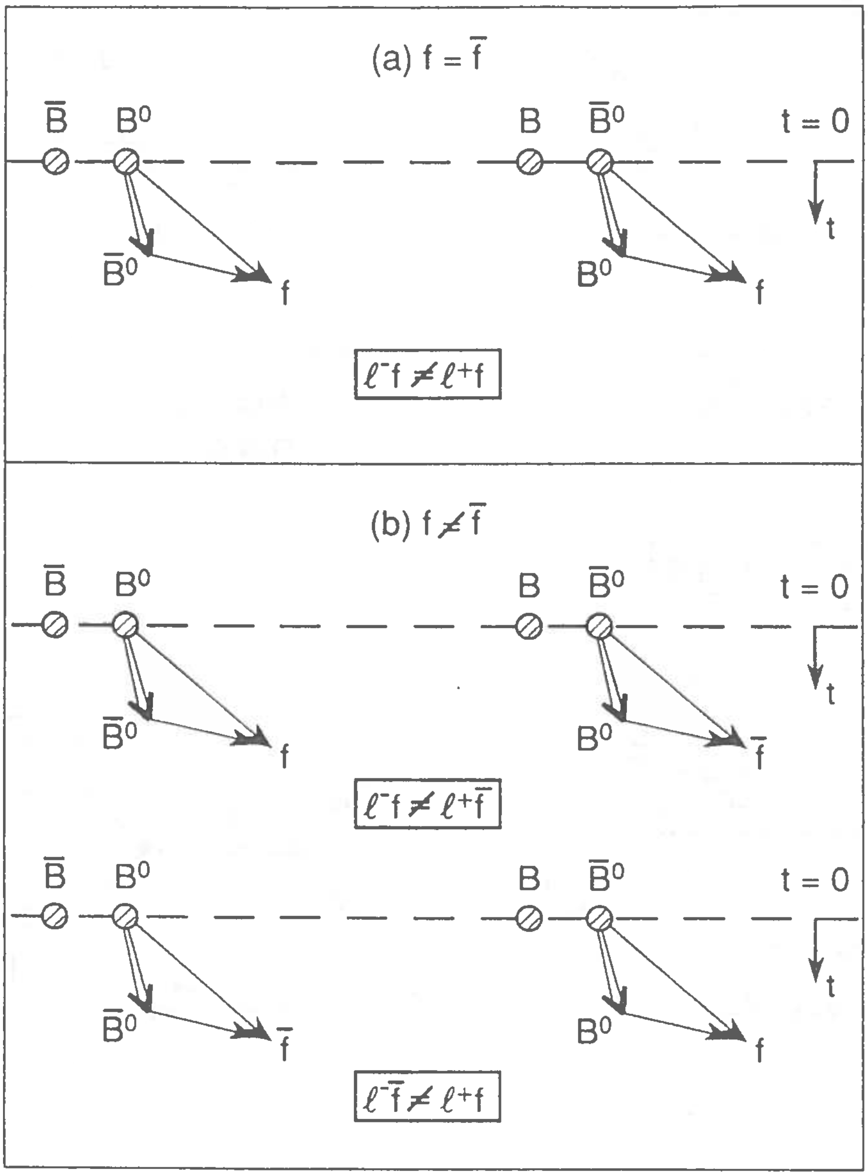

Fig. 4.3 - The B^0 or $\overline{B}^0$ produced at time $t = 0$ and responsible for the final state considered. In Section 4.3 the tagging will be considered to occur with the $B^\pm \rightarrow l^\pm X$ processes. a) Case when $f = \overline{f}$ leading to the comparison of events with $l^- f$ and $l^+ f$ in the final states, b) $f \neq \overline{f}$ yielding the comparison of $l^- f$ with $l^+ \overline{f}$ or $l^+ f$ with $l^- \overline{f}$.

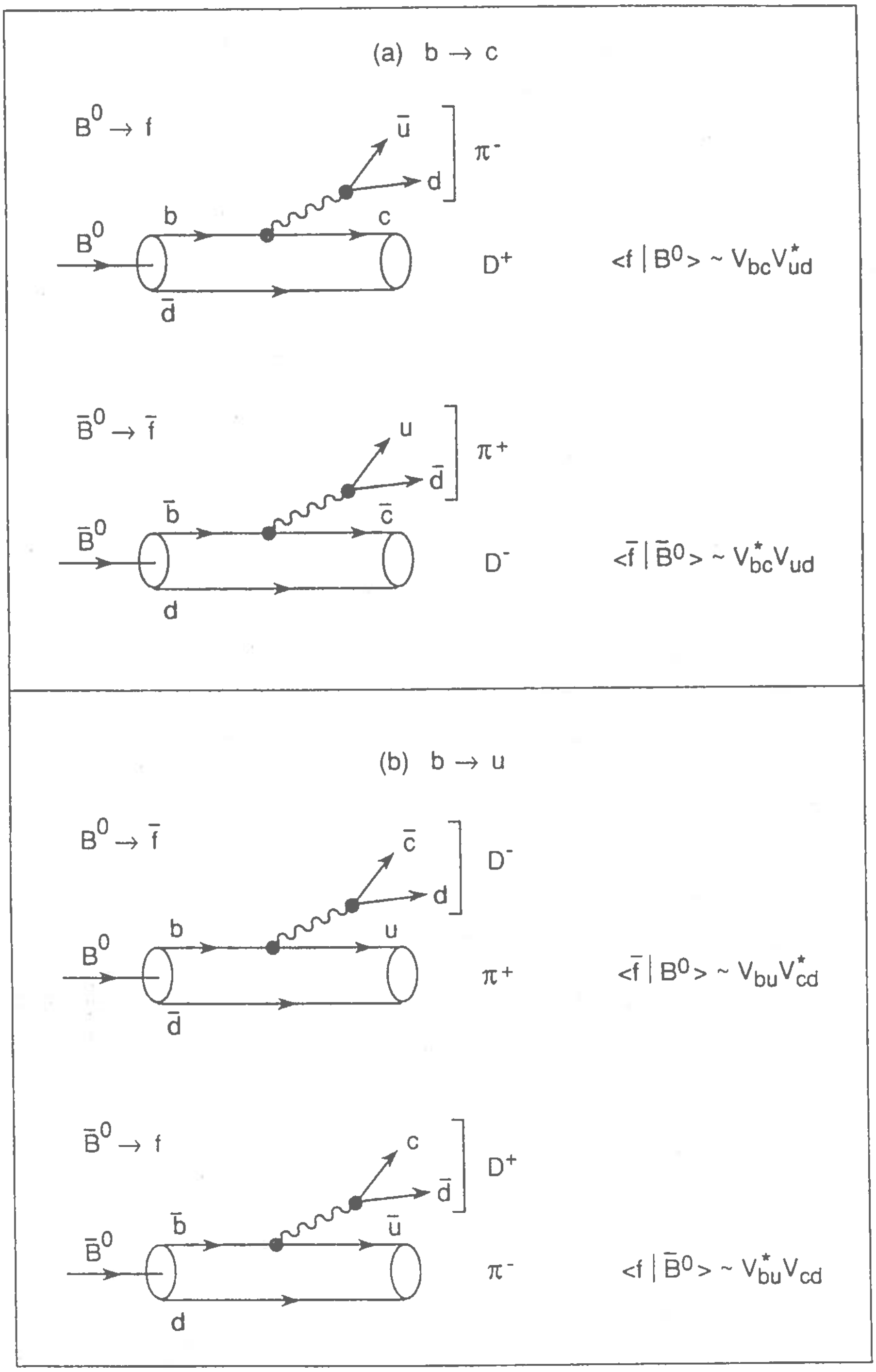

Fig. 4.4 - Graphs contributing to the $B_d^0 \to f$ and $\overline{B}_d^0 \to \overline{f}$ by means of $b \to c$ are displayed in (a). The decays involving $b \to u$ transitions are shown in (b). The set of CKM matrix elements entering in each graph is also indicated.

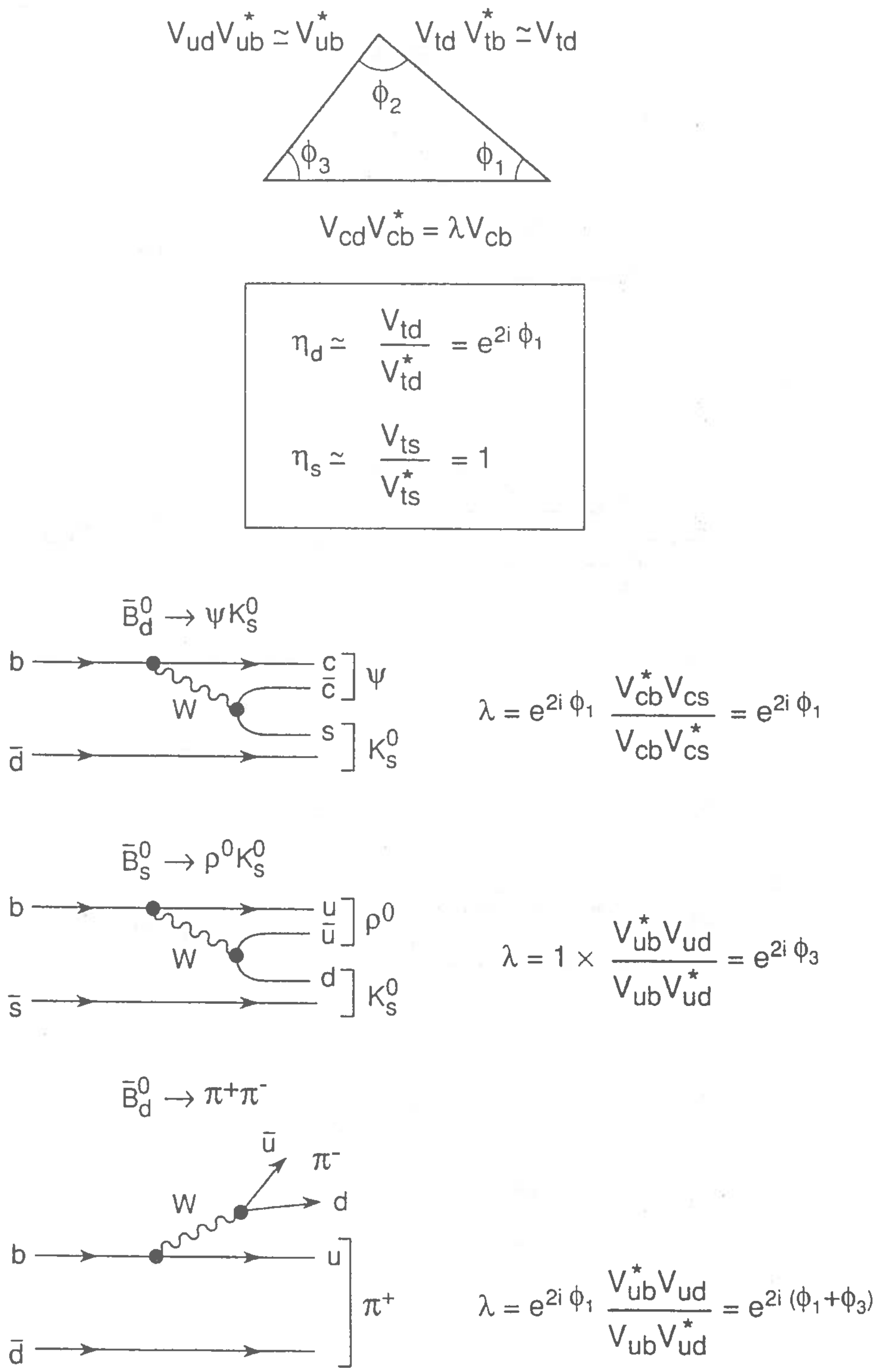

Fig. 4.5 - A unitary triangle in the complex plane (top) due to equation (2.18b), $V_{ud}V_{ub}^* + V_{cd}V_{cb}^* + V_{td}V_{tb}^* = 0$. In the Wolfenstein parametrization, the angles $\phi_{1,2,3}$ are due to the complex V_{ub} and V_{td} elements. Also shown are diagrams describing $B_{d,s}^0$ decays where $\phi_{1,2,3}$ could be estimated from the CP violation parameters $Im\lambda \equiv \sin 2\phi_j$.

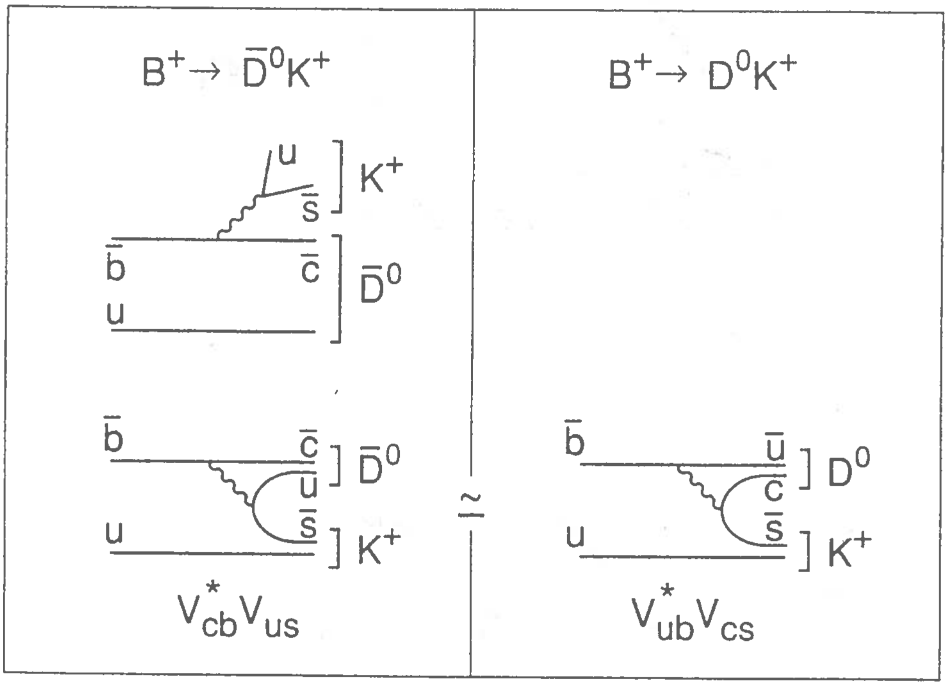

Fig. 4.6 - The spectator diagrams contributing to the $B^+ \rightarrow \overline{D}^0 K^+, D^0 K^+$ decays. The CKM matrix elements entering in these diagrams are also indicated.

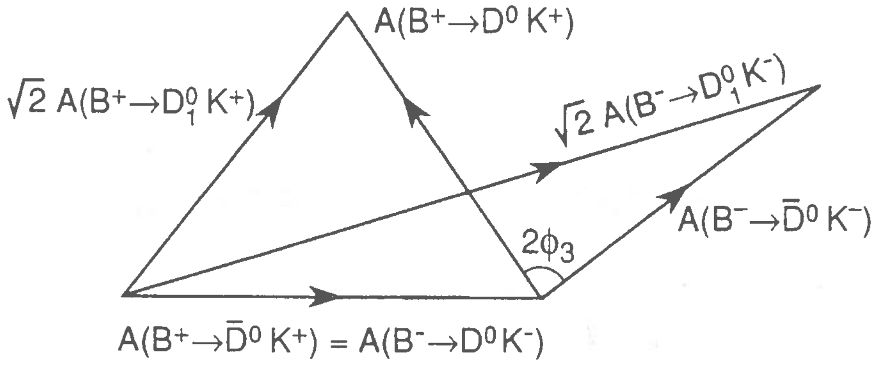

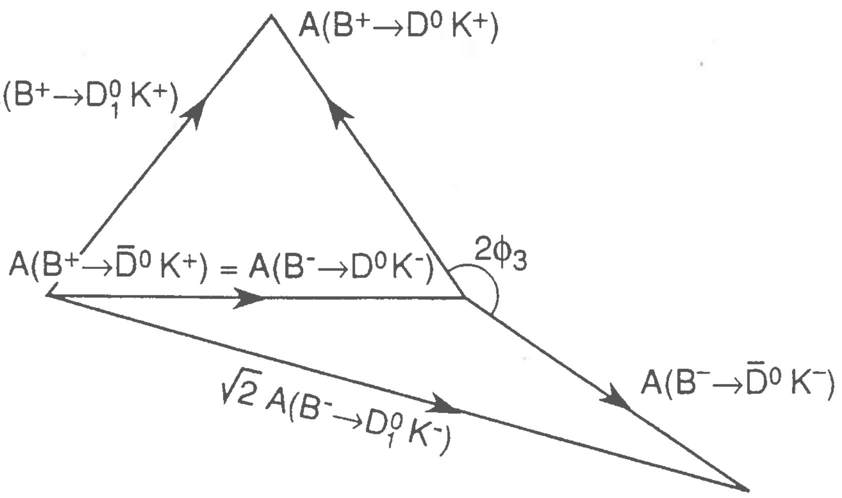

Fig. 4.7 - Relations in the complex plane between the decay amplitudes of the $B^+ \to \overline{D}^0 K^+$, $B^+ \to D^0 K^+$ and the $B^+ \to \overline{D}_1^0 K^+$ processes as well as those obtained from the B^- decay. The two-fold ambiguity of ϕ_3 is shown due to the unknown relative positions of the two triangles.

5 - B production in pN interactions

5.1 - Introduction

At large c.m. energies ($\sqrt{s} > 1$ TeV), the pp interactions are expected to have large $\sigma(b\bar{b})$ cross-sections and hence large production rates of beauty hadrons (see the comments given in Chapter 1). We will therefore discuss in more detail the B-physics that can be studied with the help of pp interactions. In particular, we will examine the problems related to the search for CP violation in the B^0 decay. Before doing this, let us note some difficulties addtional to those due to the production of different type of beauty-hadron pairs produced in pp (or pN) collisions (see Chapter 3).

In pp interactions the B and $\overline{B}$ are not obliged to be produced in equal amounts, in contrast to the $p\overline{p}$ (or e^+e^-) interactions. Therefore, the comparison of the $B \to f$ with $\overline{B} \to \overline{f}$ decay searching for CP violation through a measured asymmetry parameter, as for instance,

$$A_m = \frac{N(l^+f) - N(l^-\overline{f})}{N(l^+f) + N(l^-\overline{f})} \tag{5.1}$$

(see Chapter 4) may have some complications. Indeed, $A_m \neq 0$ would not necessarily prove the existence of CP violation effects. Let us now discuss this difficulty.

a) Beauty hadrons and their c.c. production

In the case where B and $\overline{B}$ are produced in equal amounts in hadron-hadron interactions, the relative production rates of the various types of beauty hadrons are assumed to be given by the relative production rates of the extracted sea quarks able to form with b (or $\overline{b}$) the beauty hadrons. As already discussed in Chapter 3, this is usually represented at large c.m. energies ($\sqrt{s} \geq 1$ TeV) by[1]

$$\begin{aligned} b\overline{u} : b\overline{d} : b\overline{s} : bqq &= p_u : p_d : p_s : p_n \\ &\simeq 0.38 : 0.38 : 0.14 : 0.10 \; . \end{aligned} \tag{5.2}$$

Let us recall that the p_k values, obtained from Monte Carlo calculations, are the probabilities of producing given beauty hadrons ($p_u + p_d + p_s + p_n = 1$). The same probabilities will be given for the charge conjugate (c.c.) beauty hadrons as the pair production $q\overline{q} \equiv u\overline{u}, d\overline{d}, s\overline{s}$ leads to the same number of q_j and $\overline{q}_j$.

For real pN interactions, however, the combinations of produced b or $\bar{b}$ with valence quarks contained in the beam particles change the equality of B and $\overline{B}$ production[2]. This can happen when a $\bar{b}$ quark combines with a u or d quark to form a B^+ or a B_d^0 meson, thus increasing these meson productions, or when the b forms a beauty baryon with a di-quark system contained in a beam particle (see Fig. 5.1). The additional bqq production decreases the number of $\overline{B} \equiv b\bar{q}$ events. One then has the following tendencies due to the b and $\bar{b}$ combinations with the valence quarks[3]:

$$\begin{aligned} \bar{b}q \text{ combination} \Rightarrow\ & N(\bar{b}u) \text{ increases} \\ & N(\bar{b}d) \text{ increases} \\ & N(\bar{b}s) \text{ decreases} \end{aligned} \tag{5.3}$$

$$\begin{aligned} bqq \text{ combination} \Rightarrow\ & N(b\bar{u}) \text{ decreases} \\ & N(b\bar{d}) \text{ decreases} \\ & N(b\bar{s}) \text{ decreases} \end{aligned} \tag{5.4}$$

(N denoting the number of beauty-hadrons produced in a given experiment). One notes that both effects increase the difference between the $B_{u,d}$ and $\overline{B}_{u,d}$ production. For pp interactions one expects that

$$\frac{N(\bar{b}u)}{N(b\bar{u})} \geq \frac{N(\bar{b}d)}{N(b\bar{d})} > 1 \tag{5.5a}$$

$$N(bqq) > N(\bar{b}\bar{q}\bar{q}) \ . \tag{5.5b}$$

In pn interactions, the total number of u and d quarks entering in beam-particle interactions are equal, leading to $N(\bar{b}u)/N(b\bar{u}) = N(\bar{b}d)/N(b\bar{d})$ in addition to (5.5b). One should also have:

$$\left[\frac{N(B^+)}{N(B^-)}\right]_{pp} > \left[\frac{N(B^+)}{N(B^-)}\right]_{pn} \tag{5.6a}$$

$$\left[\frac{N(B_d^0)}{N(\overline{B}_d^0)}\right]_{pp} < \left[\frac{N(B_d^0)}{N(\overline{B}_d^0)}\right]_{pn} \tag{5.6b}$$

while an equal difference between B_s^0 and $\overline{B}_s^0$ should appear in pp and pn interactions. The above expressions are only indications, as no phase space was taken into account and only combinations of b and $\bar{b}$ with valence quarks have been considered.

Table 5.1 - Examples of some B decays having a $J/\psi \to \mu^+\mu^-$ and charged partigles only in the final state. The total branching ratio $BR(tot)$ is calculated with the branching ratios of the B mesons (BR) and $BR(J/\psi \to \mu^+\mu^-) = 0.06$.

Channel	BR	$BR(tot)$	Final state
$B^+ \to J/\psi K^+$	$7.7\ 10^{-4}$	$4.6\ 10^{-5}$	$K^+\mu^+\mu^-$
$B_d^0 \to J/\psi K^*(892)$	$1.3\ 10^{-3}$	$7.8\ 10^{-5}$	$K^+\pi^-\mu^+\mu^-$
$K^* \to K^+\pi^-$	0.67		
$B_s^0 \to J/\psi\phi$	$5\ 10^{-3}$	$1.5\ 10^{-4}$	$K^+K^-\mu^+\mu^-$
$\phi \to K^+K^-$	0.49		

From the above remarks, it follows that the $N(B)/N(\overline{B})$ ratios that may have an influence on the search for CP violation in the B decay have to be measured. This can be done by using decay channels where CP violation effects are not expected. Channels with J/ψ in the final state will be particularly convenient as $J/\psi \to l^+l^-$ is planned to be used for the triggering process in several experiments studying pN interactions[4]. Table 5.1 indicates some reactions that can be used to measure the $N(B)/N(\overline{B})$ ratios. In the first two cases, each reaction can be compared with its charge conjugate one by identifying the outgoing $K^\pm$. For these channels the tree diagrams are expected to contribute mainly to the decay processes (Fig. 5.2). In fact, penguin diagrams contribute also to the decay mechanism (small contribution) as one has in the $b \to c\bar{c}s$ process two charge conjugate quarks (see Fig. 5.2). By using one of the unitar properties of the CKM matrix ($\sum V_{js}V_{jb}^* = 0$), one sees easily that the essential contribution du to the penguin diagrams has the same CKM matrix elements ($V_{cs}V_{cb}^*$) appearing in the tree diagram[6]. This fact avoids CP violation effects as no difference between the modulus of the two B and $\overline{B}$ decay amplitudes can occur. One obtains from the measurement of these decay rates the $N(B^+)/N(B^-)$ and $N(B_d^0)/N(\overline{B}_d^0)$ ratios at the c.m. energy considered.

For the same reasons no CP violation effect should appear in the $B_s^0, \overline{B}_s^0 \to J/\psi\phi$ decay. As the final state $f = J/\psi\phi$ is self-conjugate, the comparison of B_s^0 and $\overline{B}_s^0$ production can only be made between the tagged $N(l^+f)$ and $N(l^-f)$ events, or with the A_m parameter.

b) Advantages of unequal B and $\overline{B}$ production?

The unequal $B/\overline{B}$ in the pN production could also lead to some advantages[2]. Let us consider the $B_d^0 \to f$ and $\overline{B}_d^0 \to f$ decay with $f = \overline{f}$. The time-dependent rates can be written by formula (4.24) if the tagging is made with the $B^{\pm}$, namely

$$\frac{dN(B_d^0 \to f)}{d\tau_d} \propto N(B_d^0)\; e^{-\tau_d}\, [1 - n\ \sin x_d\tau_d] \qquad (5.7a)$$

$$\frac{dN(\overline{B}_d^0 \to f)}{d\tau_d} \propto N(\overline{B}_d^0)\; e^{-\tau_d}\, [1 + n\ \sin x_d\tau_d] \qquad (5.7b)$$

with $n \equiv \mathrm{Im}\lambda$. As usual, τ_d is the meson decay time in lifetime units and expressed in the meson rest frame while x_d is the mixing parameter of the B_d^0 or $\overline{B}_d^0$ meson. Without any tagging procedure, the time-dependence of the decay producing the f state is given by:

$$\frac{dN(B_d^0 \to f)}{d\tau_d} + \frac{dN(\overline{B}_d^0 \to f)}{d\tau_d} \propto e^{-\tau_d}\, [1 - \overline{A}\, n\ \sin x_d\tau_d] \qquad (5.8a)$$

$$\overline{A} = \frac{N(B_d^0) - N(\overline{B}_d^0)}{N(B_d^0) + N(\overline{B}_d^0)}\ . \qquad (5.8b)$$

Thus, the unequal amount of B_d^0 and $\overline{B}_d^0$ production can introduce an oscillation despite the fact that no tagging is applied and if $|n| > 0$.

As the tagging procedure is not needed for the present case, one could eventually consider pp interactions with large luminosities (at the LHC, the maximal predicted luminosity is $L \simeq 10^{34}\ \mathrm{cm}^{-2}\mathrm{s}^{-1}$, although the luminosity for the study of beauty physics is usually considered to be $L \simeq 10^{33}\ \mathrm{cm}^{-2}\mathrm{s}^{-1}$). Clearly, a detailed investigation has to be carried out in order to estimate the detection efficiency for events which may have a charged multiplicity larger than in the usual pp collisions. In addition, the luminosity $L = 10^{34} cm^{-2}s^{-1}$, for instance, would correspond to $\sim 10^9$ interactions per second, leading to experimental difficulties. Note also that it would be very useful to study the possibility of increasing $\overline{A}$ by eventual cuts on the emission angle and/or the momentum of the outgoing $B_d^0, \overline{B}_d^0$ mesons[3].

5.2 - Time dependence of the B^0 decay

In order to avoid the problems related to unequal amounts of B and $\overline{B}$ production, one could also study the time-dependence of the $B_d^0 \to f$ or/and $\overline{B}_d^0 \to \overline{f}$ decay taking into account the tagging procedure. A time oscillation dependence will prove the existence of CP violation effects and is, in fact, not sensitive to the unequal amounts of B and $\overline{B}$ production (see below). Let us now estimate the oscillation dependence of the B_d^0 ($\overline{B}_d^0$) decay when these mesons are produced in pN interactions.

Similarly as for the studying of mixing (Section 3.5), we consider the $B_d^0 \to f$ decay and the tagging with the semileptonic decay of the associated beauty baryon produced in the same event. Here, however, the situation will be different. The experimental reconstruction of the daughter f state will not sign the type of the parent meson as, both $B_d^0, \overline{B}_d^0$ mesons are able to decay into the f (or $\overline{f}$) state. This leads to a more tedious though straightforward calculation.

For an example of the calculation let us again consider the $l^- fX$ final state. The beauty-hadron pairs produced at time $t = 0$ and responsible for the final state considered are:

(1) $B^- B_d^0$

(2) $N_b B_d^0$

(3) $\overline{B}_s^0 B_d^0$ and $B_s^0 \overline{B}_d^0$ (coherent mixture)

(4) $\overline{B}_d^0 B_d^0$.

For the general cases, the double-differential time expressions have been derived in Appendix 5.A. Let us here consider case 4 of Section 4.6. The final state is self-conjugate ($f = \overline{f}$), there is no CP violation in the mixing procedure ($|\eta|^2 = 1$) and in the decay amplitudes ($| < f|B^0 > | = | < f|\overline{B}^0 > |$), assuming, in addition, that the complex part of the decay amplitudes is only due to the CKM matrix elements. Remember that this is equivalent to (4.23), i.e.

$$\boxed{\begin{aligned} \overline{\lambda} &= \lambda^* \\ |\, \overline{\lambda}\, | &= |\, \lambda \,| = 1 \end{aligned}}$$

leading to the following expressions[6,7] (see Appendix 5.A)

$$\frac{d\sigma_1(l^- f)}{dt_- dt_d} = |T|^2 e^{-(\Gamma_- t_- + \Gamma_d t_d)} \left[1 - n \ \sin \Delta M_d t_d\right] \tag{5.9a}$$

$$\frac{d\sigma_2(l^- f)}{dt_N dt_d} = |T'|^2 e^{-(\Gamma_N t_N + \Gamma_d t_d)} \left[1 - n \ \sin \Delta M_d t_d\right] \tag{5.9b}$$

$$\frac{d\sigma_3(l^- f)}{dt_s dt_d} = |T|^2 e^{-(\Gamma_s t_s + \Gamma_d t_d)} \left[1 - n \ (\sin(\Delta M_s t_s + \Delta M_d t_d) + \right. \tag{5.9c}$$

$$\left. + n \ \sin \Delta M_s t_s \cos \Delta M_d t_d \times (1 - \mathrm{Re}\eta_d) + \frac{\delta}{2} \sin \Delta M_s t_s)\right]$$

$$\frac{d\sigma_4(l^-f)}{dt_1dt_2} = |T|^2 e^{-\Gamma_d(t_1+t_2)} \left[1 - n\ (\sin \Delta M_d(t_1 \pm t_2)\right] \tag{5.9d}$$

using again $T =< l^-X \mid \overline{B} >< f \mid B_d^0 >$ and $T' =< l^-X \mid N_b >< f \mid B_d^0 >$. The CP violation parameter is represented again by $n = \text{Im}\lambda \equiv \sin 2\phi$ and where ϕ can be one of the three values predicted by the standard model with three generations. The derivation of these formulae are given in Appendix 5.A which also gives an estimate for δ.

The integration of these distributions over the decay time of the beauty hadron used for tagging purposes[2] gives the required distributions (Appendix 5.A).

$$\frac{d\sigma_1(l^-f)}{d\tau_d} = \frac{|T|^2}{\Gamma_+\Gamma_d} e^{-\tau_d} \left[1 - n\ \sin x_d\tau_d\right] \tag{5.10a}$$

$$\frac{d\sigma_2(l^-f)}{d\tau_d} = \frac{|T'|^2}{\Gamma_N\Gamma_d} e^{-\tau_d} \left[1 - n\ \sin x_d\tau_d\right] \tag{5.10b}$$

$$\frac{d\sigma_3(l^-f)}{d\tau_d} = \frac{|T|^2}{\Gamma_s\Gamma_d} e^{-\tau_d} \left[1 - \frac{n}{1+x_s^2}(x_s\ \cos x_d\tau_d\ \text{Re}\eta_d + \right. \tag{5.10c}$$

$$\left. + \sin x_d\tau_d) + \frac{x_s}{2(1+x_s^2)}\ \delta\right]$$

$$\frac{d\sigma_4(l^-f)}{d\tau_d} = \frac{|T|^2}{\Gamma_d^2} e^{-\tau_d}\left[1 - \frac{n}{1+x_d^2}(x_d\ \cos x_d\tau_d \pm \sin x_d\tau_d)\right] . \tag{5.10d}$$

With the same notation of Chapter 3, Γ_-, $\Gamma_{d,s}$ and Γ_N are the the decay widths of the $B^-, B_{d,s}^0$ and N_b, respectively. The mixing of the $B_{d,s}^0$ meson is given by $x_{d,s}$ whereas $\tau_d = t_d/\overline{\tau}_d$. For estimates of the distributions due to formula (5.10), one can consider, as above, that the amplitudes are nearly equal and that

$$\Gamma_+ = \Gamma_d = \Gamma_s \simeq \frac{\Gamma_N}{\epsilon} .$$

In Chapter 3, we already mentioned that the term with the $\pm$ sign in the time distribution, corresponding to the charge-conjugation value ± 1 of the $B_d^0\overline{B}_d^0$ system, vanishes for c.m. energies well above the $B\overline{B}$ threshold production. The observed $d\sigma(l^-f)/d\tau_d$ distribution will then be obtained by adding, incoherently, the equations (5.10a) to (5.10d), each of them being weighted by the production values of the quarks considered, for instance, from the probabilities given by expression

(5.2). With these values, one obtains that

$$\frac{d\sigma(l^- f)}{d\tau_d} = \sum_{j=1}^{4} p_d\, p_j\, \frac{d\sigma_j(l^- f)}{d\tau_d}$$

is not very sensitive to the variation of p_i to within a few percent. As an example[2], we consider the distribution obtained for the $l^+ f$ case with $n = 0.25$, $x_d = 0.72$ and $x_s = 8$ (Ref. 2). Assuming that the various Γ_i widths are nearly equal ($\epsilon = 1$), one obtains the distribution of Fig. 5.3 taken from Ref. 2, the $|T|^2\, e^{-\tau}/\Gamma_i\Gamma_d$ being factorized out using $|T| = |T'|$. This distribution was calculated with $\mathrm{Re}\eta_d \simeq 1$. This approximation is not very important as the oscillation introduced by formula (5.10c) is here nrgligible. For comparison we also present in Fig. 5.3 the distribution obtained by tagging only B^+. One sees that this distribution has a larger oscillation amplitude than in the general case.

In the absence of CP violation in the decay amplitude ($|\overline{T}| = |T|$), the formulae (5.10) can also be used for the $l^+ f$ case by simply changing $n \to -n$. Both time distributions obtained from the $l^- f$ and $l^+ f$ could be fitted simultanously taking into account the opposite n signs. Unequal amounts of B and $\overline{B}$ production will not really affect the oscillation behavior of $d\sigma(l^\pm f)/d\tau_d$ but only introduce a small difference in the number of events contributing to the $d\sigma(l^- f)/d\tau_d$ and $d\sigma(l^+ f)/d\tau_d$ distributions. Note also that formula (5.10c) is not very sensitive to the B_s^0 mixing parameter, as one expects a large x_s value. The situation will be different for the B_s^0 decay, as $s \leftrightarrow d$ [(5.10c) will then become sensitive to the mixing but not (5.10d)].

One has to emphasize that the time-dependence measurement will not be simple. Small oscillations (small frequencies) will certainly require important statistics of events (the B_d^0 case where $x_d \sim 0.7$) while large oscillations (B_s^0 with $x_s \geq 10$) will also need time measurements with acceptable accuracies. Nevertheless, CP violation parameters for B_s^0 could, practically, only be measured with the time-dependence distribution (see the comments in Section 4.5).

5.3 - The integrated cross-sections

If the relative amount of B and $\overline{B}$ production in pp (or pN) is known or if these differences are negligible, a comparison between the, eventual corrected, $\sigma(l^- fX)$ and $\sigma(l^+ fX)$ cross-section could also be used to search for CP violation effects. By integrating the distributions[2] given by (6.11), one obtains the following expressions for the cross-sections[8] containing the weighting $p_d\ p_j$ factors:

$$\sigma_{1+2}(l^- f) = (p_\pm + \frac{p_N}{\epsilon})\ p_d\ |T|^2 \left[1 - n\ \frac{x_d}{1+x_d^2}\right] \tag{5.11a}$$

$$\sigma_3(l^- f) = p_s\ p_d\ |T|^2 \left[1 - n\ \frac{(x_d + x_s\ \mathrm{Re}\eta_d)}{(1+x_s^2)\ (1+x_d^2)} + \frac{x_s\ \delta}{2(1+x_s^2)}\right] \tag{5.11b}$$

$$\sigma_4(l^- f) = p_d\ p_d\ |T|^2 \left[1 - n\ \frac{x_d}{(1+x_d^2)^2}\right] \tag{5.11c}$$

[remember that $\epsilon = \Gamma_N/\Gamma_i$, $|T| = |T'|$, while the Γ_i are here included into $|T|^2$].

The total $\sigma(l^- f)$ cross-section will then be obtained by adding incoherently the above expressions. Assuming still that there is no CP violation in the decay amplitudes ($|T| = |\overline{T}|$), formulae (5.11a) to (5.11c) can be applied to the $l^+ f$ case by transforming $n \to -n$. Then, with the $\Sigma[\sigma_i(l^- f) \pm \sigma_i(l^+ f)]$ expressions obtained from (5.11), the asymmetry parameter (5.1) becomes

$$A = -\left[\frac{n x_d}{1+x_d^2}\ (p_\pm + \frac{p_N}{\epsilon}) + \frac{n(x_s + x_d)}{(1+x_s^2)(1+x_d^2)}\ p_s + \frac{n x_d}{(1+x_d^2)^2}\ p_d\right] \tag{5.12a}$$

$$A = -\frac{n x_d}{1+x_d^2}\left[\ p_\pm + \frac{p_N}{\epsilon} + \frac{(x_s + x_d)}{(1+x_s^2)^2 x_d}\ p_s + \frac{1}{1+x_d^2}\ p_d\right]. \tag{5.12b}$$

taking $\mathrm{Re}\eta_d \simeq 1$. The term in front of the bracket in (5.12b) represents the asymmetry obtained by using only $B^\pm$ (or/and $N_b, \overline{N}_b$) for the tagging procedure [equation (4.25b)] which we will denote here by $A_\pm$. The expression inside the bracket of (5.12b) that we symbolize by D' has a value of $D' < 1$. This D' factor is often called a dilution factor of the asymmetry parameter (as $|A| \leq |A_\pm|$) due to the mixing phenomenon. This definition is perhaps not the best one as it is difficult to condemn the mixing process. Without mixing ($x_{d,s} = 0$), one will necessarily have in the standard model $A = 0$, with or without CP violation effects.

<u>Remarks about asymmetry measurements</u>

The fact that $|A_\pm| > |A|$ does not necessarily mean that it would be more efficient to search for CP violation in the B^0 decay by tagging only $B^\pm$ decays (for simplicity we do not consider here the $\overline{N}_b$ and N_b case). This can be seen as follows.

Using the probabilities p_j given by (5.2), $x_d = 0.7$ and $x_s = 15$, one obtains from formulae (4.25b) and (5.12) that

$$A_\pm \simeq 0.46 \ \sin 2\phi \quad \text{and} \quad A \simeq 0.36 \ \sin 2\phi \tag{5.13}$$

now replacing n by $\sin 2\phi$. The number of events, $N = N(l^- f) + N(l^+ f)$, needed to measure an asymmetry parameter $A = [N(l^- f) - N(l^+ f)]/N$ with n_s standard deviations is given by

$$N = n_s^2 \ [\frac{1 - A^2}{A^2}] \ . \tag{5.14}$$

For measuring the asymmetry parameters $A_\pm$ and A with the same number of standard deviations for a given $\sin 2\phi$ value one would, therefore, need the following ratio of $pp \to b\bar{b}X$ events

$$\frac{N_\pm(b\bar{b})}{N(b\bar{b})} = \frac{1}{p_\pm} \frac{1 - A_\pm^2}{1 - A^2} \frac{A^2}{A_\pm^2} \simeq 1.5 \ \frac{1 - [0.46 \sin 2\phi]^2}{1 - [0.36 \sin 2\phi]^2}$$

with the chosen p_j values given by formula (5.2) and the expression (5.12a). Here $N_\pm(b\bar{b})$ and $N(b\bar{b})$ are the number of $b\bar{b}$ events tagged with semileptonic decay of $B^\pm$ or by any beauty hadron decay, respectively. This means that in the present example, one would have

$$\boxed{N_\pm(b\bar{b}) > N(b\bar{b}) \ .} \tag{5.15}$$

even if one assumes that the $B^\pm$ reconstruction efficiency in an experiment will be ~ 100 %. Therefore, the decrease of the oscillation (example of Fig. 5.3) does no decrease the quality of the A measurement with respect to that of $A_\pm$ for a given experiment.

5.4 - Mistagging effects

Let us now discuss some dilution effects which decrease the experimental value of the asymmetry parameter and render more difficult the observation of CP violation phenomena. Let us consider the effects due to the mistagging of the leptons used for the tagging procedure. Error in the identification of the leptons will decrease the measured asymmmetry parameter A_m given by equation (5.1). This can occur in the following cases:

A) the cascade process, $b \to c \to l^+$ $(\bar{b} \to \bar{c} \to l^-)$ where the l has the opposite charge to that of the $b \to l^-$ $(\bar{b} \to l^+)$ decay (Fig. 5.4),

B) the l's coming from other decaying particles (K, π, for example),

C) the punchthrough in the detector (charge and leptons wrongly identified).

Mistagging of $e^\pm$ and $\mu^\pm$ will certainly be different for cases B and C, as they depend essentially on the detector used in a given experiment. Note also that all cases usually contribute equally to the misidentification of l^+ and l^- in the final state (apart from some specific experiments that we will not discuss here).

Assuming that the correct (wrong) number of events is represented by $N^c_\pm$ $(N^w_\pm)$, the measured asymmetry will be given by

$$A_m = \frac{N^c_+ + N^w_+ - N^c_- - N^w_-}{N_t} , \tag{5.16}$$

N_t representing the total number of true and wrong tagged events. The real A value, described by formula (5.12a), and the fraction of wrong tagging (w) are here defined by

$$A = \frac{N^c_+ - N^c_-}{N^c_+ + N^c_-} = \frac{N^w_- - N^w_+}{N^w_+ + N^w_-} \tag{5.17a}$$

$$w = \frac{N^w_+ + N^w_-}{N_t} = 1 - \frac{N^c_+ + N^c_-}{N_t} . \tag{5.17b}$$

One then obtains that the measured asymmetry parameter is given by $A_m = A(1-2w)$. The $D'' = 1 - 2w$ is a real dilution effect, as the misstagging of the leptons decrease the A parameter. Moreover, detected $l^\pm f$ samples contain always a fraction of background events (N_{back}), together with the events due to the considered decays (N_{sig}). Therefore a further decrease in the A parameter by $D''' = N_{sig}/(N_{sig} + N_{back})$ will occur. Finally, the measured asymmetry can be expressed by

$$A_m = A \times D'' \times D''' \equiv A\,(1-2w)\,\frac{N_{sig}}{N_{sig} + N_{back}} \tag{5.18}$$

where one can also represent the A parameter by separating some of the mixing influence namely, $A = A_\pm \times D'$. In any case the D''' could be obtained easily from the data of a given experiment. Further corrections can also be included in order to describe the real values of the observed A_m. Let us now discuss the possibilities of measuring w.

5.5 - Measurement of w

In order to estimate w, one can compare $B^{\pm} \to f^{\pm}$ or $B_d^0 \to f$ with $\overline{B}_d^0 \to \overline{f}$ when CP violation should not occur in the decay. For the $B_d^0, \overline{B}_d^0$ decay one considers cases where $f \neq \overline{f}$ and where the final state signs the parent type (B or $\overline{B}$). Then the measurement in an experiment of the number of events having these kinds of decays [$N_m(f^{\pm})$, $N_m(f)$ and $N_m(\overline{f})$] allows one to estimate the expected number of events having the final states $f^{\pm}, f$ or $\overline{f}$ in addition to the tagging lepton [$N(l^{\pm} f^{\mp})$, $N(l^- f)$ and $N(l^+ \overline{f})$]. A difference between the $N(lf)$ estimates and the observed number of events [$N_m(lf)$] allows an estimate of the dilution parameter w for the cases A to C. Let us discuss this in more details.

a) The $B^{\pm} \to f^{\pm}$ decay

Let us first consider the $B^+ \to f^+$ decays. The events having $l^- f^+ X$ in the final state will be produced by the following beauty hadron pairs appearing at the production time ($t = 0$):

(1) $B^- B^+$

(2) $N_b B^+$

(3) $\overline{B}_d^0 B^+$

(4) $\overline{B}_s^0 B^+$.

Then the relations between the expected number of $l^- f^+ X$ events [$N(l^- f^+)$] and the observed ones [$N_m(f^+)$] will be given by[10]

$$\frac{N(l^- f^+)}{N_m(f^+)} = BR(\overline{B} \to l^- X) \times [p_{\pm} + p_d\, \beta_d + p_s\, \beta_s + \frac{p_N}{\epsilon}] \,, \tag{5.19}$$

where $BR(\overline{B} \to l^- X)$ represents the B semileptonic branching ratio taking into account that $BR(\overline{B} \to l^- X) \simeq BR(N_b \to l^- X)/\epsilon$. Note that $\beta_{d,s}$ [see formula (3.14)] is defined by

$$\beta_{d,s} \equiv 1 - \chi_{d,s} = \frac{B_{d,s}^0 \to B_{d,s}^0}{B_{d,s}^0 \to B_{d,s}^0 + B_{d,s}^0 \to \overline{B}_{d,s}^0} \tag{5.20}$$

is introduced as $\overline{B}_{d,s} \to B_{d,s}^0$ does not contribute to the $l^- f X$ final state. The measured number of events $N_m(l^- f^+)$ thus allows us to obtain

$$w \simeq \frac{N(l^- f^+) - N_m(l^- f^+)}{N(l^- f^+)} \ . \tag{5.21}$$

The same type of evaluation could also be obtained with the $l^+ f^- X$ final state. In fact, larger statistics could be obtained by taking the $B^+ \to f^+$ and $B^- \to f^-$ decays, yielding

$$w \simeq \frac{N(l^- f^+) + N(l^+ f^-) - N_m(l^- f^+) - N_m(l^+ f^-)}{N(l^- f^+) + N(l^+ f^-)} \ . \tag{5.22}$$

The $B^\pm \to J/\psi K^\pm$ channels, already proposed for studying the $N(B^+)/N(B^-)$ ratio in pN interactions (Section 5.1), can also be used for measuring w. If B^+ and B^- are not produced in equal amounts corrections have to be applied.

b) The $B_d^0 \to f$ process

At high c.m. energy ($\sqrt{s} \geq 1$ Tev), the identification of $K^\pm$ is usually not simple from the experimental point of view. However, the second channel given in Table 5.1, $B_d^0 \to J/\psi K^*, K^* \to K^+ \pi^-$ with its c.c., can also be used to estimate w. The additional constraint that the effective mass of the $K\pi$ system has to be equal to the K^* mass will facilitate the identification of the B_d^0 and $\overline{B}_d^0$ mesons. But we have to take into account the coherence of the mixing processes when a pair of neutral beauty mesons is produced. The $l^- f X$ final state could now be produced by the following pairs of beauty hadrons (produced at $t = 0$):

(1) $B^- B_d^0$

(2) $N_b B_d^0$.

(3) $\overline{B}_s^0 B_d^0$ and $B_s^0 \overline{B}_d^0$ (coherent mixture)

(4) $\overline{B}_d^0 B_d^0$

For these cases the production rates (P_j) can be calculated with the wave functions describing the decay processes[7] without CP violation effects, and leading to[9]

$$P_1 \propto BR(B \to lX)\ p_\pm p_d \tag{5.23a}$$

$$P_2 \propto BR(B \to lX)\ \frac{p_N}{\epsilon} p_d \tag{5.23b}$$

$$P_3 \propto BR(B \to lX) \left[1 + \frac{1 - x_d x_s \mathrm{Re}\eta_d}{(1+x_d^2)\,(1+x_s^2)}\right] \frac{p_s p_d}{2} \tag{5.23c}$$

$$P_4 \propto BR(B \to lX) \left[1 + \frac{1}{(1+x_d^2)^2}\right] \frac{p_d^2}{2} \tag{5.23d}$$

(Appendix 5.B). The factor 1/2 in formulae (5.23c) and (5.23d) allows one to have $P_{3,4} \propto BR(B \to lX)p_{s,d}p_d$ if $x_d, x_s \to 0$. One also notices here that the contribution of (5.23c) will be negligible with respect to the other cases. Similarly to the previous case, we obtain

$$\frac{N(l^- f)}{N_m(f)} = BR(b \to l^- X)\Bigg[\left(1 + \frac{1 - x_d x_s \mathrm{Re}\eta_d}{(1+x_s^2)(1+x_d^2)}\right)\frac{p_s}{2} + \\ + \left(1 + \frac{1}{(1+x_d^2)^2}\right)\frac{p_d}{2} + p_\pm + \frac{p_N}{\epsilon}\Bigg] \; , \tag{5.24}$$

assuming again that the decay amplitudes are identical in the four cases. By measuring the $N_m(f)$ and $N_m(\overline{f})$ as well as $N_m(l^- f)$ and $N_m(l^+ \overline{f})$ one gets a formula similar to (5.22) but where $f^+ \to f$ and $f^- \to \overline{f}$.

5.6 - Some comparison with $\Upsilon(nS) \to B\overline{B}$

The production of $B^0_{d,s}$ mesons through the $e^+e^- \to \Upsilon(nS) \to B^0\overline{B}^0$ processes ($n = 4, 5$) lead to different complications for searching CP violation effects. This is due to the fact that only a pair of $B^0\overline{B}^0$ can be produced. The $d\sigma(l^- f)/(dt_1 dt_2)$ and the $d\sigma(l^- f)/dt_1$ distributions are given by formulae (5.9d) and (5.10d) expressed here in the forms:

$$\frac{d\sigma(l^- f)}{dt_1 dt_2} = |T|^2 e^{-\Gamma_d(t_1+t_2)} \left[1 - n \left(\sin \Delta M_d(t_1 + \eta_c t_2)\right)\right] \tag{5.25a}$$

$$\frac{d\sigma(l^- f)}{d\tau_d} = \frac{|T|^2}{\Gamma_d^2} e^{-\tau_d}\left[1 - \frac{n}{1+x_d^2}(x_d \; \cos(x_d \tau_d) + \eta_c \sin(x_d \tau_d))\right] \; . \tag{5.25b}$$

The total integrated cros-section becomes now

$$\sigma(l^- f) = \frac{|T|^2}{\Gamma_d^2}\left[1 - \frac{n \; x_d}{(1+x_d^2)^2} \; (1 + \eta_c)\right] \; . \tag{5.26}$$

For the $\Upsilon(4S) \to B_d^0 \overline{B}_d^0$ decay the charge conjugate parameter has the value of $\eta_c = -1$ (as the relative orbital momentum between the two mesons is $l = 1$).

Therefore, $\sigma(l^- f)$ as well as $\sigma(l^+ f)$, obtained by transforming $n \longrightarrow -n$, cannot depend on the CP violation parameter n. One then always has an asymmetry parameter $A = 0$, whether or not CP violation effects are present. Expressions (5.25a) and (5.25b) show, however, that the decay-time distributions are sensitive to the CP violation parameter.

Therefore, the search for CP violation in the $B_d^0, \overline{B}_d^0$ decays requires the measurement of the decay-time distributions. In the case of e^+e^- colliders where the incident $e^\pm$ momentum are identical, the momentum of the produced B mesons in tth laboratory system is small ($\sim$ 600 MeV/c). The decay times of the mesons are then not measurable. Asymmetry colliders were then considered in order to have large B momentum in the laboratory system and enable measurement of the decay time[11].

Appendix 5.A

Formulas for the B_d^0 decay

As an exercise, let us derive the time dependences of the $l^- f$ state when $f = \overline{f}$ appears from the B_d^0 or $\overline{B}_d^0$ decays. As considered in Chapters 3 and 4, this can occur from the following pairs of beauty hadrons produced at time $t = 0$ in pp interactions,

(1) $B^- B_d^0$

(2) $N_b B_d^0$

(3) $\overline{B}_s^0 B_d^0$ and $B_s^0 \overline{B}_d^0$ (coherent mixture)

(4) $\overline{B}_d^0 B_d^0$

Let us now consider the time dependence of the B_d^0 in the various cases.

Cases (1) and (2)

These cases have already been studied in Chapter 3. The initial vector state describing case (1) is

$$|\phi >= |B^-(t_-) > |B_d^0(t_d) > \tag{3.22}$$

where t_- (t_d) correspond to the proper time of the B^- (B_d^0) state in its rest frame. The amplitude then becomes

$$A(l^- f) \equiv < l^- f \mid \phi >=< l^- X | B^-(t_-) > < f | B_d^0(t_d) > \ .$$

Using formula (3.8), one obtains the expressions

$$\begin{aligned} A(l^- f) &=< l^- X | B^-(t_-) > \left[< f \mid B_d^0 > f_+(t_d) + < f \mid \overline{B}_d^0 > \eta_d f_-(t_-) \right] \\ &=< l^- X | B^-(t_-) >< f \mid B^0 > \left[f^+(t_d) + \lambda f_-(t_d) \right] \end{aligned}$$

where $\lambda = \eta_d < f \mid \overline{B}_d^0 > / < f \mid B_d^0 >$ [formula (4.13)]. From this amplitude one obtains the time-differential cross-sections

$$\frac{d\sigma_1}{dt_- dt_d} = \frac{|T|^2}{2} e^{-(\Gamma_- t_- + \Gamma_d t_d)} \left[1 + |\lambda|^2 + \cos \Delta M_d t_d \left[1 - |\lambda|^2 \right] - 2 \mathrm{Im} \lambda \sin \Delta M_d t_d \right] \ .$$

Using the usual conditions for the final state $f = \overline{f}$ (see case 4 in Section 4.6) one has $|\lambda| = 1$. The time dependence can then be expressed by

$$\boxed{\begin{aligned} \frac{d\sigma_1}{dt_- dt_d} &= |T|^2\, e^{-(\Gamma_- t_- \Gamma_d t_d)}\, [1 - \mathrm{Im}\lambda \sin \Delta M_d t_d] \\ \frac{d\sigma_1}{dt_d} &= \frac{|T|^2}{2\Gamma_-}\, e^{-\Gamma_d t_d}\, [1 - \mathrm{Im}\lambda \sin \Delta M_d t_d] \end{aligned}}$$

where $T =< l^- X|B^- >< f|B_d^0 >$ corresponds to formulae (5.9a). As stated in the text, point 2 has the same formula but with the transformation of $\Gamma_- \to \Gamma_N$ and $T \to T'$ as the $< l^- X|B^- >$ part of the amplitude might be different from the $< l^- X|N_b >$ one (see the discussion in Chapters 3 and 4).

Case 3

The initial state vector is now given by

$$|\phi >= |B_s(t_s) > |\overline{B}_d(t_d) > +|\overline{B}_s(t_s > |B_d(t_d) > \ . \tag{3.24}$$

Still using the equations of (3.8), one gets successively

$$\begin{aligned} < l^- f|\phi > &=< l^-|B_s^0 > \eta_s f_-(t_s) < f|\overline{B}_d^0(t_d) > + < l^-|\overline{B}_s^0 > f_+(t_s) < f|\overline{B}_s^0 > \\ &= T\left[\frac{f_-(t_s)f_-(t_d)}{\eta_d} + f_+(t_s)f_+(t_d) + \lambda(\frac{f_-(t_s)f_+(t_d)}{\eta_d} + f_+(t_s)f_-(t_d))\right] \end{aligned}$$

with $T =< l^- X|\overline{B}^0 >< f|B^0 >$ and $\eta_s = 1$. One thus obtains the double differential cross-section

$$\begin{aligned} \frac{d\sigma(l^- f)}{dt_s dt_d} = |T|^2\Bigg[&\left|\frac{f_-(t_s)f_-(t_d)}{\eta_d} + f_+(t_s)f_+(t_d)\right|^2 + \\ &+ |\lambda|^2\left|\frac{f_-(t_s)f_+(t_d)}{\eta_d} + f_+(t_s)f_-(t_d)\right|^2 + 2\mathrm{Re}\left[\lambda\Big(\eta_d f_-^*(t_s)f_+^*(t_d) + \right. \\ &\left. + f_+^*(t_s)f_-^*(t_d)\Big) \times \Big(\eta_d^* f_-(t_s)f_+(t_d) + f_+(t_s)f_+(t_d)\Big)\right]\Bigg] \ . \end{aligned}$$

Denoting the three terms in the brackets of the above equation by T_{1-3} and using the approximations (3.10), one obtains

$$T_1 = \frac{e^{-(\Gamma_s t_s + \Gamma_d t_d)}}{4} \Big[(1 - \cos\Delta M_s t_s)(1 - \cos\Delta M_d t_d) + (1 + \cos\Delta M_s t_s) \\ \times (1 + \cos\Delta M_d t_d) - \sin\Delta M_s t_s \ \sin\Delta M_d t_d) \ 2\mathrm{Re}\eta_d \Big]$$

yielding

$$T_1 = \frac{e^{-(\Gamma_s t_s + \Gamma_d t_d)}}{2} \Big[\ 1 + \cos(\Delta M_s t_s + \Delta M_d t_d) + \\ + \sin(\Delta M_s t_s) \sin(\Delta M_d t_d) \ (1 - \mathrm{Re}\eta_d) \Big] \ .$$

By a similar calculation one obtains for the second term:

$$T_2 = \frac{e^{-(\Gamma_s t_s + \Gamma_d t_d)}}{2} |\lambda|^2 \Big[\ 1 - \cos(\Delta M_s t_s + \Delta M_d t_d) \\ - \sin(\Delta M_s t_s) \sin(\Delta M_d t_d) \ (1 - \mathrm{Re}\eta_d) \Big] \ .$$

A straightforward calculation gives for the third term

$$T_3 = - \frac{e^{-(\Gamma_s t_s + \Gamma_d t_d)}}{2} \Big[2\mathrm{Im} \ \lambda \big[\sin(\Delta M_d t_d + \Delta M_s t_s) + \\ + \sin(\Delta M_d t_d) \sin(\Delta M_s t_s) \ (1 - \mathrm{Re}\eta_d) \big] - \mathrm{Re}\lambda \ Im\eta_d \sin\Delta M_s t_s \Big] \ .$$

Adding the three terms one gets the final expression for the double differential cross-section

$$\frac{d\sigma(l^- f)}{dt_s dt_d} = \frac{|T|^2}{2} e^{-(\Gamma_s t_s + \Gamma_d t_d)} \Big[\ 1 + |\lambda|^2 + (1 - |\lambda|^2) \Big(\cos(\Delta M_s t_s + \Delta M_d t_d) + \\ + \sin\Delta M_s t_s \ \sin\Delta_d t_d \times (1 - \mathrm{Re}\eta_d) \Big) - 2\mathrm{Im}\lambda \Big(\sin(\Delta M_s t_s + \Delta M_d t_d) + \\ - \sin\Delta M_s t_s \cos\Delta M_d t_d \ (1 - \mathrm{Re}\eta_d) \Big) + \mathrm{Re}\lambda \ \mathrm{Im}\eta_d \sin\Delta M_s t_s \ \Big] \ .$$

The integration of the last expression over t_s gives

$$\frac{d\sigma_3}{dt_d} = \frac{|T|^2}{\Gamma_s} e^{-\tau_d} \left[1 - \frac{\mathrm{Im}\lambda}{1+x_s^2}(x_s \cos x_d\tau_d \times \mathrm{Re}\eta_d + \sin x_d\tau_d) \right.$$
$$\left. \frac{x_s}{2(1+x_s^2)} \mathrm{Re}\lambda \; \mathrm{Im}\eta_d\right]$$

which is equattion (5.10c) where $\delta == \mathrm{Re}\lambda \; \mathrm{Im}\eta_{\mathrm{d}}$.

Case 4

Let us now consider the $B_d^0\overline{B}_d^0$ system which can be described by a state vector depending on the charge conjugate of the system $\eta_c = \pm 1$,

$$| \phi >=| B(t_1) >| \overline{B}(t_2) > +\eta_c \mid \overline{B}(t_1) >| B(t_2 > \tag{3.26}$$

labelled by their desintegration time $t_{1,2}$ in their proper rest frame. In the same way as in case 3, one gets an amplitude for the $l^- f$ final state

Let us now consider the $B^0\overline{B}^0$ case. To this end we use the amplitudes given in Section 3.5, i.e.

$$A(l^-f) = T\Big[f_-(t_1)f_-(t_2) + \eta_c f_+(t_1)f_+(t_2) + \lambda\big(f_-(t_1)f_+(t_2) + \eta_c f_+(t_1)f_-(t_2)\big)\Big]$$
$$A(l^+\overline{f}) = \overline{T}\Big[f_+(t_1)f_+(t_2) + \eta_c f_-(t_1)f_-(t_2) + \overline{\lambda}\big(f_+(t_1)f_-(t_2) + \eta_c f_-(t_1)f_+(t_2)\big)\Big]$$

and we will still assume that $|T| = |\overline{T}|$. It is easy to see that the time-dependence of $|A(l^+f)|^2$ and $|A(l^-\overline{f})|^2|$ will be identical except that λ is replaced in the second case by $\overline{\lambda}$. For the l^+f final state, for instance, one obtains the following double differential cross-section

$$\frac{d\sigma(l^-f)}{dt_1dt_2} = |T|^2\Big[\Big|f_-(t_1)f_-(t_2) + \eta_c f_+(t_1)f_+(t_2)\Big|^2$$
$$+ |\lambda|^2\Big|f_-(t_1)f_+(t_2) + \eta_c f_+(t_1)f_+(t_2)\Big|^2 + 2\mathrm{Re}\,\Big[\lambda\Big(f_-(t_1)f_+(t_2)$$
$$+ \eta_c f_+(t_1)f_-(t_2)\Big) \times \Big(f_-^*(t_1)f_-^*(t_2) + \eta_c f_+^*(t_1)f_+^*(t_2)\Big)\Big]\Big] .$$

If, as above, we define the three terms by T_{1-3} and use formula (3.10) we find easily that

$$T_1 = \frac{e^{-\Gamma(t_1+t_2)}}{2}\Big[1 + \cos\Delta M t_1 \;\cos\Delta M t_2 - \eta_c \sin\Delta M t_1 \;\sin\Delta M t_2\Big]$$
$$= \frac{e^{-\Gamma(t_1+t_2)}}{2}\Big[1 + \cos\Delta M(t_1 \pm t_2)\Big]$$

where the $\pm$ sign coresponds to $\eta_c = \pm 1$. The same kind of calculation gives for the second and third term

$$T_2 = |\lambda|^2 \frac{e^{-\Gamma(t_1+t_2)}}{2}\Big[1 - \cos\Delta M t_1 \;\cos\Delta M t_2 + \eta_c \sin\Delta M t_1 \;\sin\Delta M t_2\Big]$$
$$= |\lambda|^2 \frac{e^{-\Gamma(t_1+t_2)}}{2}\Big[1 - \cos\Delta M(t_1 \pm t_2)\Big]$$

and

$$T_3 = \frac{e^{-\Gamma(t_1+t_2)}}{2} 2\mathrm{Re}\Big[i\lambda(\sin\Delta m t_2 \;\cos\Delta M t_1 + \eta_c \sin\Delta M t_1 \;\cos\Delta M t_2)\Big]$$
$$= -2\,\frac{e^{-\Gamma(t_1+t_2)}}{2} \sin\Delta M(t_1 \pm t_2)\ \mathrm{Im}\lambda\ .$$

One thus obtains the differential cross-section

$$\frac{d\sigma(l^- f)}{dt_1 dt_2} = \frac{|T|^2}{2} e^{-\Gamma(t_1+t_2)}\Big[1 + \cos\ \Delta M(t_1 \pm t_2)$$
$$+ |\lambda|^2[1 - \cos\Delta M(t_1 \pm t_2)] - 2\mathrm{Im}\lambda \times \sin\ \Delta M(t_1 \pm t_2)\Big]\ .$$

The $|\lambda| = 1$ condition and the integration over the t_1 variable gives the $t_d \equiv t_2$ distribution, i.e., formula (5.10d)

$$\boxed{\frac{d\sigma_4(l^- f)}{dt_d} = \frac{|T|^2}{\Gamma_d} e^{-\tau_d}[1 - \frac{n}{1 + x_d^2}(x_d\ \cos(\Delta M_d t_d) \pm \sin(\Delta M_d t_d \tau_d))]\ .}$$

Appendix 5.B

Formulas for the $B_d^0 \to J/\psi K^*$ decay

As an additional exercise, let us show how the formulae (5.23) have been estimated. The expression of (5.23a) is evident, the production rate P_1 is proportionnal to the semileptonic branching ratio and to the $p_i p_j$ weigthing factor. The only difference appearing in (5,23b) is the ϵ factor as the total width of beauty baryons and B meson are different. Let us now consider the two other cases where mixing has to be taken into account.

Formula (5.23c) for the $B_s^0\overline{B}_d^0 + \overline{B}_s^0 B_d^0$ case

For the considered $B_d^0 \to J/\psi K^{*0}$ with $K^{*0} \to K^+ + ...$, the final state can only come from the B_d^0, hence $\lambda = 0$. The double-differential time distribution found in the previous Appendix becomes with $\lambda = 0$ to:

$$\frac{d\sigma(l^+ f)}{dt_s dt_d} = \frac{|T|^2}{2} e^{-(\Gamma_s t_s + \Gamma_d t_d)} \Big[1 + \cos(\Delta M_s t_s + \Delta M_d t_d) + $$

$$+ \sin \Delta M_s t_s \; \sin \Delta M_d t_d) \times (1 - \mathrm{Re}\eta_d) \Big] \; .$$

This leads to the single differential expression of

$$\frac{d\sigma_4(l^- f)}{dt_d} = \frac{|T|^2}{2\Gamma_s} e^{-\Gamma_d t_d} [1 + \frac{1}{1+x_s^2} (\cos(\Delta M_d t_d) - x_s \; \mathrm{Re}\eta_d \sin(\Delta M_d t_d \tau_d))] \; .$$

A further integration over t_d gives the expression for the cross-section,

$$\sigma(l^- f) = \frac{|T|^2}{2\Gamma_s \Gamma_d} \left[1 + \frac{1 - x_s x_d \mathrm{Re}\eta_d}{(1+x_s^2)\,(1+x_d^2)} \right] \; .$$

This is the expression used for the production rate but normalized in such a way that if $x_s = x_d = 0$, one has a formula similar to (5.23a).

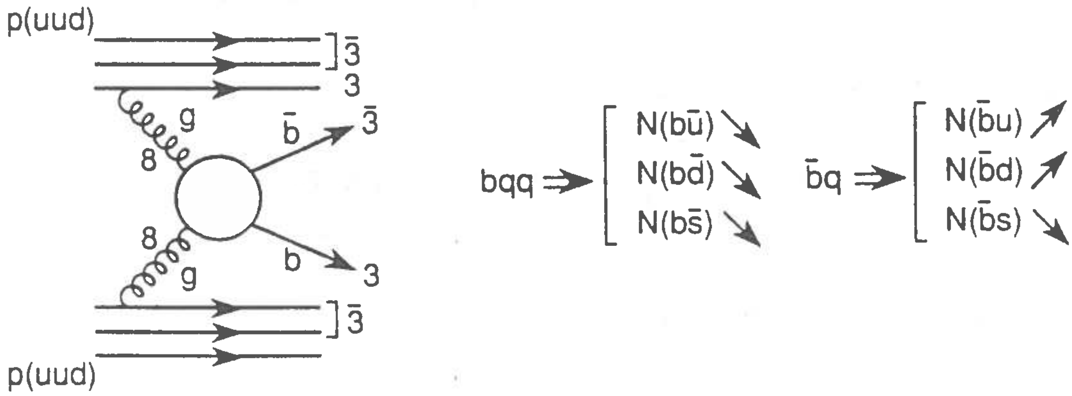

Fig. 5.1 - The possible bqq and $\bar{b}q$ combinations of the produced b and $\bar{b}$ with the valence quarks in pp interactions. The tendencies of the production of beauty mesons are also indicated, N denoting a number of events. The numbers shown in the figure give the color values of the produced quarks.

Formula (5.23d) for $B_d^0\overline{B}_d^0$ case

The double-differential cross-section is given by (Appendix 5.A)

$$\frac{d\sigma(l^- f)}{dt_1 dt_2} = \frac{|T|^2}{2} e^{-\Gamma_d(t_1+t_2)} \Big[1 + \cos\ \Delta M(t_1 + \eta_c t_2) + |\lambda|^2 [1 - \cos \Delta M(t_1 + \eta_c t_2)] - 2\mathrm{Im}\lambda \times \sin\ \Delta M(t_1 + \eta_c) \Big] \ .$$

With $\lambda = 0$, the integration over t_1 gives

$$\frac{d\sigma}{dt_2} = \frac{|T|^2}{2\Gamma_d} e^{-\Gamma_d t_2} \left[1 + \frac{\cos \Delta M_d t_2}{1 + x_d^2} - \frac{\sin \Delta M_d t_2}{1 + x_d^2} \eta_c x_d \right] \ .$$

The integration over t_2 gives the cross-section,

$$\sigma(l^- f) = \frac{|T|^2}{2\Gamma^2} \left[1 + \frac{(1 - \eta_c x_d^2)}{(1 + x_d^2)^2} \right] \ .$$

Taking into account that the number of events with relative even or odd orbital momentum between the outgoing mesons are equal, one finally obtains

$$\sigma(l^- f) = \frac{|T|^2}{\Gamma_d^2} \left[1 + \frac{1}{(1 + x_d^2)^2} \right] \ .$$

With the same normalization as before, one obtains expression (5.23c).

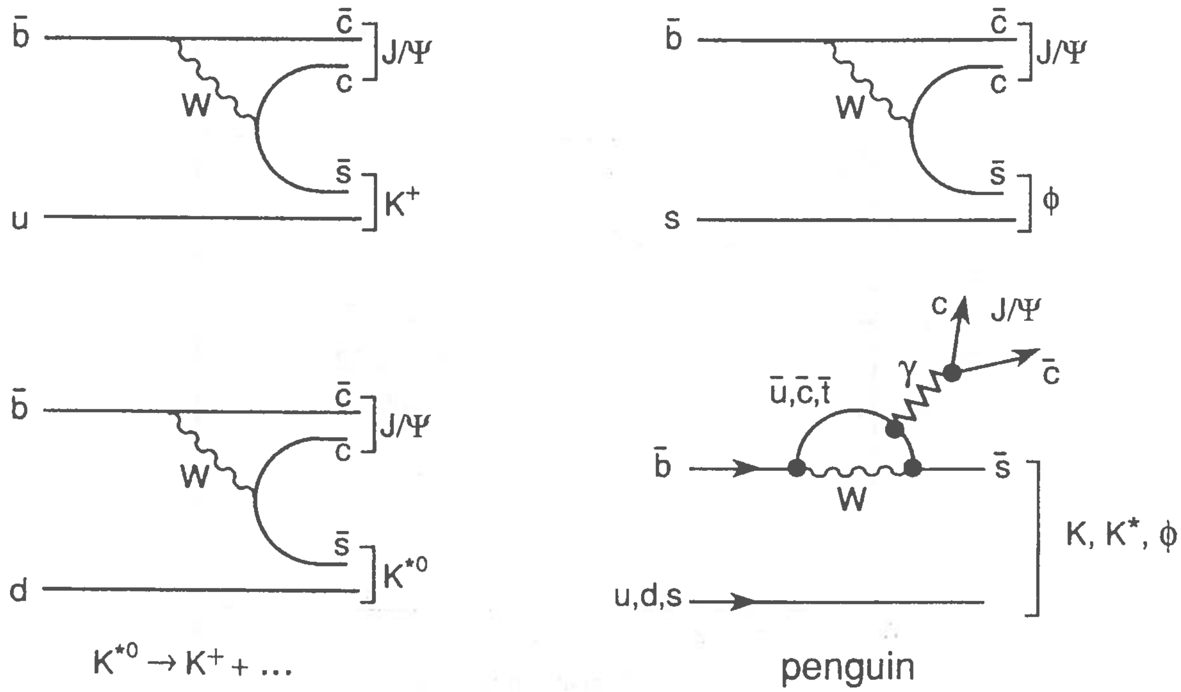

Fig. 5.2 - Diagrams contributing to the $B^+ \to J/\psi K^+$,$B_d^0 \to J/\psi K^{*0}$ and $B_s^0 \to J/\psi \phi$ decays.

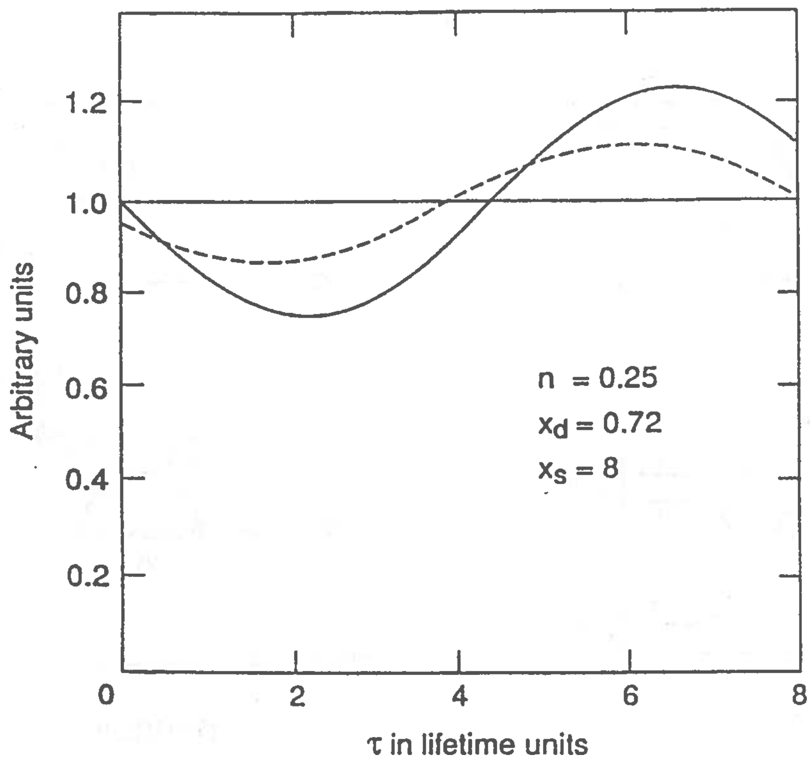

Fig. 5.3 - The time-dependent decay distribution obtained from the decays into $l^+ f$ ($B_d^0, \overline{B}_d^0 \to f$) for the general case (dashed line) or by tagging only with B^+ mesons (full line), the exponential part has been factorized out (taken from Ref. 2).

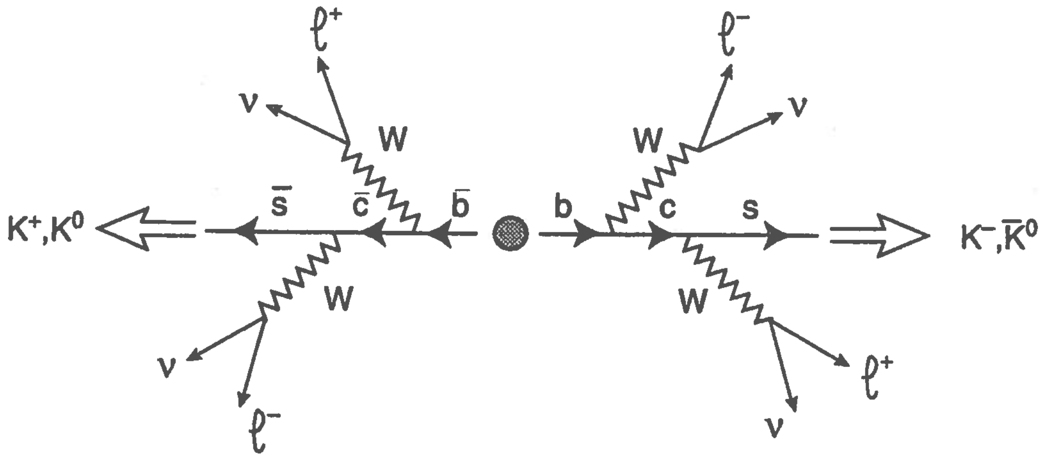

Fig. 5.4 - In the production of a $b\bar{b}$ pair, the charge of the leptons appearing in the semileptonic decay of the b or c quarks (or their c.c. ones) are indicated. One also show the charge of the K mesons resulting from the $b \to c \to s$ (or it c.c.) process.

6 - The beauty baryon

6.1 - Production and decays

a) Production rates

In this chapter we consider the beauty baryons, including their decay properties as well as their production in pN interactions. The decay can be studied efficiently in reactions where the beauty baryon production is significant. For instance, B-factories at c.m. energies around $\sqrt{s} \simeq 10$ GeV cannot be used for studyding these features, as their $\sqrt{s}$ are below the threshold corresponding to beauty baryon production, or just above if $\sqrt{s}$ can be somewhat increased. In contrast, pp interactions at the LHC project ($\sqrt{s} \simeq 14$ TeV) are expected to have a large beauty baryon cross-section (see below).

Table 6.1 presents various beauty baryons that could be produced in pN interactions, the charge conjugate (c.c.) ones not being indicated. Excited states are also not shown. Therefore, all the baryons have a spin of S=1/2, apart from the bbb state having S=3/2. The masses of these particles are those used in the PYTHIA Monte Carlo program[1] except for the measured Λ_b mass[2]. We use the following notation: the baryon with isospin $I = 1$ will be denoted by Σ, whereas Ξ will be taken for baryons having $I = 1/2$. For $I = 0$, we use Λ unless each quark forming a baryon has $I = 0$, in which case the notation will be Ω. The subscripts of Σ, Ξ, Λ, and Ω indicate the number and the type of the heavy quarks ($Q \equiv b, c$) contained in the considered baryon (as above, the light quarks will be denoted by $q \equiv u, d, s$). Note that the baryons containing only one heavy quark will be represented by $N_b \equiv bq_1q_2$ or $N_c \equiv cq_1q_2$ (and by $\overline{N}_b, \overline{N}_c$ for their c.c. states).

The production rates of beauty baryons in pN interactions at $\sqrt{s} \geq 2$ TeV are not really known today. Estimates of the cross-section $\sigma(bq_1q_2)$ for a given N_b state can be made from the ratio $\sigma(bq_1q_2)/\sigma(\bar{b}b)$ calculated, from various models. As used previously, $\sigma(b\bar{b})$ represents the $pp \to b\bar{b}X$ cross-section at the c.m. energy considered. For example, the PYTHIA Monte Carlo program allows the obtaining of the above ratios for baryons having only one heavy quark $Q \equiv b, c$. Then using a model dependent value of $\sigma(b\bar{b})$, one gets estimates of beauty baryon cross-sections. With $\sigma(b\bar{b}) \simeq 300$ μb, which is the order of magnitude considered for $\sqrt{s} \simeq 14$ TeV, one obtains the following estimates for the N_b and $\overline{N}_b$ production cross-sections in pp interactions with the help of the Monte Carlo calculation[3]:

Table 6.1 - Various beauty baryons (N_b) using the notation explained above. The charge and the quarks forming the baryons are also given. The mass values are those of the model used in the PYTHIA Monte Carlo program[1], apart from the mass of the Λ_b, which has been measured[2].

	Quarks	Charge	Mass (GeV)
Λ_b	bud	0	5.64
Σ_b	buu	+1	5.80
	bdu	0	"
	bdd	−1	"
Ξ_b	bsu	0	5.84
	bsd	−1	"
Ξ_{bc}	bcu	+1	7.01
	bcd	0	"
Ξ_{2b}	bbu	0	10.42
	bbd	−1	"
Ω_b	bss	−1	6.12
Ω_{bc}	bcs	0	7.19
Ω_{b2c}	bcc	+1	8.31
Ω_{2b}	bbs	−1	10.60
Ω_{2bc}	bbc	0	11.71
Ω_{3b}	bbb	−1	15.11

$$\begin{aligned} &\sigma(\Lambda_b) \simeq 24.0\ \mu\text{b}\ , \quad \sigma(\overline{\Lambda}_b) \simeq 23.2\ \mu\text{b} \\ &\sigma(\Sigma_b) \simeq 4.0\ \mu\text{b}\ , \quad \sigma(\overline{\Sigma}_b) \simeq 3.8\ \mu\text{b} \\ &\sigma(\Xi_b) \simeq 3.3\ \mu\text{b}\ , \quad \sigma(\overline{\Xi}_b) \simeq 3.2\ \mu\text{b} \\ &\sigma(\Omega_b) \sim 0.03\ \mu\text{b}\ , \quad \sigma(\overline{\Omega}_b) \sim 0.03\ \mu\text{b}\ . \end{aligned} \tag{6.1}$$

The difference between the N_b and $\overline{N}_b$ production rates appears as the combination of the b ($\overline{b}$) quark with the valence quarks contained in the beam particles has been taken into account[1] and yielding $\sigma(N_b) \geq \sigma(\overline{N}_b)$. The difference values given above can only be considered as indications. The various cross-sections have to be measured. This could be done easily when pN interactions at large $\sqrt{s}$ will be available, as no mixing and tagging have to be considered in the beauty-baryon decays.

Estimates of the $\sigma(bcq)$ cross-sections are based on the fact that the velocites of the bound b, c and q quarks have to be (nearly) equal in a choosen frame. This means that the momentum of the light quark will be negligible with respect to the momenta of the b or c quark. The kinematics as well as the QCD interactions in the final state will thus depend essentially on the bc system. Therefore a rough estimate of $\sigma(bcq)$ could be written as[4]

$$\sigma(bcq) \simeq \sigma(\overline{B}_c)\ G \times \eta_q\ , \tag{6.2}$$

($\overline{B}_c \equiv b\bar{c}$) where $G = 1/2$ is a color factor comparing the bcq color singlet with the $b\bar{c}$ one[5]. The estimate of η_q is obtained from the probability of producing a given q quark. To this end one can, for instance, consider

$$bu : bd : bs : bqq = 0.38 : 0.38 : 0.14 : 0.10\ , \tag{3.30}$$

already used for $\sqrt{s} \simeq 14$ TeV (Chapter 4). Within the present approximation, this gives

$$bcu : bcd : bcs = \eta_u : \eta_d : \eta_s = 0.42 : 0.42 : 0.16\ .$$

An estimate of the $pp \to \overline{B}_c X$ cross-section at $\sqrt{s} \simeq 14$ TeV is $\sigma(\overline{B}_c) \simeq 39$ nb (Ref. 6). By taking into account both $\overline{B}_c$ and $\overline{B}_c^*$ production according to reference 6, one has the estimate of $\sigma(\overline{B}_c$ or $\overline{\mathrm{B}}_\mathrm{c}^*) \simeq 60$ nb. Using this last value and formula (6.2), one obtains the following estimates at $\sqrt{s} \simeq 14$ TeV:

$$\sigma(\Xi_{bc}) \sim 1.3\ 10^{-2}\ \mu\text{b} \tag{6.3a}$$

$$\sigma(\Omega_{bc}) \sim 5\ 10^{-3}\ \mu\text{b}\ . \tag{6.3b}$$

For beauty baryons having two b quarks or three heavy quarks one can use the following limits[4]:

$$\sigma(bbq) < \sigma(b\bar{b})\ \frac{\sigma(b\bar{b})}{\sigma_{in}}\ \eta_q$$

$$\sigma(bQ_1Q_2) < \sigma(b\bar{b})\ \frac{\sigma(Q_1\overline{Q}_1)\ \sigma(Q_2\overline{Q}_2)}{\sigma_{in}^2}\ ,$$

where $\sigma_{in} \simeq 60$ mb (Ref. 7) is the expected inelastic pp cross-section at $\sqrt{s} = 14$ TeV (let us recall that σ_{in} is the total cross-section minus the elastic and the diffractive ones). The upper limit in the above formula is due to the fact that one

Table 6.2 - Examples for the $1/2 \to 1/2 + 0$ spin configuration. The branching ratios $BR(\Lambda \to p\pi^-) = 0.64$ and $BR(K_s^0 \to \pi^+\pi^-) = 0.69$ are not indicated.

Channel	BR	$BR(tot)$	Final state
$\Lambda_b \to \Lambda D^0$ $D^0 \to K^-\pi^+$	$\sim 10^{-3}$ $\sim 3.7\ 10^{-2}$	$\sim 2\ 10^{-5}$	$pK^-\pi^+\pi^-$
$\Lambda_b \to \Lambda \overline{D}^0$ $\overline{D}^0 \to K^+\pi^-$	$\sim 2\ 10^{-4}$ $\sim 3.7\ 10^{-2}$	$\sim 5\ 10^{-6}$	$pK^+\pi^-\pi^-$
$\Lambda_b \to \Lambda_c^+\pi^-$ $\Lambda_c^+ \to pK^+\pi^-$ $\Lambda_c^+ \to pK^0$	$\sim 2\ 10^{-1}$ $\sim 3.2\ 10^{-2}$ $\sim 1.6\ 10^{-2}$	 $\sim 6\ 10^{-3}$ $\sim 10^{-3}$	 $pK^+\pi^+\pi^-$ $p\pi^+\pi^+\pi^-$
$\Xi_b^0 \to \Lambda D^0$ $D^0 \to K^-\pi^+$	$\sim 2\ 10^{-2}$ $\sim 3.7\ 10^{-2}$	$\sim 5\ 10^{-4}$	$pK^-\pi^+\pi^-$
$\Xi_b^- \to \Xi^- D^0$ $\Xi^- \to \Lambda\pi^-$ $D^0 \to K^-\pi^+$	$\sim 10^{-3}$ ~ 1 $\sim 3.7\ 10^{-2}$	$\sim 2\ 10^{-5}$	$pK^-\pi^+\pi^-\pi^-$
$\Xi_b^- \to \Xi_c^0\pi^-$ $\Xi_c^0 \to \Xi^-\pi^+$ $\Xi^- \to \Lambda\pi^-$	$\sim 2\ 10^{-1}$ $\sim 5.8\ 10^{-3}$ ~ 1	$\sim 7\ 10^{-4}$	$p\pi^+\pi^-\pi^-\pi^-$

Table 6.3 - Examples for the $1/2 \to 1/2 + 1$ spin configuration with $BR(J/\Psi \to \mu^+\mu^-) = 0.06$.

Channel	BR	$BR(tot)$	Final state
$\Lambda_b \to \Lambda J/\Psi$	$\sim 2\ 10^{-2}$	$\sim 8\ 10^{-4}$	$p\pi^-\mu^+\mu^-$
$\Xi_b^0 \to \Lambda J/\Psi$	$\sim 10^{-3}$	$\sim 4\ 10^{-5}$	$p\pi^-\mu^+\mu^-$
$\Xi_b^- \to \Xi^- J/\Psi$ $\Xi^- \to \Lambda\pi^-$	$\sim 2\ 10^{-2}$ ~ 1	$\sim 8\ 10^{-4}$	$p\pi^-\pi^-\mu^+\mu^-$
$\Omega_b^- \to \Omega^- J/\Psi$ $\Omega^- \to \Lambda K^-$	$\sim 2\ 10^{-2}$ 0.68	$\sim 5\ 10^{-4}$	$pK^-\pi^-\mu^+\mu^-$
$\Omega_b^- \to \Xi^- J/\Psi$ $\Xi^- \to \Lambda\pi^-$	$\sim 2\ 10^{-2}$ ~ 1	$\sim 8\ 10^{-4}$	$p\pi^-\pi^-\mu^+\mu^-$

does not take into account the probability that the produced bQ_1Q_2 quarks will form a baryon.

b) Decay processes

In the following we consider beauty hadrons containing only one heavy quark (b or c) and decaying into two particles, namely

$$\begin{aligned} N_b &\to Y + M \\ &\to N_c + M \end{aligned}$$

(and their charge conjugate reactions) where $Y \equiv \Lambda, \Xi, \Omega$ represents the hyperons. Here the meson M could have a spin of 0 or 1 corresponding to the following spin configurations:

$$1/2 \to 1/2 + 0 \ , \qquad 1/2 \to 1/2 + 1 \ . \tag{6.4}$$

The spin value S=1 for the meson $M = J/\psi$ is of particular interest as the leptons coming from the $J/\psi \to l^+l^-$ can be used for the triggering process in pp collisions[3]. Tables 6.2 and 6.3 indicate some beauty-baryon decays having the spin configurations given by (6.4). The examples shown in these tables have final states with only charged particles that could be detected easily.

For the decays described by Table 6.2 and 6.3, we will discuss the parameters sensitive to CP violation effects in the beauty-baryon decay. Because of the spin of the particles appearing in the decay processes, the final state will not be a parity eigenstate. This is because of the various (L) waves due to different orbital momenta (l) between the daughter particles, namely

$$\begin{aligned} 1/2 \to 1/2 + 0 \quad &\Rightarrow \quad L = S, P \\ 1/2 \to 1/2 + 1 \quad &\Rightarrow \quad L = S_{1/2}, P_{1/2}, P_{3/2}, D_{3/2} \ , \end{aligned} \tag{6.5}$$

the indices in the last equation indicating the sum of the spins of the outgoing meson and baryon. The methods of searching for CP violation effects in the beauty-baryon decays, different from the B decay cases, will be discussed in some detail here below.

Another aspect related to the production process consists in observing the polarization of the beauty baryon produced. Knowledge of the polarization will allow the measuring of decay parameters sensitive to CP violation effects (see below). Let us remember that in the $pN \to N_b(\overline{N}_b)X$ interactions, the polarization of N_b (or $\overline{N}_b$) in its rest frame can only be along $\hat{n}$, the normal to the production plane (see Fig. 6.1). This plane is defined here by the momenta of the incident proton ($\vec{p}_{inc}$) and the outgoing N_b or $\overline{N}_b$ ($\vec{p}_{out}$) produced in the laboratory (or in the c.m.) system, i.e. $\hat{n} = \vec{p}_{inc} \times \vec{p}_{out} / |\vec{p}_{inc} \times \vec{p}_{out}|$. In the following we will consider the knowledge of the polarization measurement as an attempt to have a better understanding of the production process, in addition to the usefulness of searching CP violation effects.

6.2 - The N_b decaying into two particles with S=1/2, 0

a) Introduction

The cases that we consider are similar to the $\Lambda \to p\pi$ and $\Xi \to \Lambda\pi$ studied about 30 years ago. The decay processes have been described in detail[8]. In the following we will recall some of these features in order to examine the interests of studying beauty baryon decays.

The weak decay in the cases under consideration will be described by S and P waves (corresponding to relative orbital momenta of $l = 0, 1$, respectively, between the outgoing particles). The partial waves for the decay of a given N_b or (its CP) $\overline{N}_b$ state can be written as[8,9]:

$$S = \sum_k S_k \exp i(\delta_k^S + \phi_k^S) , \quad \overline{S} = -\sum_k S_k \exp i(\delta_k^S - \phi_k^S) \qquad (6.6)$$

$$P = \sum_k P_k \exp i(\delta_k^P + \phi_k^P) , \quad \overline{P} = \sum_k P_k \exp i(\delta_k^P - \phi_k^P) \qquad (6.7) ,$$

where $\delta_k^{S,P}$ correspond to the phases due to final-state interaction while $\phi_k^{S,P}$ are the weak decay phases. Here a bar sign appearing on any quantity denotes that it is related to the $\overline{N}_b$ decay. The sum is given on the various isospin transitions between the initial ($\vec{I}_i$) and final ($\vec{I}_f$) state. The indice k indicates, however, the isospin value of the final state. For the decay channels discussed here the sommation will be at most over two terms. Note that in the present approach, the CP violation effects in the weak decay could only occur from the weak phases $\phi_k^{S,P}$. One has also to note that the relations between the $\phi_k^{S,P}$ and the CKM matrix elements are not evident, as they are model dependent[10].

The partial decay widths of the N_b (Γ) and $\overline{N}_b$ ($\overline{\Gamma}$) baryons are given by

$$\boxed{\Gamma \propto |S|^2 + |P|^2 , \quad \overline{\Gamma} \propto |\overline{S}|^2 + |\overline{P}|^2 .} \qquad (6.8)$$

From formulae (6.6) and (6.7), one sees that in the case of CP violation ($\phi^{S,P} \neq 0, \pi$) in the $N_b, \overline{N}_b$ decay, the width inequality $\Gamma \neq \overline{\Gamma}$ could only occur when more than one isospin transition leads to final states with a non unique isospin value[8,9]. In the beauty-baryon examples given in Table 6.2, the S and P waves in each case have the same I_f value. Therefore, one will always have $\Delta = (\Gamma - \overline{\Gamma})/(\Gamma + \overline{\Gamma}) = 0$ whether or not CP violation is present[9] (a situation similar to the $\Xi \rightarrow \Lambda\pi$ decay). Decay parameters have then to be used to search for CP violation effects in the beauty baryon decays.

In the general case, one has (Appendix 6.A)

$$\Delta = \frac{\Gamma - \overline{\Gamma}}{\Gamma + \overline{\Gamma}} \tag{6.9}$$

$$= \frac{-2\sum_{i<j}\left[S_iS_js(\delta_i^S - \delta_j^S)s(\phi_i^S - \phi_j^S) + P_iP_js(\delta_i^P - \delta_j^P)s(\phi_j^P - \phi_j^P)\right]}{\sum_i(S_i^2 + P_i^2) + \sum_{i<j}\left[S_iS_jc(\delta_i^S - \delta_j^S)c(\phi_i^S - \phi_j^S) + P_iP_jc(\delta_i^P - \delta_j^P)c(\phi_i^P - \phi_j^P)\right]}$$

(where here $s \equiv \sin$, $c \equiv \cos$). The numerator in the last equation depends only on sines terms and will, therefore, also lead to $\Delta = 0$ in the absence of final-state interactions ($\delta_j^{S,P} = 0$). If Δ can be different from zero for some specific decay channels, the relative production rates of N_b and $\overline{N}_b$ in the considered pN collisions have to be measured before interpreting any observed Δ value.

Because of the difficulties introduced by the isospin transitions for the measurements of Δ, let us now consider the decay (or correlation) parameters that can be used to search for CP violation effects. They were in fact utilized for studying the hyperon decays and could also be utilized fo the beauty baryon decay. The correlation or decay parameters between the S and P waves are defined by[8,9]:

$$\alpha = \frac{2\mathrm{Re}\,(S^*P)}{|S|^2 + |P|^2} \tag{6.10a}$$

$$\beta = \frac{2\mathrm{Im}\,(S^*P)}{|S|^2 + |P|^2} \tag{6.10b}$$

$$\gamma = \frac{|S|^2 - |P|^2}{|S|^2 + |P|^2} \tag{6.10c}$$

($\alpha^2 + \beta^2 + \gamma^2 = 1$). Similar relations are obtained for the $\overline{N}_b$ parameters, $\overline{\alpha}, \overline{\beta}, \overline{\gamma}$ using the above relations with $S \rightarrow \overline{S}$ and $P \rightarrow \overline{P}$. In the absence of CP violation in the $N_b, \overline{N}_b$ decays, the weak phases $\phi_k^{S,P}$ vanish. Then by using formulae (6.6), (6.7) and (6.10), one will have

$$\boxed{\alpha + \overline{\alpha} = 0\,, \quad \beta + \overline{\beta} = 0\,, \quad \gamma = \overline{\gamma}\,.} \tag{6.11}$$

In reality, the search for CP violation effects with the decay parameters has been applied by testing the non-zero values of the following ratios:

$$A = \frac{\Gamma\alpha + \overline{\Gamma}\overline{\alpha}}{\Gamma\alpha - \overline{\Gamma}\overline{\alpha}} \simeq \frac{\alpha + \overline{\alpha}}{\alpha - \overline{\alpha}} = \frac{\mathrm{Re}\,(S^*P + \overline{S}^*\overline{P})}{\mathrm{Re}\,(S^*P - \overline{S}^*\overline{P})} \tag{6.12a}$$

$$B = \frac{\Gamma\beta + \overline{\Gamma}\overline{\beta}}{\Gamma\beta - \overline{\Gamma}\overline{\beta}} \simeq \frac{\beta + \overline{\beta}}{\beta - \overline{\beta}} = \frac{\mathrm{Im}\,(S^*P + \overline{S}^*\overline{P})}{\mathrm{Im}\,(S^*P - \overline{S}^*\overline{P})} \tag{6.12b}$$

$$B' = \frac{\Gamma\beta + \overline{\Gamma}\overline{\beta}}{\Gamma\alpha - \overline{\Gamma}\overline{\alpha}} \simeq \frac{\beta + \overline{\beta}}{\alpha - \overline{\alpha}} = \frac{\mathrm{Im}\,(S^*P + \overline{S}^*\overline{P})}{\mathrm{Re}\,(S^*P - \overline{S}^*\overline{P})}\,. \tag{6.12c}$$

An eventual unequal amount of N_b and $\overline{N}_b$ production has no importance here, as one compares decay parameters and not N_b with $\overline{N}_b$ events. With the formulae given in Appendix 6.A, one obtains for the general cases the following expressions of the A, B and B' parameters:

$$A = \frac{-\sum_{i,j} S_i P_j \sin(\delta_j^P - \delta_i^S)\sin(\phi_j^P - \phi_i^S)}{\sum_{i,j} S_i P_j \cos(\delta_j^P - \delta_i^S)\cos(\phi_j^P - \phi_i^S)} \tag{6.13}$$

$$B = \frac{-\sum_{i,j} S_i P_j \cos(\delta_j^P - \delta_i^S)\sin(\phi_j^P - \phi_i^S)}{\sum_{i,j} S_i P_j \sin(\delta_j^P - \delta_i^S)\cos(\phi_j^P - \phi_i^S)} \tag{6.14}$$

$$B' = \frac{\Gamma\beta + \overline{\Gamma}\overline{\beta}}{\Gamma\alpha - \overline{\Gamma}\overline{\alpha}} \simeq \frac{\beta + \overline{\beta}}{\alpha - \overline{\alpha}} \propto -\sum_{i,j} S_i P_j \sin(\phi_i^P - \phi_j^S)\,. \tag{6.15}$$

The B parameter tests (in principle) the time reversal invariance related to the $N_b, \overline{N}_b$ decays (see below) that should be equivalent to CP invariance (CPT rule). For simplicity, we assumed in the B' equation that the differences of $\delta_j - \delta_i$ and $\phi_j - \phi_i$ are small, allowing an approximation of the cosine of these difference by 1. The parameter B' does not depend then on the phases due to the final-state interactions, an important advantage in searching for CP violation effects. For a given CP violation effect one notes[9] that $|B| \gg |A| \gg |\Delta|$, indicating that the measurements of β and $\overline{\beta}$ might be very useful, although difficult (next paragraph).

Table 6.4 - For the spin configuration $1/2 \to 1/2 + 0$, the Γ, α, β relations between the N_b and $\overline{N}_b$ decays for CP conservation or violation. In each case final-state interactions (FSI) were assumed or neglected.

CP conservation		CP violation	
FSI	No FSI	FSI	No FSI
$\Gamma = \overline{\Gamma}$	$\Gamma = \overline{\Gamma}$	$\Gamma \neq \overline{\Gamma}^*$	$\Gamma = \overline{\Gamma}$
$\alpha = -\overline{\alpha}$	$\alpha = -\overline{\alpha}$	$\alpha \neq -\overline{\alpha}$	$\alpha = -\overline{\alpha}$
$\beta = -\overline{\beta}$	$\beta, \overline{\beta} = 0$	$\beta \neq -\overline{\beta}$	$\beta = \overline{\beta}$

* With only one isospin transition, one has $\Gamma = \overline{\Gamma}$ (see text).

Note that for CP violation effects where the final state interactions (FSI) having a small effect ($\delta_k^S, \delta_k^P \to 0$) one obtains that $A \to 0$ and $B \to \infty$ yielding $\alpha = -\overline{\alpha}$ and $\beta = \overline{\beta}$, respectively.

The relations between the various parameters are given in Table 6.4 for CP conservation or violation in the beauty baryon decay. They are obtained by using formulae (6.13) and (6.14). For each case we consider the presence of final-state interactions or decay processes where the final state could be neglected.

Let us repeat that non-zero values of the β or $\overline{\beta}$ parameters are related to the violation of the time reversal (T) applied to the considered decay process (see the next section), and hence to the CP violation (CPT rule). However, final-state interactions can also lead to $\beta, \overline{\beta} \neq 0$. Table 6.4 indicates the relations between β and $\overline{\beta}$ that could indicate the violation of time reversal.

Remarks about the $\Lambda \to p\pi^-$ decay

Let us remember the expressions obtained for the $\Lambda \to p\pi^-$ decays where $I_f = 3/2, 1/2$. Experimental evidence has shown that the decay transition with $I_f = 3/2$ is much smaller than that having $I_f = 1/2$ in the final state (the ratio is about 1/30). Using also the fact that $|S| > |P|$, one can approximate formula (6.9) by (see also Appendix 6A)

$$\Delta = \frac{\Gamma - \overline{\Gamma}}{\Gamma + \overline{\Gamma}} \simeq -2\,\frac{S_3}{S_1}\,\sin(\delta_1^S - \delta_3^S)\,\sin(\phi_1^S - \phi_3^S)\,. \tag{6.16}$$

With these assumptions, one obtains the following approximations for the Λ ratios:

$$A = \frac{\alpha + \overline{\alpha}}{\alpha - \overline{\alpha}} = -\mathrm{tg}(\delta_1^P - \delta_1^S)\,\mathrm{tg}(\phi_1^P - \phi_1^S) \tag{6.17a}$$

$$B = \frac{\beta + \overline{\beta}}{\beta - \overline{\beta}} = -\frac{\mathrm{tg}(\phi_1^P - \phi_1^S)}{\mathrm{tg}(\delta_1^P - \delta_1^S)} \qquad (6.17b)$$

$$B' = \frac{\beta + \overline{\beta}}{\alpha - \overline{\alpha}} = -\mathrm{tg}(\phi_1^P - \phi_1^S) \ . \qquad (6.17c)$$

We see that here $A, B, B' \neq 0$ are due to interferences between the S and P waves having both the same final isospin value, $I_f = 1/2$.

b) The α and β measurements

The α and β parameters indicated above for a given $N_b \to f$ (and its c.c.) channel are related to the polarization of N_b and that of the baryon (hyperon or charmed baryon) appearing in the N_b decay. Before examining these features, let us recall that in hadron hadron interactions the N_b polarization (in the N_b rest frame) can only be along $\hat{n}$, the normal to the production plane (Fig. 6.1).

For the present discussion let us consider the weak decay of $\Lambda_b \to \Lambda D^0$ with $\Lambda \to p\pi^-$ although the estimated $BR(\Lambda_b \to \Lambda D^0)$ branching ratio given in Table 6.2 is rather small. In fact, any other decay channel given in this table could be used for the present discussion. Nevertheless, for simplicity, we use the $\Lambda_b \to \Lambda D^0$ channel, which will be compared with the $\overline{\Lambda}_b \to \overline{\Lambda}\overline{D}^0$ one.

Similarly as with the study of the $\Lambda \to p\pi$ and $\Xi \to \Lambda\pi$ decays[8], let us characterize the $\Lambda_b \to \Lambda D^0$ decay by the angular distribution of Λ in the Λ_b rest frame by $I(\hat{\Lambda})$ and use $I(\hat{p})$ for that of the proton distribution in the Λ rest frame (coming from $\Lambda \to p\pi^-$), hence

$$I(\hat{\Lambda}) = 1 + \alpha(\Lambda_b)\ \vec{P}(\Lambda_b)\ \hat{\Lambda} \qquad (6.18a)$$

$$I(\hat{p}) = 1 + \alpha(\Lambda)\ \vec{P}(\Lambda)\ \hat{p} \ , \qquad (6.18b)$$

where $\alpha(N)$ denotes here a decay parameter related to a given N decay channel into two particles [see formula (6.10a)]. We recall that the polarization of Λ_b and Λ are defined in their rest frame. The $\hat{\Lambda}$ ($\hat{p}$) is the momentum direction (one unit) of the Λ (p) in the Λ_b (Λ) rest frame. In the following we will often use Θ representing the angle between the Λ and the polarization directions in the production c.m. system $[\vec{P}(\Lambda_b)\hat{\Lambda} \equiv P(\Lambda_b)\cos\Theta]$, as shown in Fig. 6.1. The probability of a given configuration of the Λ_b and Λ decay per unit of solid angles $d\Omega(\hat{\Lambda})/4\pi$ and $d\Omega(\hat{p})/4\pi$ could be given by:

$$f(\hat{\Lambda}, \hat{p}) = \left[1 + \alpha(\Lambda_b)\ \vec{P}(\Lambda_b)\ \hat{\Lambda}\right] \times \left[1 + \alpha(\Lambda)\ \vec{P}(\Lambda)\ \hat{p}\right] \ , \qquad (6.19)$$

whereas the probability of observing the Λ polarization $\vec{P}(\Lambda)$ in its rest frame will be[8]:

$$I(\hat{\Lambda})\vec{P}(\Lambda) = \left[\alpha(\Lambda_b) + \vec{P}(\Lambda_b)\hat{\Lambda}\right] \hat{\Lambda} + \beta(\Lambda_b)(\vec{P}(\Lambda_b) \times \hat{\Lambda}) + \gamma(\Lambda_b)\left[\hat{\Lambda} \times (\vec{P}(\Lambda_b) \times \hat{\Lambda})\right] \ . \quad (6.20)$$

Under time reversal, spin, polarization, the $\hat{\Lambda}$ and the $\hat{p}$ directions, change sign. Therefore, the left-handed side of equation (6.20) changes sign, whereas the same feature can only occur on the right-hand side if $\beta = 0$. Thus, time-reversal invariance in the beauty baryon decay requires $\beta = 0$, although final-state interactions can lead to $\beta \neq 0$, see formulae (6.10a) and (6.10b) and Table 6.4.

As is well known, formula (6.20) indicates that $\beta(\Lambda_b)$ and $\gamma(\Lambda_b)$ can only be measured if $P(\Lambda_b) \neq 0$. For simplicity, let us define the proton emission angle (θ_{1-3}) from the Λ decay in its rest frame with respect to the coordinate system shown in Fig. 6.1. One then has

$$\cos\theta_1 = \frac{\hat{p}\ \left(\hat{\Lambda} \times (\hat{n} \times \hat{\Lambda})\right)}{|\hat{\Lambda} \times (\hat{n} \times \hat{\Lambda}|} \quad (6.21)$$

$$\cos\theta_2 = \frac{\hat{p}\ (\hat{n} \times \hat{\Lambda})}{|\hat{n} \times \hat{\Lambda}|} \quad (6.22)$$

$$\cos\theta_3 = \hat{p}\ \hat{\Lambda}\ , \quad (6.23)$$

yielding the following angular distributions[11] (see Appendix 6.B):

$$I(\theta_3) \propto 1 + \alpha(\Lambda_b)\alpha(\Lambda)\cos\theta_3 \quad (6.24)$$

$$I(\theta_2) \propto 1 - \frac{\pi}{4}\ P(\Lambda_b)\beta(\Lambda_b)\alpha(\Lambda)\cos\theta_2 \quad (6.25)$$

$$I(\theta_1) \propto 1 - \frac{\pi}{4}\ P(\Lambda_b)\gamma(\Lambda_b)\alpha(\Lambda)\cos\theta_1\ . \quad (6.26)$$

The experimental angular distributions corresponding to formula (6.24) allow one to measure $\alpha(\Lambda_b)$ with a method independent of the value and knowledge of $P(\Lambda_b)$ as, $\alpha(\Lambda) \equiv \alpha(\Lambda \to p\pi^-) = 0.64$ is well known. In contrast, $\beta(\Lambda_b)$ and $\gamma(\Lambda_b)$ could only be measured if $P(\Lambda_b) \neq 0$ is known. This polarization can be obtained from the angular distribution of Λ in the Λ_b rest frame [formula (6.18a)], once $\alpha(\Lambda_b)$ is known. The measurement of $\beta(\Lambda_b)$ could then be carried out by using the angular distribution given by formula (6.25). The validity of the time-reversal (T) invariance of the $\Lambda_b \to \Lambda D^0$ decay could then be tested by comparing $\beta(\Lambda_b)$ with $\overline{\beta}(\overline{\Lambda}_b) \equiv \overline{\beta}$. The various steps for measuring $\alpha(N_b)$, $P(N_b)$ and $\beta(N_b)$ are summarized in Fig. 6.2.

Comments about the α parameter

Models have been used to describe the $\Lambda_b \to \Lambda_c^+\pi^-$ and $\Lambda_c^+ \to \Lambda\pi^+$ decays[12–14]. By using only spectator diagrams (factorizable contribution), it is predicted that $\alpha(\Lambda_b)$, $\alpha(\Lambda_c) \simeq \pm 1$ [and $\overline{\alpha}(\overline{\Lambda}_b), \overline{\alpha}(\overline{\Lambda}_c) \simeq \mp 1$]. No time reversal violation could then be measured with β as $\beta(\Lambda_b), \beta(\Lambda_c) \to 0$ (because of the relation $\alpha^2 + \beta^2 + \gamma^2 = 1$). The $\alpha(\Lambda_c^+ \to \Lambda\pi^+)$ have been measured[15] and found to be compatible with 1. In any case, the decay parameters α and $\overline{\alpha}$ have to be measured for the N_b and $\overline{N}_b$ decay channels.

6.3 - The N_b decaying into two particles with S=1/2, 1

These cases will be somewhat more complicated because of the spin configuration $1/2 \to 1/2 + 1$. However, here also, the contribution of only one isospin transition between the initial and final state leads to the equality of the partial widths of the considered N_b and $\overline{N}_b$ decays ($\Gamma = \overline{\Gamma}$), yielding $\Delta = 0$. The decay channels given as examples in Table 6.3 will then all have $\Delta = 0$. Also here one has to consider other parameters which can be used to search for CP violation in these decay channels.

The angular distribution of the hyperon or N_c ($N_b \to Y + M, N_c + M$) with respect to the polarization direction of the N_b in its rest frame (angle Θ) has a form similar to formula (6.18a), namely[13,16]

$$I(\Theta) \propto 1 \pm \alpha'(N_b) P(N_b) \cos\,\Theta\ . \tag{6.27}$$

The α' parameter depends on the various orbital momenta between J/Ψ and Y and can be expressed by[16]

$$|\alpha'(N_b)| = \frac{|2\ \mathrm{Re}\ (S^*_{1/2}\ P_{1/2} + D^*_{3/2} P_{3/2})|}{|S_{1/2}|^2 + |P_{1/2}|^2 + |P_{3/2}|^2 + |D_{3/2}|^2}\ . \tag{6.28}$$

The indices indicate the sum of the spins of the outgoing particles, namely 3/2 or 1/2. For the present case, the angular distribution of one of the daughter particles of the emitted baryon (Y or N_c, denoted here by N) in the baryon rest frame is also linear in $\cos\theta_3$ (Ref. 13),

$$I(\theta_3) \propto 1 \pm \alpha''(N_b)\alpha(N) \cos\theta_3\ . \tag{6.29}$$

The comparison of this distribution with experimental data allows one to obtain α'', which can be compared with the value deduced from the c.c. channel ($\overline{\alpha}''$).

The coefficient α'' is, however, different from that appearing in formula (6.27), in contrast to the $1/2 \to 1/2 + 0$ case. Therefore, $\alpha'(N_b)$ can only be measured with distribution (6.27) if the polarization $P(N_b)$ is known. The comparison of α' with $\overline{\alpha}'$ or α'' with $\overline{\alpha}''$ through the parameters

$$A' = \frac{\alpha' + \overline{\alpha}'}{\alpha' - \overline{\alpha}'} \quad \text{or} \quad A'' = \frac{\alpha'' + \overline{\alpha}''}{\alpha'' - \overline{\alpha}''} \tag{6.30}$$

could be used to search for CP violation (see Fig. 6.2).

Remarks about the $\alpha'(\Lambda_b)$ parameter

There are several models[17] predicting the $\alpha'(\Lambda_b)$ value for the $\Lambda_b \to \Lambda J/\Psi$ decay. With the free quark decay $b \to c\bar{c}s$ constraining the $c\bar{c}$ effective mass to be near the J/Ψ mass, the estimate is $\alpha'(\Lambda_b) \sim 0.43$. By using an exclusive model[17], the estimate becomes $\alpha'(\Lambda_b) \simeq 0.19 - 0.26$. With this order of magnitude one can appreciate the measurement precision of $\alpha'(\Lambda_b)P(\Lambda_b)$ expected for a proposed experiment.

6.4 - The polarization of the beauty baryons

The polarization of the hyperons $Y \equiv \Lambda, \Sigma, \Xi$ has been measured in several p-target experiments[18–20] ($pN \to YX, \overline{Y}X$) with p incident momentum around $400 - 800$ GeV/c. The polarization of Λ has been observed, in contrast to the $\overline{\Lambda}$ which vanishes in the same type of interaction[20]. For Ξ^- and $\overline{\Xi}^+$ the situation is different, as both have nearly the same polarization[18,20] in the pN production with an incident momentum of around 800 GeV/c. The polarization measurement of beauty baryons could certainly be useful for a better understanding of the production mechanism. Furthermore, as already discussed above, the knowledge of the polarization of N_b and $\overline{N}_b$ could be helpful for searching CP violation in the decay of the beauty baryon. By considering the decay of the beauty hadron into two particles

$$\begin{aligned} N_b &\to Y + M \\ &\to N_c + M \ , \end{aligned}$$

as indicated in Table 6.2 ($1/2 \to 1/2+0$), as well as their charge conjugate reactions, one could measure and compare the polarization of N_b and $\overline{N}_b$. The search for CP violation with the β and $\overline{\beta}$ parameters could then be attempted if one finds that $P(N_b)$ and $P(\overline{N}_b) \neq 0$ (Section 6.2 and Fig. 6.2).

From the channels indicated in Table 6.2, the $\Lambda_b \to \Lambda_c^+ \pi^-$ channel appears to have the largest branching ratio. By using the distribution (6.18a), written here in the form:

$$I(\Theta) = 1 + \alpha(\Lambda_b \to \Lambda_c^+ \pi^-)\ P(\Lambda_b) \cos\Theta\ , \tag{6.31}$$

one can measure the quantity $\alpha(\Lambda_b \to \Lambda_c^+\pi^-)P(\Lambda_b)$. As mentioned above, theoretical models[12–14] predict that the decay parameters $|\alpha(\Lambda_b \to \Lambda_c^+\pi^-)| = |\alpha(\Lambda_c^+ \to \Lambda\pi^+)| \simeq 1$ using only spectator diagrams (factorizable contributions) as shown in Fig. 6.3. As already noted, the $|\alpha(\Lambda_c^+ \to \Lambda\pi^+)|$ parameter has been measured and is compatible with 1 (Ref. 15). Assuming that the same type of mechanism will contribute to the Λ_b ($\overline{\Lambda}_b$) decay (see Fig. 6.3), one can expect that $|\alpha(\Lambda_b \to \Lambda_c^+\pi^-)| = 1$. Then the polarizations $P(\Lambda_b)$ could be measured directly from the distributions given by (6.31). In the same way one could obtain $P(\overline{\Lambda}_b)$ assuming that one has also $|\alpha(\overline{\Lambda}_b)| \simeq 1$,

For the $1/2 \to 1/2 + 1$ spin configuration, one can measure the $\alpha'(N_b)P(N_b)$ quantity using the angular distribution given by formula (6.27), namely

$$I(\Theta) \propto 1 \pm \alpha'(N_b)P(N_b)\cos\Theta\ .$$

By fitting the experimental data with the above type of equation for the N_b and $\overline{N}_b$, we could compare $\alpha'(N_b)P(N_b)$ and $\overline{\alpha}'(\overline{N}_b)P(\overline{N}_b)$. With the assumption that $\alpha' \simeq \overline{\alpha}'$, one obtains information about the relation between $P(N_b)$ and $P(\overline{N}_b)$.

6.5 - Suggestions

In this chapter we discussed some interesting features of studying beauty baryon ($N_b \equiv bqq$ and its c.c.) decays. Such investigations could be made successfully in pN (or $\overline{p}N$) interactions at c.m. energies $\sqrt{s} > 1$ TeV. In this domain the production rate of beauty baryon is expected to be large.

We recalled here several aspects which were utilized for the analysis of hyperon decays and which could also be used for some of the N_b decay channels. Within the statistics actually available, no CP violation effects have been observed in the hyperon decays. Nevertheless, the search for CP violation in the $N_b, \overline{N}_b$ decays has to be studied. This kind of study will certainly give a better understanding of baryon decay but could, perhaps, also lead to the discovery of new aspects of weak decays. The construction of the LHC will provide a large production of $N_b, \overline{N}_b$. This should encourage us to prepare detectors which could also give us the possibility of a detailed investigation of the beauty baryon decays.

Appendix 6.A

The CP violation parameters ($1/2 \to 1/2 + 0$)
a) The Λ decay case

As an example, let us first consider the $\Lambda \to p\pi^-$ decay where two isospin transitions $I_f = 3/2, 1/2$ are present (using now the indice $k = 2I_f$). One has then

$$\begin{aligned} S =& S_1 \ \exp\ i(\delta_1^S + \phi_1^S) \ + S_3 \ \exp\ i(\delta_3^S + \phi_3^S) \\ P =& P_1 \ \exp\ i(\delta_1^P + \phi_1^P) \ + P_3 \ \exp\ i(\delta_3^P + \phi_3^P) \\ \overline{S} =& - S_1 \ \exp\ i(\delta_1^S - \phi_1^S) \ - S_3 \ \exp\ i(\delta_3^S - \phi_3^S) \\ \overline{P} =& P_1 \ \exp\ i(\delta_1^P - \phi_1^P) \ + P_3 \ \exp\ i(\delta_3^P - \phi_3^P)\ . \end{aligned} \tag{6.A1}$$

For the S waves, for instance, one obtains

$$\begin{aligned} |S|^2 &= S_1^2 + S_3^2 + 2S_1S_3 \ \cos(x+y) \\ |\overline{S}|^2 &= S_1^2 + S_3^2 + 2S_1S_3 \ \cos(x-y)\ , \end{aligned}$$

with $x = \delta_1^S - \delta_3^S$ and $y = \phi_1^S - \phi_3^S$. This gives the expressions:

$$\begin{aligned} |S|^2 - |\overline{S}|^2 &= 4S_1S_3 \ \sin x \sin y \\ |S|^2 + |\overline{S}|^2 &= 2(S_1^2 + S_3^2) + 4S_1S_3 \ \cos x \cos y\ . \end{aligned}$$

Similar expressions can be obtained for the P waves where $x, y \to x', y'$, with this time, $x' = \delta_1^P - \delta_3^P$ and $y' = \phi_1^P - \phi_3^P$. One then obtains

$$\Delta = \frac{\Gamma - \overline{\Gamma}}{\Gamma + \overline{\Gamma}} \tag{6.A2}$$

$$= \frac{-2\left[S_1S_3 \ s(\delta_1^S - \delta_3^S)\ s(\phi_1^S - \phi_3^S) + P_1P_3 \ s(\delta_1^P - \delta_3^P)s(\phi_1^P - \phi_3^P)\right]}{\sum_{1,3}(S_i^2 + P_i^2) + \left[S_1S_3 \ c(\delta_1^S - \delta_3^S)c(\phi_1^S - \phi_3^S) + P_1P_3 \ c(\delta_1^P - \delta_3^P)c(\phi_1^P - \phi_3^P)\right]}$$

where $s \equiv \sin$, $c \equiv \cos$. Here the interference terms (the expression appearing in the numerator) is due to waves having the same orbital momentum but different I_f values. From (6A.1), one obtains formula (6.16) assuming that $S_3 < S_1$ and $S_{1,3} > P_{1,3}$

b) **The general case for the $1/2 \to 1/2 + 0$ decay**

Using the formulae (6.6) and (6.7) relating the S, P with the $\overline{S}$, $\overline{P}$ waves as well as formula (6.8) and (6.10) defining the Γ, α, β parameters, it is straightforward to obtain the following expressions[8,9]:

$$\Delta = \frac{\Gamma - \overline{\Gamma}}{\Gamma + \overline{\Gamma}} \tag{6.A3}$$

$$= \frac{-2\sum_{i<j}\left[S_iS_js(\delta_i^S - \delta_j^S)s(\phi_i^S - \phi_j^S) + P_iP_js(\delta_i^P - \delta_j^P)s(\phi_j^P - \phi_j^P)\right]}{\sum_i(S_i^2 + P_i^2) + \sum_{i<j}\left[S_iS_jc(\delta_i^S - \delta_j^S)c(\phi_i^S - \phi_j^S) + P_iP_jc(\delta_i^P - \delta_j^P)c(\phi_i^P - \phi_j^P)\right]},$$

(where here $s \equiv \sin$, $c \equiv \cos$) and

$$A \simeq \frac{\alpha + \overline{\alpha}}{\alpha - \overline{\alpha}} = \frac{\text{Re }(S^*P + \overline{S}^*\overline{P})}{\text{Re }(S^*P - \overline{S}^*\overline{P})} \tag{6.A4}$$

$$= \frac{-\sum_{i,j} S_iP_j \sin(\delta_j^P - \delta_i^S)\sin(\phi_j^P - \phi_i^S)}{\sum_{i,j} S_iP_j \cos(\delta_j^P - \delta_i^S)\cos(\phi_j^P - \phi_i^S)}$$

$$B \simeq \frac{\beta + \overline{\beta}}{\beta - \overline{\beta}} = \frac{\text{Im }(S^*P + \overline{S}^*\overline{P})}{\text{Im }(S^*P - \overline{S}^*\overline{P})} \tag{6.A5}$$

$$= \frac{-\sum_{i,j} S_iP_j \cos(\delta_j^P - \delta_i^S)\sin(\phi_j^P - \phi_i^S)}{\sum_{i,j} S_iP_j \sin(\delta_j^P - \delta_i^S)\cos(\phi_j^P - \phi_i^S)}.$$

Let us recall that the δ phases are due to final-state interactions while the ϕ represent the weak decay phases which may lead to CP violation effects. The numerators in (6.A3) and (6.A4) contain only sin terms. Therefore, in the absence of the final-state interactions one will always have $\Delta = A = 0$. By comparing the expressions of (6.A3), (6.A4) and (6.A5), one usually expects that $|B| > |A| > |\Delta|$ in the case of CP violation. The expressions given above have been used in order to indicate the relations given in Table 6.4. Here the summation is at most over two terms.

As the angles corresponding to the differences of $\delta_j - \delta_i$ and $\phi_j - \phi_i$ are expected to be small, one often uses the above formulae with $\cos(\delta_j - \delta_i) \simeq \cos(\phi_j - \phi_i) \simeq 1$. In this approximation the ratio

$$B' = \frac{\Lambda\beta + \overline{\Lambda}\overline{\beta}}{\Lambda\alpha - \overline{\Lambda}\overline{\alpha}} \simeq \frac{\beta + \overline{\beta}}{\alpha - \overline{\alpha}} \propto -\sum_{i,j} S_iP_j \sin(\phi_i^P - \phi_j^S) \tag{6.A6}$$

does not depend on the phases due to the final-state interactions. The measurement of this ratio could then be of great interest.

Appendix 6.B

The decay angular distributions ($1/2 \to 1/2 + 1$)

Let us demonstrate formulae (6.24) to (6.26). To this end we use formula (6.19),

$$f(\hat{\Lambda}, \hat{p}) = \Big[1 + \alpha(\Lambda_b)\ \vec{P}(\Lambda_b)\ \hat{\Lambda}\Big] \times \Big[1 + \alpha(\Lambda)\ \vec{P}(\Lambda)\ \hat{p}\Big]\ , \tag{6.19}$$

in which we replace $\vec{P}(\Lambda)$ by using formula (6.20), written here as:

$$\vec{P}(\Lambda) = \frac{1}{I(\hat{\Lambda})}\Bigg(\Big[\alpha(\Lambda_b) + \vec{P}(\Lambda_b)\hat{\Lambda}\Big]\ \hat{\Lambda} + \beta(\Lambda_b)(\vec{P}(\Lambda_b) \times \hat{\Lambda}) + \gamma(\Lambda_b)\ \Big[\hat{\Lambda} \times (\vec{P}(\Lambda_b) \times \hat{\Lambda})\Big] \Bigg)\ .$$

For transforming formula (6.19) we use the unit vectors along the coordinate system in the Λ rest frame (Fig. 6.1), namely

$$\hat{X} = \frac{\Lambda \times (\vec{n} \times \hat{\Lambda})}{\sin\theta}\ ,\quad \hat{Y} = \frac{\vec{n} \times \hat{\Lambda}}{\sin\theta}\ ,\quad \hat{Z} = \hat{\Lambda}\ ,$$

where θ is the angle between $\vec{n}$ and Λ in the Λ_b rest frame ($\hat{\Lambda}\vec{n} = \cos\theta$). The emission angles θ_j (j =1-3) of the proton in the Λ rest frame are then defined by:

$$\hat{p}\hat{X} = \cos\theta_1\ ,\quad \hat{p}\hat{Y} = \cos\theta_2\ ,\quad \hat{p}\hat{Z} \equiv \hat{\Lambda}\hat{p} = \cos\theta_3\ .$$

Formula (6.19) now becomes:

$$f(\theta, \theta_j) = 1 + \alpha(\Lambda)\alpha(\Lambda_b)\cos\theta_3 + P(\Lambda)\big[\alpha(\Lambda_b)\cos\theta + \alpha(\Lambda)\cos\theta\ \cos\theta_3 + \beta(\Lambda_b)\alpha(\Lambda)\sin\theta\ \cos\theta_2 + \gamma(\Lambda_b)\alpha(\Lambda)\sin\theta\ \cos\theta_1\big]\ .$$

In order to have only the θ_j dependence, the integration of the above equation on $d\Omega = 2\pi d(\cos\theta)$ leads to:

$$f(\theta_j) \propto 2(1 + \alpha(\Lambda)\alpha(\Lambda_b)\cos\theta_3) + P(\Lambda)\big[-\beta(\Lambda_b)\alpha(\Lambda)\frac{\pi}{2}\ \cos\theta_2 - \gamma(\Lambda_b)\alpha(\Lambda)\frac{\pi}{2}\ \cos\theta_1\big]\ .$$

To have a distribution depending only on a given θ_j, one has to integrate the last equation over the solid angles corresponding to the remaining angles. One then obtains formulae (6.24) to (6.26).

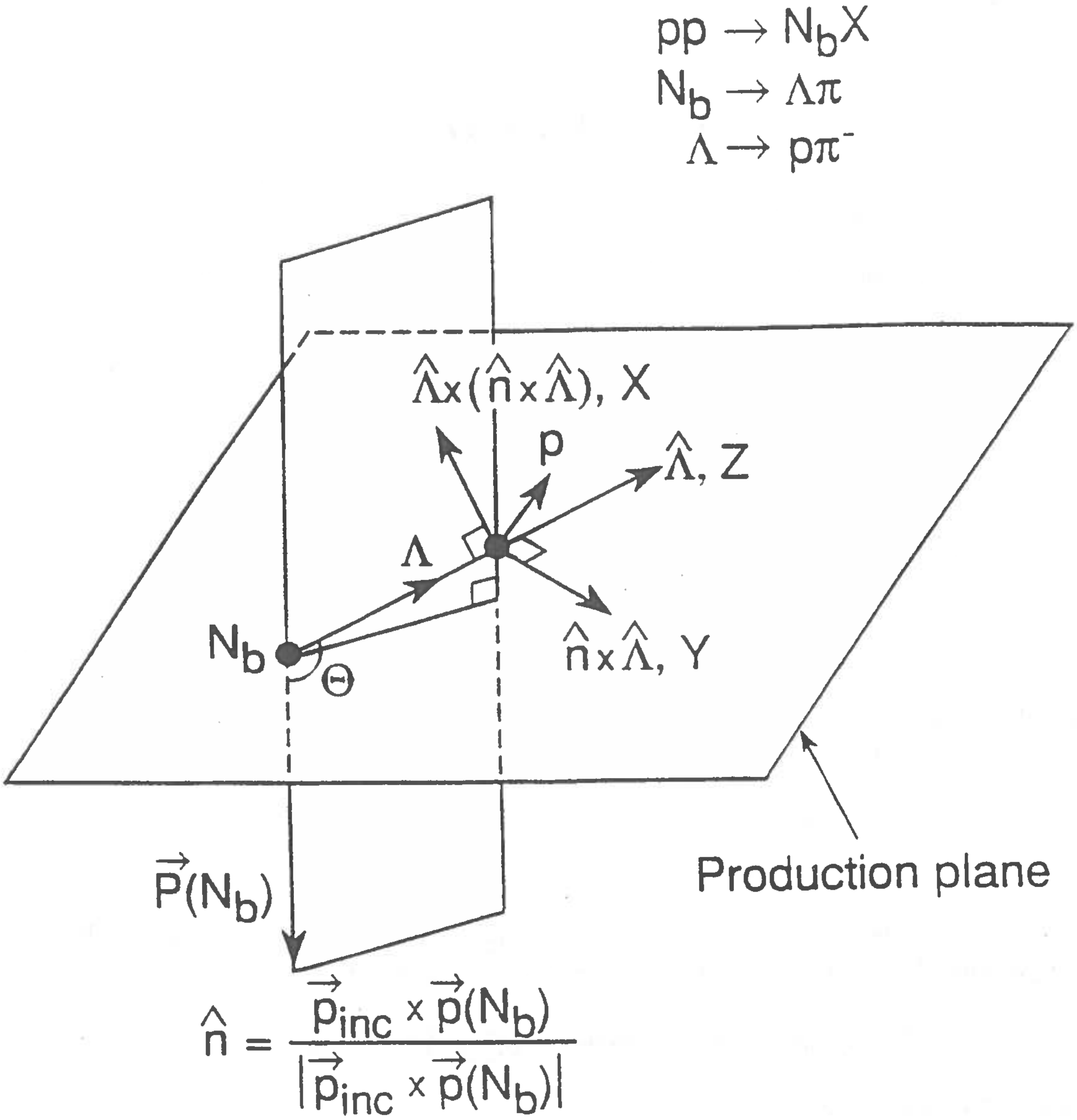

Fig. 6.1 - The production plane of the $pp \rightarrow N_b X$ reaction and the $\vec{P}(N_b)$ polarization normal to this plane. The X, Y, Z represent the coordinate system used in the Λ rest frame for defining the p angular (θ_{1-3}) distributions coming from the $\Lambda \rightarrow p\pi$ decay. Here Θ is the Λ emission angle with respect to the $P(N_b)$ direction in the N_b rest frame.

$a)\ 1/2 \to 1/2 + 0\ ,\quad \Lambda_b \to \Lambda + \pi$, $\Lambda \to p + \pi^-$	
$I(\Theta) = 1 + \alpha(\Lambda_b)P(\Lambda_b)\cos\Theta$	1
$I(\theta_3) \propto 1 + \alpha(\Lambda_b)\alpha(\Lambda)\cos\theta_3$	2
$I(\theta_2) \propto 1 - \frac{\pi}{4}\ P(\Lambda_b)\beta(\Lambda_b)\alpha(\Lambda)\cos\theta_2$	3
$I(\theta_1) \propto 1 - \frac{\pi}{4}\ P(\Lambda_b)\gamma(\Lambda_b)\alpha(\Lambda)\cos\theta_1$	4

$$\Delta = \frac{\Gamma - \overline{\Gamma}}{\Gamma + \overline{\Gamma}} \quad ?$$
$$A \simeq \frac{\alpha + \overline{\alpha}}{\alpha - \overline{\alpha}}$$
$$B \simeq \frac{\beta + \overline{\beta}}{\beta - \overline{\beta}} \quad ?$$
$$|B| \geq |A| \geq |\Delta|\ .$$

$b)\ 1/2 \to 1/2 + 1\ ,\quad \Lambda_b \to \Lambda + J/\psi$, $\Lambda \to p + \pi^-$	
$I(\Theta) = 1 + \alpha'(\Lambda_b)\ P(\Lambda_b)\cos\Theta$	1
$I(\theta_3) \propto 1 + \alpha''(\Lambda_b)\alpha(\Lambda)\cos\theta_3$	2

$$\Delta = \frac{\Gamma - \overline{\Gamma}}{\Gamma + \overline{\Gamma}} \quad ?$$
$$A' \simeq \frac{\alpha' + \overline{\alpha}'}{\alpha' - \overline{\alpha}'} \quad ?$$
$$A'' \simeq \frac{\alpha'' + \overline{\alpha}''}{\alpha'' - \overline{\alpha}''}\ .$$

Fig. 6.2 - The angular distributions for some examples of Λ_b decay channels. a) $1/2 \to 1/2 + 0$: The distribution 2 gives $\alpha(\Lambda_b)$, allowing $P(\Lambda_b)$ to be obtained with equation 1. Once $P(\Lambda_b) \neq 0$ is measured, one can obtain $\beta(\Lambda_b)$ (same procedure for $\overline{\Lambda}_b$). b) $1/2 \to 1/2 + 1$: Equation 2 gives $\alpha''(\Lambda_b)$, while $\alpha'(\Lambda_b)$ can only be measured if $P(\Lambda_b) \neq 0$ is known. The ? signs near some of the asymmetry parameters (Δ, B, A', A'') indicate that they can only be used to search for CP violation effects under some conditions (see text).

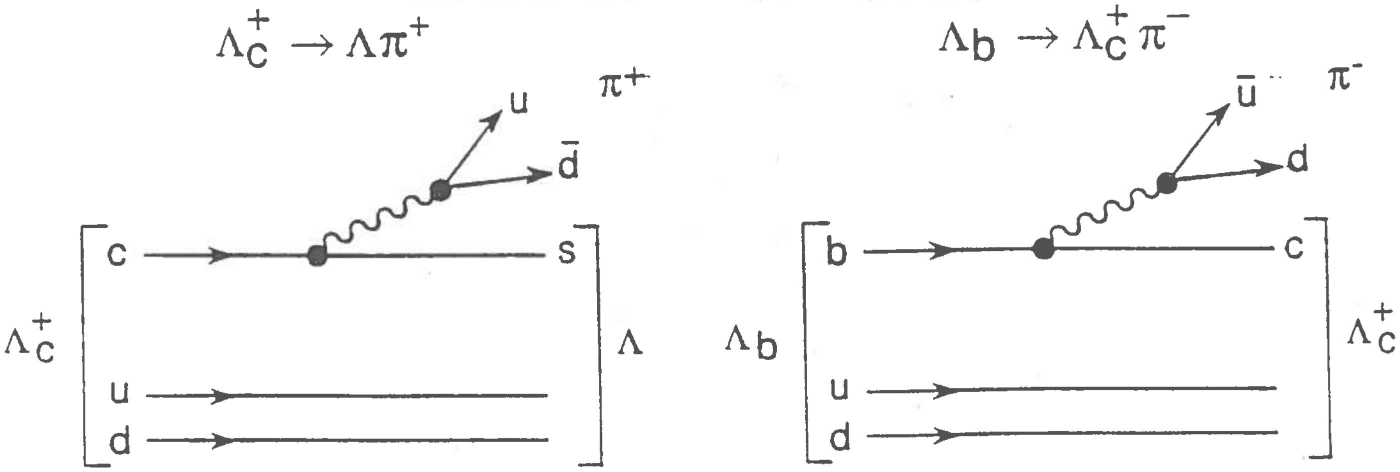

Fig. 6.3 - Spectator diagrams responsible for the $\Lambda_c^+ \to \Lambda\pi^-$ and $\Lambda_b \to \Lambda_c^+\pi^-$ decays.

References

Chapter 1

1) F.E. Close, "An Introduction to Quarks and Partons", Academic Press (1979).
2) R.E. Marshak, Conceptual Foundations of Modern Particle Physics, World Scientific Publishing Co. Pte. Ltd. (1993).
3) Preliminary results from the CDF experiment at FERMILAB (1994).
4) Review of Particle Properties, Phys. Rev. D50, No 3, (1994) 1173.
5) E. Eichten et al., Phys. Rev. D21 (1980) 203;
J.L. Richardson, Phys. Lett. B82 (1979) 272;
A. Martin, Phys. Lett. B93 (1980) 338.
6) W. Buchmuller and S.-H. H. Tye, Phys. Rev D24 (1981) 132.
7) M. Krammer and H. Kraseman, DESY Report 79/20, 1979.
8) H. Grosse and A. Martin, Phys. Rep 60 (1980) 341;
A. Martin, Potential models: predictive rigorous results, CERN-TH.6933/93 (1993).
9) See for instance: La Revista del Nuovo Cimento 11 (1981) and references quoted therein.
10) A. Fridman, Fort. Phys. 34 (1986) 397 and quoted references.
11) G.A. Schuler, Quarkonium production and decays, CERN-TH.7170/94 Report (1994).
12) K. Ueno et al., Phys. Rev. Lett 32 (1979) 486.
13) For a D wave, the orbital momentum will lead to $\psi(0) \to 0$. Then the partial widths given by formula (1.1) and (1.2) will tend to vanish. No resonances will then be observed
14) R. Van Royen and V.F. Weisskopf, Nuov. Cimento 50 (1967) 617 and 51 (1967) 383.
15) T. Appelquist and H.D. Politzer, Phys. Rev. Lett. 34 (1975) 43 and Phys. Rev. D12 (1975) 1404;
A. De Rujula and S.L. Glashow, Phys. Rev. Lett. 34 (1975) 46.
16) Proc., B-factories, The State of the Art in Accelerators, Detector and Physics Workshop, SLAC-400 Report (1992).
17) The Compact Muon Solenoid (CMS), CERN/LHCC 92-3 (1992);
B Physics and CP Violation Studies with the CMS Detector at the LHC, International Journal of Mod. Phys. A Vol 9, No24 (1994).

18) General-Purpose *pp* Experiment at the Large Hadron Collider at CERN (ATLAS), CERN/LHCC 92-4 (1992).

19) M.M. Block and R.N. Cahn, Phys. Lett. 188B (1987) 143;
M.M. Block, F. Halzen and B. Margolis, Phys. Rev. D45 (1992) 839.

20) G.A. Schuler and T. Sjöstrand, CERN-TH.6837/93 Report (1993).

21) A. Fridman and A. Snyder, Proc. of the Large Hadron Collider Workshop, CERN 90-10 and ECFA 90-133, Vol. II, p. 218 (1990).

22) K.J. Foley et al., Proceedings of the Workshop on Experiments, Detectors and Experimental Areas for the Supercollider, Berkeley, July 7-17 (1987).

Chapter 2

1) S.Weinberg, Rev. Mod. Phys. 52 (1980) 515;
A. Salam, Rev. Mod. Phys. 52 (1980) 529;
S.L. Glashow, Rev. Mod. Phys. 52 (1980) 539.

2) C. Bouchiat, J. Iliopoulos and Ph. Meyer, Phys. Lett. 38B (1972) 519.

3) M. Kobayashi, T. Maskawa, Prog. Theor. Phys. 49 (1973) 652;
N. Cabibbo, Phys. Rev. Lett. 10 (1963) 531.

4) M.K. Gaillard, L. Maiani, Quarks and Leptons, Cargese (1979) p. 433.

5) Reference 10 in Chapter 1

6) C. Jarlskog, Advanced Series On Direction in High Energy Physics, Vol 3, World Scientific (1989) p. 33.

7) L. Wolfenstein, Phys. Rev. Lett 51 (1983) 1945.

8) J.D Bjorken and I. Dunietz, Phys. Rev. D36 (1987) 2109.

9) L.L. Chau Phys. Rep. 95, N0 1 (1980) 3.

10) M.K. Gaillard, B.W. Lee, J.L. Rosner, Rev. Mod. Phys. 47 (1975) 277;
J. Ellis, M.K. Gaillard, D.V. Nanopoulos, Nucl. Phys. B100 (1975) 313;
J.P. Leveille, Proceedings of the CLEO Collaboration Workshop, Cornell Report CLNS 51/505, July 1981.

(11) R. Rückl, Elementary Particles, XCII Corso, 1987, Soc. Italiana di Fisica, Bologna, Italy.

(12) V. Baur, H. Fritzsch, Phys. Lett. B109 (1982) 402;
J.L. Cortes, X.Y. Pham, A. Toundsi, Phys. Rev. D25 (1982) 188;
T. Inami and C.S. Lim, Prog. Theor. Phys. 65 (1981) 297.

(13) Reference 4 in Chapter 1.

(14) A. Ali and D. London, ECFA Workshop on a European B-Meson Factory, ECFA 93/151 and DESY 93-053 Report (1993) p. 42.

Chapter 3

1) J.S. Haguelin, M.B. Wise, Nucl. Phys. B189 (1981) 87; J.S. Haguelin, Ibid B193 (1981) 123;
A. Ali, Z.Z. Aydin, Nucl. Phys. B148 (1979) 165;
I.I. Bigi, A. I. Sanda, Nucl. Phys. B193 (1981) 85;
L.L. Chau, W.Y. Keung, Phys. Rev. D29 (1984) 592.

2) A.J. Buras, W. Slominski, H. Steger, Nucl. Phys. B238 (1984) 529.

3) I.I. Bigi, A.I. Sanda, Phys. Rev. D29 (1984) 1393.

4) See for instance: Weak Interactions of Leptons and Quarks, E.D. Commins and H.P. Bucksbaum, Cambridge University Press, 1983.

5) I.I. Bigi, A.I. Sanda, Nucl. Phys. B193 (1981) 85.

6) L.L. Chau, Phys. Rep. 95, No 1 (1980) 3.

7) I. Dunietz, J.L. Rosner, Phys. Rev. D34 (1986) 1404.

8) A. Fridman, Mixing and CP Violation in the B-System, lecture notes, CERN-EP 88-123 (1988).

9) A. Pais, S.B. Treiman, Phys. Rev. D12 (1975) 2744.

10) Reference 4 in Chapter 1.

11) CLNS 91-1043 report (1991) and quoted references.

12) See also: T. Inami and C.S. Lim, Progr. Theor. Phys. 65 (1981) 297.

13) A. Ali, C. Jarlskog, Phys. Lett. 144B (1984) 266.

14) Reference 3 in Chapter 1.

15) As the D meson has a smaller mass than the B, one might expect that phase space effects will become more important for the D decay than for the B decay. This could lead to $[\Delta\Gamma/\Delta M]_D > [\Delta\Gamma/\Delta M]_B$ and not allow one to neglect the y parameter for the D mesons.

16) P. Roudeau, Talk given at the Plenary Session of Heavy Flavors at the Glasgow Conference (1994).

17) H.-U. Bengtsson and T. Sjöstrand, Computer Phys. Commun. 46 (1987) 43; T. Sjöstrand, Report CERN-TH.6488/92 (1992).

18) L.B. Okun, V.I. Zakharov, B.M. Pontecorvo, Lett. Nuovo Cimento 13 (1975) 218.

Chapter 4

1) References 6 and 7 in Chapter 3.

2) Reference 9 in Chapter 2.

3) B. Kayser, Testing the standard model of CP violation in all manner of B decay modes, Proceedings of the Second International Symposium on Paticles, Strings and Cosmology, Boston, March 1991.

4) Reference 2 in Chapter 3.

5) Reference 5 in Chapter 3.

6) Reference 8 in Chapter 3.

7) Proceedings of the Workshop on B Physics at Hadron Accelerators, Snowmass, Colorado June 21 - July 2, 1993.

(8) M. Gronau and D. Wyler, Phys. Lett. B256 (1991) 172.

Chapter 5

1) These estimates are obtained from models used with the PHYTIA Monte Carlo calculations. See Reference 17 in Chapter 3. The given values depend somewhat from the c.m. energy but one often uses those given by (5.2) for for $1 \leq \sqrt{s} \leq 20$ Tev.

2) M. Chaichian and A. Fridman, Phys. Lett. B298 (1993) 218.

3) A. Fridman and O. Mai, Remarks about the Measurement of B Decay at HERAB, Note unpublished (1994).

4) References 17 and 18 in Chapter 1

5) H. Quinn, Phys. Rev. D50, No 3, (1994) 1632.

6) I.I. Bigi and A.I. Sanda, Nucl. Phys. B281 (1987) 41.

7) Reference 8 in Chapter 3.

8) Reference 16 in Chapter 3.

9) M. Cannalire and A. Fridman, Nuovo Cim. 106A, (1993) 251.

10) A. Fridman, Proceedings of the Workshop on B Physics at Hadron Accelerators, Snowmass, Colorado June 21 - July 2, 1993, p. 695.

11) Reference 16 in Chapter 1.

Chapter 6

1) Reference 17 in Chapter 3.

2) Reference 4 in Chapter 1.

3) A. Fridman, R. Kinnunen and N. Neumeister, Decays and Production of Beauty Baryons in pp Interactions, to be published in Physica Scripta (1995).

4) A. Fridman and B. Margolis, Beauty Baryon Production and Decays, and CKM Matrix Elements, CERN-TH 6878/93 report (1993).

5) Reference 1 in Chapter 1.

6) Chao-Hsi Chang and Yu-Qi Chen, Phys. Rev. D48 (1993) 4086.

7) Reference 20 in Chapter 1.

8) See, for instance:
T.D. Lee and C.N. Yang, Phys. Rev. 108 (1957) 1645;
J.W. Cronin and O.E Overseth, Phys. Rev. 129 (1963) 1795;
G. Källen, Elementary Particle Physics, Addison-Wesley Company Inc., Reading, Massachusetts, 1964;
T.D. Lee, Prelude in Theoretical Physics, North-Holland Publishing Company, Amsterdam, 1966;
P. Eberhard, J. Button-Shafer and D.W. Merril, UCRL-11427 Berkeley;
P.M. Dauber et al., Phys. Rev. 179 (1969) 1261.

9) J.F. Donoghue and Sandip Pakvasa, Phys. Rev. Lett. 55 (1985) 162;
J.F. Donoghue, Xiao-Gang He and Sandip Pakvasa, Phys. Rev. D34 (1986) 833.

10) X.-G He, H. Steger and G. Valencia, Phys. Lett. B272 (1991) 411.

11) A. Fridman and R. Kinnunen, Comments on Beauty Baryon Decays and CP-Violation Effects, CERN-PPE/93-61 report, Contribution to the 5th International Symposium on Heavy Flavor Physics, Montréal, July 6-10, 1993.

12) T. Mannel, W. Roberts and Z. Ryzak, Phys. Lett. B255 (1991) 593,
Parity Violation and Flavor Selection Rule in Charmed Baryon Decays, S. Pakvasa, S.P. Rosen and S.F. Tuan, Report UH-511-693-90 (1990);
T. Mannel and W. Roberts, Phys. Rev. D47 (1993) 4963.

13) J.G. Körner and M. Krämer, Phys. Lett.B275 (1992) 495.

14) J.D. Bjorken, Phys. Rev. D40 (1989) 1513.

15) H. Albrecht et al.,Phys. Lett. B274 (1992) 239;
P. Avery et al., Phys. Rev. Lett. 65 (1990) 2842.

16) H. Albrecht, A. Fridman, O. Mai, T. Oest, W. Schmidt-Parzefall and R. Kinnunen, The interest in Studying Beauty Baryon in pN Interactions at HERA, DESY 93-156 report (1993).

17) F.E. Close et al., Heavy Quark Theory and b-polarisation at LEP, preprint RAL-92-016 (1992).

18) See for instance the following articles and the references quoted therein:
K. Heller et al., Phys. Rev. Lett. 51 (1989) 2025;
J. Lach, Hyperons: Insights Baryon Structures, Lectures given at the Fourth Mexican School of Particles and Fields, Oaxtepec, Mexico (1990), FERMILAB-Conf-91/200 Report;
L. Pondron, Phys. Rep. 122, 58 (1985).

19) B. Lundberg et al., Phys. Rev. D40 (1989) 357.

20) P.M. Ho et al., Phys. Rev. Lett. 65 (1990) 1713.